Manuela Alexandrina David de Aguiar

Vector fields with heteroclinic networks

Departamento de Matemática Aplicada
Faculdade de Ciências da Universidade do Porto
Dezembro 2002

Manuela Alexandrina David de Aguiar

Vector fields with heteroclinic networks

Tese submetida à Faculdade de Ciências da Universidade do Porto para obtenção do grau de Doutor em Matemática

Departamento de Matemática Aplicada
Faculdade de Ciências da Universidade do Porto
Dezembro 2002

Ao meu marido, Emanuel

Não sei de onde venho...

...não sei para onde vou.

Sei que não vou por aí!

Acknowledgments

O prefácio, inspirado num poema de José Régio, traduz bem uma aparente aleatoriedade que tem pautado a minha vida académica e profissional. Na verdade quando ao terminar o meu 11º ano de escolaridade decidi abandonar temporariamente os meus estudos e ingenuamente ingressar no mundo do trabalho foi com a firme certeza de que um dia iria regressar.

Sim, eu sabia, tal como insistentemente me alertaram, que era preciso uma grande força de vontade. Eu tinha-a! Foi essa força de vontade de estar constantemente a aprender que me fez regressar e ficar.

Claro que tudo isto só foi possível graças ao empenho e apoio de um sem número de pessoas às quais quero agredecer.

Pessoalmente, a mais valia destes quatro anos de doutoramento foi sem dúvida o muito que aprendi. E isso, e muito mais: a motivação, a compreensão, o empenho, o apoio, a orientação devo-o agradecer às minhas orientadoras, Prof. Isabel Labouriau e Prof. Sofia Castro Gothen. Porque foram orientadoras de facto, o meu muito obrigada. Sem elas este trabalho nao teria sido possível.

O meu muito obrigada também ao Prof. M.Field pelas suas sugestões e por me ter convidado a visitá-lo na Universidade de Houston. Também ele teve um papel determinante neste meu trabalho.

Outros Professores, pelos mais diversos motivos, merecem o meu agradecimento: Prof. Ana Paula Dias, Prof. Christian Bonatti, Prof. Fernando Jorge, Prof. J.M. Gambaudo, Prof. Gueorgui Sirmnov, Prof. Helena Mena Matos, Prof. Inês Cruz, Prof. Jose Bastos, Prof. Marcelo Viana, Prof. Maria Joao Costa, Prof. Margarida Brito, Prof. Marty Golubisky, Prof. Paul Glendinnig e Prof. Silvio Gama.

Quero agradecer à Faculdade de Economia da Universidade do Porto o facto de me terem dado equiparação a bolseiro e me terem sempre apoiado durante estes quatro anos.

Agradeço ao pessoal das bibliotecas do Departamento de Matemática Aplicada, do Departamento de Matemática Pura e da Faculdade de Economia do Porto pelos seus serviços. Quero também agradecer a todos os funcionários do Departamento de Matemática Aplicada pela simpatia com que sempre me trataram.

Aos meus colegas de Doutoramento, a Stella, o Zé, a Eliana, a Carla, o Manel e

a Helena, agradeço o convívio e o apoio nos momentos que partilhamos. À Helena agradeço também a sua ajuda.

Um agradecimento especial para as minhas amigas Ana Paula e Stella. Elas, como ninguém, souberam ouvir-me, confortar-me e aconselhar-me.

Ao Filipe muito tenho a agradecer; o ser um verdadeiro amigo e o companheirismo ao longo destes anos. Agradeço também o apoio informático e o tempo que dispendeu para me ajudar a instalar diverso software. Neste campo deixo também o meu agradecimento ao Ismael e ao Pedro Campos por me terem ajudado.

Agradeço a toda a minha família. Aos meus Pais muito tenho a agradecer, a educação que me deram, o amor, o carinho e a ajuda. Em particular muito agradeço o facto de me terem ajudado e continuarem a ajudar a cuidar e educar a minha filha.

À minha filha Filipa, de quem muito me orgulho, agradeço o seu amor incondicional e peço desculpa por muitas vezes o tempo ter sido curto e a paciência também.

Finalmente, muito tenho a agradecer ao meu marido. Por no meu segundo ano da licenciatura me ter dado a oportunidade de deixar de ser trabalhadora-estudante e passar a ser só estudante, por me ter apoiado sempre ao longo destes 14 anos, pelo seu amor e carinho dedico-lhe esta tese.

E agora? -podem perguntar. Agora, com a mesma incerteza de sempre eu digo "*Não sei de onde venho ...não sei para onde vou.*", com maior certeza afirmo "*Não vou por aí!*" e com a ingenuidade de sempre termino "*Só vou por onde me levam os meus próprios passos!*".

Este trabalho foi financiado durante 3 anos por uma bolsa PRODEP - Formação de Formadores do Ensino Superior, Concurso 3/98.

Resumo

O trabalho desenvolvido ao longo desta tese tem como ponto de partida uma família de equações diferenciais apresentada e estudada por Field (Ver M.J. Field, 1996, *Lectures on Bifurcations, Dynamics and Symmetry*, Pitman Research Notes in Mathematics Series 356, Longman).

Field conjectura, com base no seu estudo analítico e numérico, a existência, para certos valores dos parâmetros, de uma rede heteroclínica envolvendo os equilíbrios e as trajectórias periódicas na dinâmica do sistema. No caso de as variedades invariantes de dimensão ≥ 2 dos equilíbrios e das trajectórias periódicas se intersectarem transversalmente, Field conjectura também a existência de dinâmica da ferradura na vizinhança da rede heteroclínica.

Nesta tese provamos as conjecturas de Field. O trabalho aqui desenvolvido indica a existência de uma rede heteroclínica de Shilnikov e prova a existência de dinâmica da ferradura na vizinhança de uma tal rede heteroclínica.

Usamos a simetria do sistema para definir a rede heteroclínica quociente. Isto sugeriu-nos uma abordagem para estudar a dinâmica na vizinhança da rede heteroclínica de Shilnikov. O estudo da dinâmica é efectuado com recurso a uma codificação da dinâmica ao longo da rede heteroclínica e a uma codificação da dinâmica local na vizinhança dos ciclos heteroclínicos na rede quociente.

Construímos exemplos simples contendo ciclos heteroclínicos de Shilnikov que são topologicamente equivalentes a ciclos heteroclínicos quocientes no exemplo de Field. Um facto importante acerca destes exemplos é que, apesar de possuírem dinâmica complexa, pela forma como são construídos, são mais fáceis de manipular analiticamente. Por exemplo, provamos analiticamente a intersecção transversal das variedades invariantes de dimensão ≥ 2.

Os exemplos que construímos ajudam a compreender o comportamento complexo no exemplo de Field. Provamos a existência de dinâmica da ferradura na vizinhança de

ciclos heteroclínicos envolvendo duas selas com autovalores complexos. Isto prova a existência de dinâmica da ferradura no caso concreto de um dos exemplos que construímos.

A codificação obtida dá uma ideia da complexidade da dinâmica no exemplo de Field. A conclusão final é que, sob certas condições, a dinâmica na vizinhança da rede heteroclínica de Shilnikov é dinâmica de ferradura de ferraduras.

Abstract

The starting point for the work in this thesis is a family of differential equations with very complicated dynamics presented and studied by Field (See Field - M.J. Field, 1996, *Lectures on Bifurcations, Dynamics and Symmetry*, Pitman Research Notes in Mathematics Series 356, Longman).

Based on his analytical and numerical studies, Field conjectures, for certain parameter values, the existence of a heteroclinic network involving equilibria and periodic trajectories in the dynamics of the system. He also conjectures, provided the invariant manifolds of dimension ≥ 2 of the equilibria and periodic trajectories intersect transversely, that the existence of such a heteroclinic network would imply horseshoe dynamics in its neighbourhood.

In this thesis we pursue Field's studies about the example. The work developed here indicates the existence of a Shilnikov heteroclinic network and proves the existence of horseshoe dynamics in the neighbourhood of such a Shilnikov heteroclinic network.

We use the symmetry of the system to define the quotient heteroclinic network. This suggests an approach to study the dynamics in the neighbourhood of the Shilnikov heteroclinic network. We codify the dynamics along the heteroclinic network and the local dynamics in the neigbourhood of the cycles in the quotient heteroclinic network. We use both codifications to charaterize the local chaotic dynamics in the neighbourhood of the network.

We construct simple examples with Shilnikov heteroclinic cycles topologically equivalent to quotient heteroclinic cycles in Field's example. These examples, although exhibiting complex dynamics, are by construction easy to study analytically. For example, we prove analytically the transverse intersection of the invariant manifolds with dimension ≥ 2, essential for Field's conjecture.

The examples we construct help understand the chaotic behaviour in Field's example. We prove the existence of horseshoe dynamics in the neighbourhood of heteroclinic

cycles involving two saddle-foci. This proves the existence of horseshoe dynamics in the specific case of one of the examples that we construct.

Our codification gives an idea of the complexity of the dynamics in Field's example. The final conclusion is that, under certain conditions, the dynamics in the neighbourhood of the Shilnikov heteroclinic network is a horsehoe of horsehoe dynamics.

Résumé

Le point de départ pour le travail presenté dans cette thèse est un exemple d'une famille d'équations différentielles avec une dynamique trés complexe qui a été presentée par Field (Voir M.J. Field, 1996, *Lectures on Bifurcations, Dynamics and Symmetry*, Pitman Research Notes in Mathematics Series 356, Longman).

Field qui a étudié analitique et numériquement cette famille, a conjecturé l'existence, pour quelques valeurs des paramètres, d'un réseau hétérocline avec équilibres et trajectoires périodiques dans la dynamique de l'exemple. Dans le cas où les variétés invariantes de dimension ≥ 2 des équilibres et des trajectoires périodiques se coupent transversalement, Field a conjecturé aussi l'existence de dynamique de fers à cheval au voisinage du réseau hétérocline.

Dans cette thèse nous poursuivrons les études de Field. Le travail développé ici indique l'existence d'un réseau hétérocline de Shilnikov et prouve l'existence de dynamique de fers à cheval au voisinage d'une tel réseau hétérocline.

Nous faisons usage de la symétrie du système pour définir le réseau hétérocline quociente. Cela nous a suggéré un abordage pour étudier la dynamique au voisinage du réseau hétérocline de Shilnikov. Nous codifions la dynamique au long du réseau hétérocline et la dynamique local au voisinage des cycles hétéroclines dans le réseau quocient. L'usage de ces deux codifications permet caractériser la dynamique local chaotique au voisinage du réseau.

Nous construirons des exemples simples avec des cycles et des réseaus hétéroclines de Shilnikov topologiquement équivalents aux cycles hétéroclines quocients dans l'exemple de Field. Un fait important sur ces exemples c'est que, nonobstant leur dynamique être complexe, par la façon comme ils sont construit, ils sont plus faciles de manipuler analitiquement. Par exemple, nous sommes capables de prouver analitiquement le coupe transversal des variétés invariantes de dimension ≥ 2.

Les exemples construis par nous aide à comprendre le comportement chaótique de

l'exemple de Field. Nous prouvons l'existence de la dynamique de fers à cheval au voisinage de cycles hétéroclines avec deux selles à valeurs propres complexes. Cela prouve l'existence de dynamique de fers à cheval dans le cas concret de l'un des exemples que nous construisons.

La codification obtenuée donne une idée de la complexité de la dynamique de l'exemple de Field. Pour conclusion finale, la dynamique au voisinage du réseau hétérocline de Shilnikov est la dynamique d'une fers à cheval de fers à cheval.

Contents

List of Figures

Chapter 1

Motivation and aims

A fundamental aspect in setting a general theory of chaotic dynamical systems is the study of specific examples. In this work we construct and study examples with chaotic dynamics.

The complicated dynamics of these examples are due to recurrent behaviour forced by the existence of dynamical objects called heteroclinic cycles and heteroclinic networks.

Roughly speaking, a heteroclinic cycle is a closed path formed by an ordered set of flow invariant sets, called nodes, and trajectories connecting each node to the next. Each heteroclinic connection belongs to the intersection of the unstable manifold of one node with the stable manifold of the next node.

A heteroclinic network is a collection of heteroclinic cycles. There are several definitions in the literature, each imposing certain conditions and properties. These are presented in chapter 2.

In this thesis we deal with equivariant ordinary differential equations. These are ordinary differential equations which are equivariant by some symmetry group. The concepts and results on the dynamics of ordinary differential equations needed for the work in this thesis, can be found, for example, in Arnold [1], Guckenheimer and Holmes [20], Palis and Melo [38]. For equivariant dynamics we refer the reader to Field [15] and Golubitsky and Schaeffer [19].

Heteroclinic cycles and heteroclinic networks are a characteristic feature of equivariant dynamical systems. This is due to the existence of flow invariant subspaces, called fixed point spaces. Most examples of structurally stable heteroclinic cycles that appear in the literature are in the context of equivariant dynamics. A review of some of

these can be found in Field [15] and Krupa [33]. Heteroclinic connections inside fixed point spaces may be robust, or structurally stable, even if the stable and the unstable manifolds of the adjacent nodes do not intersect transversely (see [13]). These connections are preserved by perturbations that preserve the symmetry of the spaces containing them. We refer to the article by Krupa [33] for a review of the theoretical and applied research on robust heteroclinic cycles.

In this work we analyse numerically an example of 'instant chaos' presented and studied by Field in [15] that has very complicated dynamics. In [15] Field conjectures that for certain parameter values this example has a Shilnikov heteroclinic network involving equilibria and periodic trajectories. He also conjectures the transverse intersection of the invariant manifolds with dimension ≥ 2. We make numerical observations of this example that confirm Field's conjectures and use them to establish assumptions on the dynamical behaviour of the example.

This serves as motivation for the construction of simple examples, having part of the complex behaviour conjectured for Field's example.

In [36], Lauterbach and Roberts show that forced symmetry breaking, i.e., perturbing the equations slightly so that some of the symmetries are broken, can naturally lead to the existence of structurally stable heteroclinic cycles. They give examples for dynamical systems with broken spherical symmetry. In [35], Lauterbach *et al* undertake a systematic study of such a situation, obtaining necessary and sufficient conditions for the existence of heteroclinic cycles in dynamical systems with broken symmetries, for general Lie groups.

In this work we use forced symmetry breaking to construct a class of examples having structurally stable heteroclinic cycles with some heteroclinic connections not contained in fixed point spaces. The heteroclinic connections that are not inside fixed point spaces are contained in the transverse intersection of invariant manifolds with dimension greater than or equal to 2, as is expected in Field's example.

We prove analytically the transverse intersection of the invariant manifolds in the examples that we construct. The construction of the examples is an analytic proof that what we observe numerically in Field's example can really exist.

The study of the simple examples helps to understand complex dynamics in general.

The existence of recurrent behaviour in the neighbourhood of heteroclinic phenomena implies periodic behaviour. Moreover, in the general situation of the examples we study, the existence of heteroclinic connections that result from the transverse

intersection of invariant manifolds with dimension ≥ 2, implies more complicated dynamics. We prove that it implies local horseshoe dynamics in the neighbourhood of the heteroclinic cycles and networks, as conjectured by Field.

The term *Shilnikov heteroclinic network* (this term was first used by Field in [15]) is used to refer to a heteroclinic network containing invariant saddles with complex eigenvalues with Shilnikov phenomena, i.e., a heteroclinic network with local horseshoe dynamics. The name of Shilnikov is associated to this phenomena since it was he who first studied, Shilnikov [41], the existence of local horseshoe dynamics in the neighbourhood of homoclinic and heteroclinic phenomena involving saddles with complex eigenvalues.

Although there is a lot of work on the existence, structural stability and asymptotic stability of heteroclinic cycles and networks, there seems to be little work on the study of the local dynamics in their neighbourhood. In [39], Reissner addresses this question in the context of spatio-temporal symmetric systems.

The Shilnikov heteroclinic network in Field's example is a particularly complex heteroclinic network with heteroclinic connections between the different equilibria, that are saddle-foci, between equilibria and periodic trajectories, and between distinct periodic trajectories. We use the symmetry in Field's example to reduce the network to a quotient heteroclinic network.

The characterization of the local dynamics in the neighbourhood of the quotient heteroclinic cycles relies on the study of the local dynamics in the neighbourhood of generic heteroclinic cycles topologically equivalent to them and to the examples that we construct. We define symbolic dynamics and conclude that, under certain conditions, the chaotic local dynamics in the neighbourhood of the heteroclinic cycles that we construct and the quotient heteroclinic cycles of Field's example is horseshoe dynamics.

We characterize the chaotic local dynamics in the neighbourhood of the heteroclinic network in Field's example using symbolic dynamics that describe the dynamics along the heteroclinic network and symbolic dynamics that describe the local dynamics in the neighbourhood of the quotient heteroclinic cycles. We conclude that the chaotic local dynamics in the neighbourhood of the Shilnikov heteroclinic network of Field's example is a horseshoe of horseshoe dynamics.

Our approach gives an idea of the complexity of the dynamics in Field's example and can be used to study the local dynamics in the neighbourhood of heteroclinic networks

of the same kind.

In the next chapter we give the definition of heteroclinic cycle and heteroclinic network that we are going to consider in this thesis and then we review the existent definitions. In chapter 3, we describe Field's example and our numerical simulations. Then, we characterize the structure of the heteroclinic network in Field's example and give an outline of the rest of the thesis.

I declare that, to the best of my knowledge and unless where otherwise stated, all the work presented in this thesis is original.

Chapter 2

Heteroclinic cycles and networks

2.1 Definitions

We adopt the definitions of heteroclinic cycle and heteroclinic complex in Field [15], but instead of using the term heteroclinic complex we use heteroclinic network as it is more commonly used.

Let X be a vector field on $\mathbf{R}^n$.

Definition 1 ([15], 6.5) *Suppose that A is a compact invariant set for the flow of X. We say that A is an* invariant saddle *if*

$$\overline{W^s(A) \setminus A}, \overline{W^u(A) \setminus A} \supset A.$$

Definition 2 ([15], 6.7) *Suppose that*

$$\mathcal{A} = \{A_i \ : \ i = 0, ..., n-1\}$$

is a finite (ordered) set of mutually disjoint invariant saddles. We say that there is a heteroclinic cycle *associated to $\mathcal{A}$, if*

$$W^u(A_i) \cap W^s(A_{i+1}) \neq \emptyset, \ i \geq 0 \ (\text{mod} \quad n).$$

We refer to the set $\Sigma \subset \mathbf{R}^n$ defined by

$$\Sigma = \cup_{i=0}^{n-1} A_i \cup (W^u(A_i) \cap W^s(A_{i+1})),$$

as the (maximal) heteroclinic cycle determined by $\mathcal{A}$.

Let $A_i, A_j \in \mathbf{R}^n$ be two invariant saddles and $W^u(A_i) \cap W^s(A_j) \neq \emptyset$. A trajectory in $W^u(A_i) \cap W^s(A_j)$ is called a *heteroclinic trajectory* or a *heteroclinic connection* from A_i to A_j. We use $A_i \to A_j$ to denote that there is such a connection.

Let X be a Γ-equivariant vector field on $\mathbf{R}^n$. Suppose that Σ is a heteroclinic cycle with associated set of invariant saddles $\mathcal{A}$. Let Γ_Σ denote the isotropy group of Σ, that is,

$$\Gamma_\Sigma = \{\gamma \in \Gamma \ : \ \gamma(\Sigma) = \Sigma\}.$$

Γ_Σ acts on the set of invariant saddles $\mathcal{A}$. If this action is transitive, i.e. given A_i, $A_j \in \mathcal{A}$, $\exists \gamma \in \Gamma_\Sigma$ such that $\gamma(A_i) = A_j$, Σ is sometimes refered as a *homoclinic cycle* (Field [15]).

Definition 3 ([15], 6.22) *Let $\mathcal{A} = \{A_i \ : \ i \in I\}$ be a finite (unordered) set of invariant saddles. We say that a flow-invariant subset Σ of $\mathbf{R}^n$ is a* heteroclinic network *if there is a finite set of (ordered) nonempty subsets $\mathcal{A}_j$ of $\mathcal{A}$ such that*

(A) Each subset $\mathcal{A}_j$ determines a heteroclinic cycle Σ_j.

(B) $\Sigma = \cup_j \Sigma_j$.

(C) If $W^u(A_k) \cap W^s(A_l) \neq \emptyset$ then, there exists j such that $W^u(A_k) \cap W^s(A_l) \subset \Sigma_j$.

(D) $\cup_j \mathcal{A}_j = \mathcal{A}$

If Σ is a heteroclinic network with associated invariant saddle set $\{A_i \ : \ i \in I\}$, then, (see[15], 6.23 (2)),

$$\Sigma = \cup_{i,j \in I} W^u(A_i) \cap W^s(A_j).$$

Suppose that Σ is a connected heteroclinic network with associated saddle set $\mathcal{A}$. Given any pair $A_j, A_k \in \mathcal{A}$, we can find a chain of trajectories joining A_j to A_k; there is a sequence $j = l_0, ..., l_N = k$ such that $W^u(A_{l_i}) \cap W^s(A_{l_{i+1}}) \neq \emptyset$, $0 \leq i < N$(see [15], 6.23 (3)).

From now on we modify the existing definitions in order to adapt them to the problems studied in this thesis.

Definition 4 *Let $\mathcal{A} = \{A_i \ : \ i \in I\}$ be a finite (unordered) set of invariant saddles, and Σ the heteroclinic network with associated saddle set $\mathcal{A}$. We say that a flow-invariant subset $\Upsilon \subset \Sigma$ is a* heteroclinic subnetwork *if there is a finite set of (ordered) nonempty subsets $\mathcal{A}_j$ of $\mathcal{A}$ such that*

(A) Each subset $\mathcal{A}_j$ determines a heteroclinic cycle Υ_j.

(B) $\Upsilon = \cup_j \Upsilon_j$.

It follows that a subnetwork is not necessarily a network and that a heteroclinic cycle is a particular case of a subnetwork.

It follows from (D) in definition 3 that a heteroclinic network with associated saddle set $\mathcal{A}$ cannot be written as a disjoint union of two networks with the same set of saddles $\mathcal{A}$. Nevertheless it can be written as a disjoint union of two subnetworks.

Sometimes it is useful to interpret a heteroclinic network as a (directed) graph. The invariant saddles are the nodes of the graph, and for each nonempty intersection $W^u(A_i) \cap W^s(A_j) \neq \emptyset$ there is an edge from node A_i to node A_j. This means that there is an edge in the graph from node A_i to node A_j for each heteroclinic connection in the network from the invariant saddle A_i to the invariant saddle A_j. It is usual to refer to the invariant saddles of the network as the nodes of the network.

In what follows we study the asymptotic stability of heteroclinic cycles and networks. A flow-invariant set S is *Lyapunov stable* if for any neighbourhood U of S there exists a neighbourhood $V \subseteq U$ of S such that all trajectories starting in V remain in U for all forward time. A flow-invariant set S is *asymptotically stable* if it is Lyapunov stable and there exists a neighbourhood V of S such that all trajectories with initial condition in V converge to S in forward time.

2.2 Overview of existing definitions

There are several definitions of the concept of heteroclinic cycle in the literature Ashwin [3], Ashwin and Field [4], Field [15], Kirk and Silber [30], Krupa and Melbourne [34], Krupa [33], Melbourne *et al* [37]. Essentially, all of them consider a *heteroclinic cycle* as a cycle of connections between ordered compact flow invariant sets usually called nodes. A heteroclinic connection between two consecutive nodes is a trajectory contained in the intersection of the unstable manifold of one node with the stable manifold of the next node.

Some definitions restrict the nodes to hyperbolic equilibria ([3], [30],[34], [33]), while others generalize to any flow invariant sets such as periodic trajectories or even chaotic sets ([4], [15], [37]).

In general, the definitions of heteroclinic cycle make no reference to the dimension of the set of heteroclinic connections between two nodes. However, the simplest and perhaps the most studied situation is that of heteroclinic cycles with one dimensional connections. In [3], Ashwin and Chossat study robust heteroclinic cycles with continua of connections. In [9] Chossat *et al* introduce the term *generalized heteroclinic cycle* to distinguish heteroclinic cycles having sets of connections with dimension greater than one.

In the context of equivariant dynamics, Melbourne *et al* [37] define heteroclinic cycle as a cycle of trajectories that start at a node and end at a conjugate of that node.

The context of equivariant dynamics has the particularity that, if there is a heteroclinic connection between two nodes, there is a conjugate heteroclinic connection between the conjugate of those nodes. Moreover, it is common to ask all trajectories along the unstable manifold of one node to be captured by the group orbit of the stable manifold of some node in the cycle (Dias *et al* [12],Krupa and Melbourne [34]).

The situation where all the nodes in the heteroclinic cycle are conjugated by symmetry is called a *homoclinic cycle* in [3], [37].

In Field and Richardson [18] the orbit of a heteroclinic cycle by the symmetry group is refered to as a *heteroclinic complex*. This is, for example, the case of the heteroclinic cycles in Guckenheimer and Holmes [21].

The concept of heteroclinic complex, more commonly refered to as *heteroclinic network*, has several different definitions in the literature. Nevertheless, in all of them it is described as a collection of heteroclinic cycles. The definitions of Field [15] and Kirk & Silber [30] present a heteroclinic network as a connected finite collection of heteroclinic cycles; any two nodes in the network can be joined by a sequence of heteroclinic connections. The definition in [15] is more general in that it allows heteroclinic cycles in the network to have empty intersection. Nevertheless, it forces every connnection between any two nodes in the network to be contained in the network.

In this sense the definition of *heteroclinic web* of Dias *et al* [12] goes further and forces the unstable manifold of any node in the network to be contained in the union of the stable manifolds of all nodes in the network.

Several definitions of heteroclinic cycle and network emerged according to the particular examples under consideration. To establish a more general definition including all the previously studied cases, Field & Ashwin present in [4] a definition of heteroclinic network that generalizes the definitions of heteroclinic network thus far, and introduce

the concept of depth in the network. They define a heteroclinic network as a flow-invariant set that is indecomposable but not recurrent.

Their definition covers many previously discussed examples of heteroclinic behaviour. As mentioned in [4], it includes the examples of 'cycling chaos' in Ashwin [2], Dellnitz *et al* [10], Field [15] but not the Shilnikov network of Field's example in ([15], appendix *A*) that we study here.

In Field's example, we establish the existence of an invariant set homeomorphic to a Cantor set in the neighbourhood of the Shilnikov network. This means that there is an infinite set of recurrent points in the neighbourhood of the network. This contradicts the existence of a finite nodal set as defined in [4] and thus does not satisfy the definition of heteroclinic network in [4].

2.3 Networks and symmetry

Let $V = \mathbf{R}^n$ and Γ a compact Lie group acting on V. Consider the system of differential equations

$$\frac{dx}{dt} + f(x, \lambda) = 0, \tag{2.1}$$

where $x \in \mathbf{V}$ and $f : \mathbf{V} \times \mathbf{R} \to \mathbf{V}$.

We say that f *commutes* with the action of Γ, or that (2.1) is Γ-*equivariant*, if

$$f(\gamma \cdot x, \lambda) = \gamma \cdot f(x, \lambda) \tag{2.2}$$

for all $\gamma \in \Gamma$, $x \in \mathbf{V}$. The maximal group Γ that commutes with f is referred to as the *symmetry group* of (2.1).

For $x \in V$, we define $\Gamma(x)$, the *orbit* of x by the group Γ, and Γ_x, the *isotropy subgroup* of x respectively, as follows,

$$\Gamma(x) = \{\gamma.x \ : \ \gamma \in \Gamma\} \subset V, \qquad \Gamma_x = \{\gamma \in \Gamma \ : \ \gamma.x = x\} \subset \Gamma.$$

It is an easy but important consequence that if x is a solution of the equivariant system (2.1), so are the elements in its Γ-orbit.

The isotropy subgroup of a solution is the subgroup of the symmetries of that solution.

To each subgroup Σ of Γ we associate the *fixed point subspace*

$$Fix(\Sigma) = \{y \in V \ : \ \sigma.y = y, \forall \sigma \in \Sigma\}.$$

An important property of fixed point subspaces is that they are invariant by the flow of (2.1).

Other concepts and results on equivariant dynamics not defined here can be found in [15], [19] (we draw the reader's attention to some notational differences).

Equivariant systems have the property that if K is a flow invariant set, then so are the sets γK, $\gamma \in \Gamma$ in its group orbit. The sets K and γK are called *conjugate.*

When dealing with heteroclinic cycles and heteroclinic networks in the context of equivariant dynamics, it may be useful to identify points in the same group orbit.

We consider a compact manifold M, a compact Lie group Γ and a Γ-equivariant flow on M, ϕ.

In the next paragraphs we discuss how, using the action of Γ on M we can reduce the phase space M to the orbit space M/Γ by identifying points in the same group orbit, and define a smooth flow on M/Γ corresponding to ϕ. Then we show that a heteroclinc cycle or network of ϕ on M transforms by the reduction to a heteroclinic cycle or network of the reduced flow on M/Γ. These results will be used later, in section 3.4, in Field's example.

Given $x, y \in M$ we define the equivalence relation:

$$x \sim y \iff x \text{ and } y \text{ are in the same group orbit.}$$

Define the set M/Γ of the equivalence classes, i.e., the set of the orbits of Γ on M. We denote by $[x] = \Gamma(x)$ the equivalence class of $x \in M$.

The set M/Γ endowed with the quotient topology is called the *orbit space* of M (with respect to Γ). See Bredon [7], chapter I, section 3. Let $\pi : M \to M/\Gamma$ denote the continuous map that takes each element x of M into its equivalence class $[x]$.

In general M/Γ is no longer a differentiable manifold. Nevertheless, the group orbits of differentiable group actions are differentiable manifolds ([7], chapter VI, section 1).

A differentiable flow on M does not need to induce a differentiable flow on M/Γ. However, by the Smooth Lifting Theorem (theorem 0.2) in Schwarz [40], this is true when Γ is a compact Lie group. More precisely, the Smooth Lifting Theorem (theorem 0.2 in [40]) states that for each smooth Γ-equivariant vector field on M, there is a corresponding smooth strata-preserving vector field on M/Γ. (For a definition of strata-preserving differentiable vector fields, see [40].)

Definition 5 *Let $\{\phi_t : t \in \mathbf{R}\}$ be a flow of a Γ-equivariant system of differential equations on M. Each map ϕ_t induces on the orbit space M/Γ the map,*

$$\begin{array}{rccc} \phi_t^q: & X/\Gamma & \to & X/\Gamma \\ & \phi_t^q \circ \pi & = & \pi \circ \phi_t. \end{array} \tag{2.3}$$

The function $\phi^q(t,.) = \phi_t^q$ in M/Γ is called the quotient flow.

Next we prove that, a heteroclinic network on M, invariant by a flow ϕ on M, induces a heteroclinic network on M/Γ, invariant by the quotient flow ϕ^q on M/Γ.

Lemma 6 *Let Σ be a heteroclinic cycle determined by a finite (ordered) set of invariant saddles $\mathcal{A} = \{A_i : i = 0, ..., n-1\}$. Then Σ/Γ is a collection of heteroclinic cycles (with nonempty intersection) associated to the set $\mathcal{A}/\Gamma$, and is given by*

$$\Sigma/\Gamma = \cup_{i=0}^{k-1}[A_i] \cup (W^u([A_i]) \cap W^s([A_{i+1}])),$$

where k is the number of equivalence classes in $\mathcal{A}/\Gamma$.

Proof: The elements B_i of $\mathcal{A}/\Gamma$ are the equivalence classes, $[A_j]$, of the elements in $\mathcal{A}$. Each element of $\mathcal{A}/\Gamma$ is the subset of the elements in $\mathcal{A}$ that are in the same group orbit.

Consider the order relation in $\mathcal{A}/\Gamma$ defined by

$$B_i < B_j \quad \text{if} \quad \exists A_k \in B_i, A_l \in B_j \quad \text{such that} \quad W^u(A_k) \cap W^s(A_l) \neq \emptyset. \tag{2.4}$$

Let $\mathcal{B}_1, ..., \mathcal{B}_r$ be the maximal subsets of $\mathcal{A}/\Gamma$ where the order relation defined above is univocally determined, and $\cup_p \mathcal{B}_p = \mathcal{A}/\Gamma$.

We show that each $\mathcal{B}_i$ determines a heteroclinic cycle Σ_i. Let $\mathcal{B}_i = \{B_j : j = 0, ..., m-1\}$. We have

$$B_j < B_{j+1} \quad \forall j = 0, ..., m-2 \ (\text{mod } m),$$

which is equivalent, by (2.4), to

$$W^u(B_j) \cap W^s(B_{j+1}) \neq \emptyset \quad \forall j = 0, ..., m-2 \ (\text{mod } m).$$

It remains to show that $W^u(B_{m-1}) \cap W^s(B_0) \neq \emptyset$. If $W^u(B_{m-1}) \cap W^s(B_1) = \emptyset$, then we would have

$$\forall A_k \in B_{m-1}, A_l \in B_0, \ W^u(A_k) \cap W^s(A_l) = \emptyset.$$

Since Σ is a heteroclinic cycle determined by $\mathcal{A}$, there would be B_s and $A_r \in B_s$ such that $W^u(A_k) \cap W^s(A_r) \neq \emptyset$. Then, we would have $B_{m-1} < B_s$, and so, $\mathcal{B}_i$ would not be a maximal subset of $\mathcal{A}/\Gamma$ where the defined order relation is univocally determined.

We must then conclude that $W^u(B_{m-1}) \cap W^s(B_0) \neq \emptyset$ and that each $\mathcal{B}_i$ determines a heteroclinic cycle Σ_i. Then

$$\Sigma/\Gamma = \cup_i^r \Sigma_i = \cup_{i=0}^{k-1} [A_i] \cup (W^u([A_i]) \cap W^s([A_{i+1}])),$$

where k is the number of equivalence classes in $\mathcal{A}/\Gamma$. □

Lemma 7 *Let $\Sigma \subset M$ be a heteroclinic network with a set of invariant saddles $\mathcal{A}$. Then Σ/Γ is a heteroclinic network with set of invariant saddles $\mathcal{A}/\Gamma$.*

Proof: Let B_i be the elements of $\mathcal{A}/\Gamma$, that are the equivalence classes, $[A_j]$, of the elements in $\mathcal{A}$.

Since Σ is a heteroclinic network there is a finite set of ordered nonempty subsets $\mathcal{A}_j$ of $\mathcal{A}$ such that each $\mathcal{A}_j$ determines a heteroclinic cycle Σ_j. By the previous lemma there are subsets $\mathcal{B}_{jk}$ of $\mathcal{A}_j/\Gamma$ such that $\cup_k \mathcal{B}_{jk} = \mathcal{A}_j/\Gamma$, each $\mathcal{B}_{jk}$ determines a heteroclinic cycle Σ_{jk} and $\cup_k \Sigma_{jk} = \Sigma_j/\Gamma$.

Assume $W^u(B_m) \cap W^s(B_n) \neq \emptyset$, then $\exists A_k \in B_m, A_l \in B_n$ such that $W^u(A_k) \cap W^s(A_l) \neq \emptyset$. Since Σ is a heteroclinic network $\exists j$ such that $W^u(A_k) \cap W^s(A_l) \in \Sigma_j$. Then $\exists k$ such that $W^u(B_m) \cap W^s(B_n) \in \Sigma_{jk}$.

Since Σ is a heteroclinic network, we have $\cup_j \mathcal{A}_j = \mathcal{A}$. This implies $\cup_j \mathcal{A}_j/\Gamma = \mathcal{A}/\Gamma$, which is equivalent to $\cup_j \cup_k \mathcal{B}_{jk} = \mathcal{A}/\Gamma$.

We conclude that there is a finite set of (ordered) nonempty sets $\mathcal{B}_{jk}$ of $\mathcal{A}/\Gamma$ such that

(A) Each $\mathcal{B}_{jk}$ determines a heteroclinic cycle Σ_{jk}.

(B) $\Sigma/\Gamma = \cup_j \cup_k \Sigma_{jk}$.

(C) If $W^u(b_k) \cap W^s(b_l) \neq \emptyset$ then, there exists j such that $W^u(b_k) \cap W^s(b_l) \subset \Sigma_{jk}$.

(D) $\cup_j \cup_k \mathcal{B}_{jk} = \mathcal{A}/\Gamma$

Thus, we conclude that Σ/Γ is a heteroclinic network with set of invariant saddles $\mathcal{A}/\Gamma$. □

Definition 8 *Given a heteroclinic network* Σ *we call* Σ/Γ *the* quotient heteroclinic network *of* Σ *by* Γ.

Analogously to the case of heteroclinic networks, we can define *quotient heteroclinic cycle* and *quotient heteroclinic subnetwork.*

Note that, in general, there is no way of getting a heteroclinic network Σ from its quotient network Σ/Γ: suppose there is a connection $[A_i] \to [A_j]$ in Σ/Γ. Then there is in Σ a connection $A_i \to \gamma A_j$ for some $\gamma \in \Gamma$. This connection does not necessarily exist for all $\gamma \in \Gamma$. Further, if we only know Σ/Γ, there is no way of deciding for which γ the connection exists.

Nevertheless, it is possible to define heteroclinic subnetworks Υ of Σ such that its group orbit by Γ is Σ. We call them *representative heteroclinic subnetworks.*

Chapter 3

Field's Example

The starting point for the work in this thesis is an example with interesting dynamics, presented and studied in appendix A of Field [15]. We describe this example in the next two sections.

In the first section we mention the results in [15] that are relevant for our study. We describe Field's conjecture on the existence of chaotic behaviour due to the possible existence of a Shilnikov heteroclinic network.

Then in section 3.2 we describe our numerical simulations and show how they provide strong evidence of the existence of a Shilnikov heteroclinic network in the dynamics of the example.

In section 3.3 we charaterize the heteroclinic network using the definitions in chapter 2 and in section 3.4 we outline the rest of the thesis.

3.1 Description, previous results and Field's conjecture

For a more detailed explanation of the contents of this section see [15], appendix A.

Consider the family of differential equations in $\mathbf{R}^4$,

$$\begin{cases} \dot{x}_1 &= \lambda x_1 - ||x||^2 x_1 + \beta(x_1^2 x_2 - y_1^2 x_2 - 2x_1 y_1 y_2) + \gamma(x_2^3 - 3x_2 y_2^2) \\ \dot{y}_1 &= \lambda y_1 - ||x||^2 y_1 + \beta(-x_1^2 y_2 + y_1^2 y_2 - 2x_1 y_1 x_2) + \gamma(-y_2^3 + 3x_2^2 y_2) \\ \dot{x}_2 &= \lambda x_2 - ||x||^2 x_2 + \beta(x_1 x_2^2 - x_1 y_2^2 + 2y_1 x_2 y_2) + \gamma(x_1^3 - 3x_1 y_1^2) \\ \dot{y}_2 &= \lambda y_2 - ||x||^2 y_2 + \beta(y_1 x_2^2 - y_1 y_2^2 - 2x_1 x_2 y_2) + \gamma(y_1^3 - 3x_1^2 y_1) \end{cases} . \quad (3.1)$$

Identifying $\mathbf{R}^4 \approx \mathbf{C}^2$ we may rewrite the equations in complex coordinates (z_1, z_2) where $z_j = x_j + iy_j, j = 1, 2$. With this notation, the family (3.1) is equivariant by the compact Lie group Γ generated by,

$$s(z_1, z_2) = (\omega z_1, \omega^2 z_2), \quad (3.2)$$

$$t(z_1, z_2) = (\overline{z}_2, z_1), \quad (3.3)$$

$$-I_V(z_1, z_2) = (-z_1, -z_2), \quad (3.4)$$

where $\omega = e^{\frac{2\pi i}{5}}$.

Lemma 9 ([15], A.7) *Representative proper fixed point spaces of* $(\mathbf{C}^2, \Gamma)$ *are given by*

(A) $\mathbf{A} = \{(x_1, 0, x_1, 0) : x_1 \in \mathbf{R}\} = Fix((t))$ *(axis of symmetry).*

(B) $\mathbf{B} = \{(x_1, 0, -x_1, 0) : x_1 \in \mathbf{R}\} = Fix((-t))$ *(axis of symmetry).*

(S) $\mathbf{S} = \{(x_1, 0, x_2, 0) : x_1, x_2 \in \mathbf{R}\} = Fix((t^2))$ *(submaximal stratum).*

(P) $\mathbf{P} = \{(0, y_1, 0, y_2) : y_1, y_2 \in \mathbf{R}\} = Fix((-t^2))$ *(maximal orbit stratum) and we have* $N((-t^2))/(-t^2) \cong \mathbf{Z}_4$.

There are exactly five axes of type (A), *five axes of type* (B), *five planes of type* (S) *and five planes of type* (P). *There are no three dimensional fixed point subspaces.*

From now on we fix parameter values as follows:

$$\lambda > 0, \quad \gamma < 0, \quad \beta > 0, \quad \gamma + 3\beta > 0 \quad \text{and} \quad |\beta + \gamma| < 2.$$

For these parameter values, by the result in lemma $A.10$ of [15] (taking $\alpha = -1$), the cubic term of (3.1) is contracting and we can apply the Invariant Sphere Theorem, Field [14], Field [15] to reduce the dynamics of (3.1) to an invariant three-dimensional

sphere that is globally attracting in the sense that every trajectory which does not contain the trivial equilibrium is forward asymptotic to it. Consequently, we restrict our attention to the flow on the topological sphere.

The following results on the dynamics on the fixed-point spaces, for the chosen parameter values, are relevant for later chapters:

- There is a pair of equilibria $\pm a(\lambda)$ on the axis **A** and a pair of equilibria $\pm b(\lambda)$ on the axis **B**. We have that $\pm a(\lambda)$ and $\pm b(\lambda)$ are the only nontrivial equilibria on **S** ([15], lemma A.11).

- For the flow restricted to **S**, the points $\pm b(\lambda)$ are sinks, $\pm a(\lambda)$ are saddles and there is a one-dimensional connection from $\pm a(\lambda)$ to $\pm b(\lambda)$ ([15], lemma A.14).

- The connection from $\pm a(\lambda)$ to $\pm b(\lambda)$ is contained in the invariant sphere. In the restriction to the invariant sphere, $\dim(W^u(b(\lambda))) = 2$ and $\dim(W^s(a(\lambda))) = 3$ and $W^u(b(\lambda))$ and $W^s(a(\lambda))$ are transverse to the plane **S** ([15], lemma A.14). See figure 3.1 (copy of figure 11 in Field [16]).

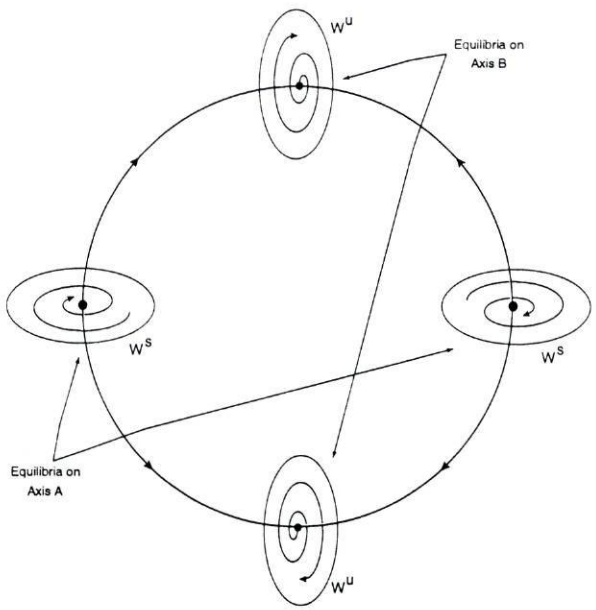

Figure 3.1: Dynamics of Field's example near the plane **S** (copy of figure 11 in [16])

- There are no nontrivial equilibria on the plane **P** ([15], proposition A.15). There is a periodic trajectory, $c(\lambda)$, obtained from the intersection of **P** and the invariant three-sphere, that attracts all points in $\mathbf{P} - \{0\}$.

- By lemma A.19 in [15] the equilibria in $[a] = \{\pm s^n a,\ n = 0, ..., 4\}$, the equilibria in $[b] = \{\pm s^n b,\ n = 0, ..., 4\}$ and the origin are the only equilibria of (3.1), where s is the element of Γ defined in (3.2).

Similar dynamics occur in the conjugates of fixed point spaces by the group Γ.

For the parameter values we are considering we expect to find heteroclinic phenomena connecting the equilibria in $[a]$ and $[b]$, and even the periodic trajectories on the plane $\mathbf{P}$, in the flow restricted to the invariant three-sphere.

Figures 3.2 and 3.3, obtained using the dynamical systems package Dstool, Guckenheimer *et al* [22], [23], [24], [25], are an evidence of the complex dynamics in Field's example, for the parameter values considered.

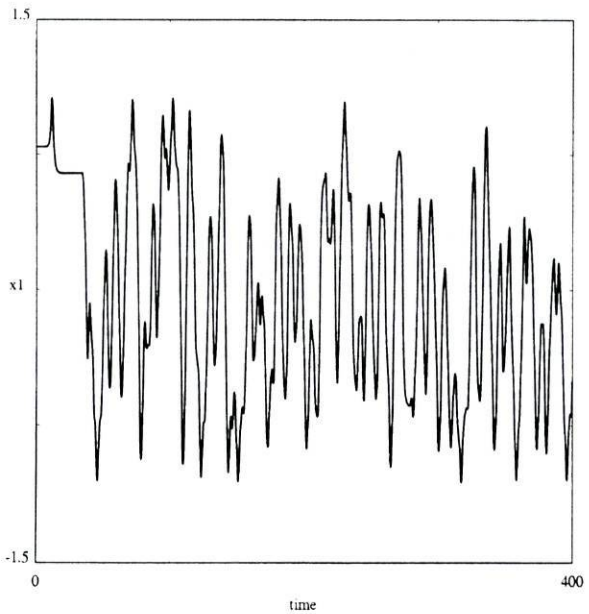

Figure 3.2: Time series for x_1 of a trajectory in Field's example when $\lambda = 1$, $\beta = 1$ and $\gamma = -0.6$

Field conjectures that,

Conjecture 10 *The Γ-orbit of $W^u(b(\lambda))$ intersects the Γ-orbit of $W^s(a(\lambda))$ transversely, and therefore the intersection is persistent.*

Conjecture 11 *Assuming the hyperbolicity of the periodic trajectory, there are also transverse intersections of the invariant manifolds of the periodic trajectories and of the invariant manifolds of the equilibria and periodic trajectories.*

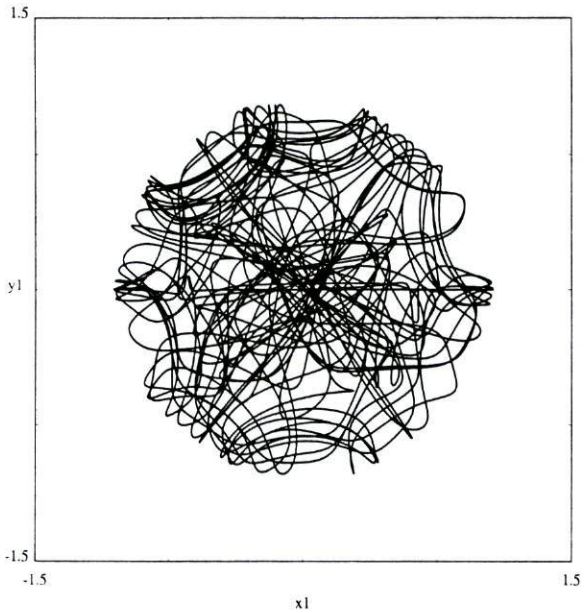

Figure 3.3: Projection in the (x_1, y_1)-plane of a trajectory in Field's example, when $\lambda = 1$, $\beta = 1$ and $\gamma = -0.6$

Conjecture 10 is enough to produce a Shilnikov network of heteroclinic cycles. Both conjectures lead to complicated dynamics.

3.2 Numerical study and definition of the heteroclinic network

For the rest of the thesis we assume $\lambda = 1$ fixed and we omit references to λ in the text.

In this section we describe the numerical evidence supporting Field's conjecture. The search for the analytical proof of the conjecture produced the work in the remaining chapters.

In our numerical study we used the dynamical systems package Dstool [22], [23], [24], [25]. Our procedure was based on the fact that asymptotically stable heteroclinic phenomena are related to nontransient intermittent behaviour: a trajectory in the neighbourhood of a heteroclinic cycle or network will move from one invariant saddle to the next *ad infinitum* spending a long time near each invariant saddle.

In our Dstool specification of Field's example we incorporated a C-routine. For each Dstool computation of a trajectory, with given initial conditions, the C-routine gives as output a sequence that identifies the invariant saddles near the trajectory.

Specifically, in the Dstool specification we consider a neighbourhood of each invariant equilibrium and periodic trajectory. At each Dstool iteration the C-routine inspects if the actual position in the phase space is within any of the neighbourhoods and in that case it prints the identification of the corresponding equilibrium or periodic trajectory and the distance in each coordinate between the actual position and that of the invariant saddle.

Appendix A contains the Dstool specification of the example and a more careful explanation of how the C-routine, `field_aux()`, works.

The sequences produced by the C-routine running Dstool, exhibit evidence of the existence of the following connections:

- from $\pm b$ to $\pm s^n(a)$ with $n \neq 0$,
- from $\pm b$ to $s^n(c)$,
- from c to $\pm s^n(a)$,
- from c to $s^n(c)$ with $n \neq 0$,

with $n \in \mathbf{Z}(mod\ 5)$ and s the element of Γ defined in (3.2).

Note that we do not know the dimension of these connections. This seems to be impossible to determine numerically.

Applying the symmetry to the connections found numerically, we obtain the following connections,

- from $s^k(\pm b)$ to $s^k(\pm s^n(a))$ with $n \neq 0$,
- from $s^k(\pm b)$ to $s^k(s^n(c))$,
- from $s^k(c)$ to $s^k(\pm s^n(a))$,
- from $s^k(c)$ to $s^k(s^n(c))$ with $n \neq 0$,

with $k, n \in \mathbf{Z}(mod\ 5)$ and s the element of the symmetry group Γ defined in (3.2).

In each fixed point subspace $s^k(\mathbf{S})$ conjugate to the plane $\mathbf{S}$ there are also the connections, found analitically by Field [15],

- from $s^k(\pm a)$ to $s^k(\pm b)$,

with $k \in \mathbf{Z}(mod\ 5)$ and s the element of the symmetry group Γ defined in (3.2).

Since the symmetry group has finite order there exist sequences of connections beginning and ending at the same equilibrium point or periodic trajectory. This supports the existence of a Shilnikov network of heteroclinic cycles involving equilibria and periodic trajectories and with the invariant manifolds with dimension ≥ 2 intersecting transversely, as conjectured by Field. We denote this network by Σ.

The periodic trajectory on plane $\mathbf{P}$ may be a hyperbolic saddle with either two- or three-dimensional unstable manifold. Numerical computations with GAIO, Dellnitz *et al* [11], Junge [29] indicate that the unstable manifold of the periodic trajectory is two-dimensional.

Numerical computations with GAIO further support the existence of a transverse intersection of the invariant manifolds with dimension ≥ 2 of the equilibria and periodic trajectories in Σ. With this transverse intersection as a hypothesis we prove the existence of horseshoe dynamics leading to the chaotic behaviour we observe numerically.

3.3 Structure and symmetry of the heteroclinic network

The network Σ has a lot of structure and symmetry and we characterize it using the concepts in chapter 2. At the same time we give a general overview of how we are going to study the local dynamics in the neighbourhood of the network based on its properties.

As we have seen in the last chapter the invariant saddles in the network can be either equilibria or periodic trajectories. There are three equivalence classes of invariant saddles, $[a]$, $[b]$ and $[c]$, which correspond, respectively, to the set of equilibria conjugate to equilibrium a, the set of equilibria conjugate to equilibrium b and the set of periodic trajectories conjugate to periodic trajectory c.

There are heteroclinic connections from elements in $[a]$ to elements in $[b]$, from elements in $[b]$ to elements in $[a] \cup [c]$ and from elements in $[c]$ to elements in $[a] \cup [c]$.

Thus, there are heteroclinic cycles, and heteroclinic subnetworks, involving only elements in $[a] \cup [b]$, in $[a] \cup [b] \cup [c]$ or in $[c]$. Let us call the subnetwork involving all the equilibria in $[a] \cup [b]$ and all the connections between them, the *maximal subnetwork of equilibria.*

There are some interesting aspects about the subnetworks which we mention next.

We define the *order* of a heteroclinic cycle or network as the number of invariant saddles that it contains.

Proposition 12 *In a heteroclinic network with precisely the connections described in section 3.2, the heteroclinic cycles in a subnetwork of equilibria are of order k with k even and $4 \leq k \leq n$, with n the number of equilibria in the subnetwork.*

Proof: The order of the heteroclinic cycles is even since the heteroclinic connections from equilibria in $[a]$ are only to equilibria in $[b]$ and vice-versa: there is no heteroclinic connection between the equilibria in $[a]$ and no heteroclinic connection between the equilibria in $[b]$.

The minimum order is 4 since there is no heteroclinic connection from $s^n b$ to $s^n a$, $n = 0, ..., 4$. The maximum order is obviously determined by the number of equilibria. □

Using combinatorics we can say that there are 160 heteroclinic cycles of order 4, 1280 of order 6, 9680 of order 8, and so on.

There are heteroclinic cycles in the subnetwork of equilibria with nonempty intersection due to a common equilibrium or to one or more common connections.

Consider a heteroclinic cycle with maximum order, say $e_1 \to e_2 \to e_3 \to ... \to e_{20} \to e_1$, with $e_i \neq e_j$ for all $i, j \in 1, ..., 20$. Assume $e_1 \in [a]$, then $e_2 \in [b]$, $e_3 \in [a]$ ... and $e_{20} \in [b]$.

We can assume e_3 to be such that there is the connection $e_{20} \to e_3$, and consider the heteroclinic cycle given by $e_3 \to e_4 \to e_5 \to ... \to e_{20} \to e_3$. The two heteroclinic cycles have 17 heteroclinic connections in common.

Theorem 13 *In a heteroclinic network with precisely the connections described in section 3.2, two different heteroclinic cycles in the maximal subnetwork of equilibria coincide in, at most,* 17 *heteroclinic connections.*

Proof: This follows from the fact that the maximal subnetwork of equilibria is of order 20, and the heteroclinic connections from equilibria in $[a]$ are only to equilibria in $[b]$ and vice-versa.

Suppose there were two such cycles, and that the common heteroclinic connections were $e_1 \to e_2 \to e_3 \to ... \to e_{19}$, with $e_i \neq e_j$ for all $i, j \in 1, ..., 19$. Assume, without lost of generality, that $e_1 \in [a]$. Then $e_{19} \in [a]$, and the remaining equilibrium, e_{20} is in $[b]$. So, the remaining heteroclinic connections in the heteroclinic cycles have to be $e_{19} \to e_{20} \to e_1$. This is absurd because, by hypothesis, the two heteroclinic cycles are different. □

To simplify our description we refer to trajectories close to the network as *paths along the network*. We use $A_i \to A_j$ to denote that there is a path from the invariant saddle A_i to the invariant saddle A_j and in fact this means that there is a segment of a trajectory close to A_i, that later becomes close to A_j, and in the meanwhile does not become close to any other invariant saddle. We say that a segment of a trajectory is a *closed path* if it starts close to, and ends close to the same invariant saddle of the network but does not intersect the invariant saddle.

An important property of the network Σ is that paths that are in the same group orbit induce local dynamics that are essentially the same up to symmetry. To exemplify,

consider the closed paths $a \to b \to sa \to sb \to a$ and $sa \to sb \to s^2a \to s^2b \to sa$. The essential difference is in the identification of the nodes of the network that are "visited" by the path.

It is possible to find subnetworks of Σ whose orbit by the symmetry group is the network Σ. We call such a network a *representative subnetwork*. See Figure 3.4 for an example of a representative subnetwork of Σ.

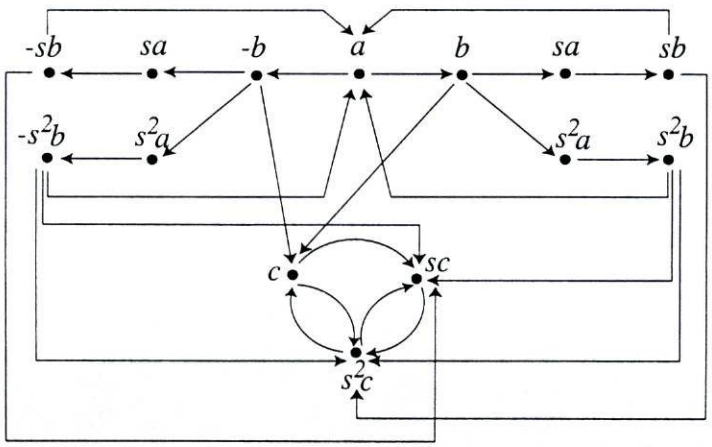

Figure 3.4: Example of a representative subnetwork of the heteroclinic network Σ in Field's example.

We can go further and say that the local dynamics induced by a visit to the closed path $a \to b \to sa \to sb \to a$ is essentially the same as the local dynamics induced by two visits to the closed path $a \to b \to a$, modulus the record of the identification of the nodes visited during the path. Nevertheless, the closed path $a \to b \to a$ is not a path along the heteroclinic network Σ, nor in a representative subnetwork. It is a path on the quotient heteroclinic network Σ/Γ.

The observations above motivated our approach to the study of the local dynamics in the neighbourhood of the network Σ. We use a codification of the dynamics along the heteroclinic network Σ and a codification of the local dynamics in the neighbourhood of the quotient network Σ/Γ to characterize the local dynamics in the neighbourhood of the heteroclinic network Σ.

Let us define the quotient heteroclinic network Σ/Γ. The invariant saddles are the equivalence classes $[a]$, $[b]$ and $[c]$. The heteroclinic connections from the equilibria in $[a]$ to the equilibria in $[b]$ are conjugated, that is, are in the same group orbit. Thus, their quotient by the symmetry group Γ is a heteroclinic connection by the quotient

flow from $[a]$ to $[b]$. The same does not happen, for example, with the heteroclinic connections from the equilibria in $[b]$ to the equilibria in $[a]$. We know, for example, that there is at least one heteroclinic connection from $\pm b$ to $\pm s^n a$ with $n \neq 0$. Then in the quotient flow there is a heteroclinic connection from $[b]$ to $[a]$ for each one of these connections. In fact, we have at least eight connections from $[b]$ to $[a]$.

In our study we consider that there is only one heteroclinic connection from $[b]$ to $[a]$. This seems to be no problem since this information is recovered later using the dynamics along the network Σ. Moreover, as we have already mentioned, we were not able to detect numerically the number of heteroclinic connections from $\pm b$ to $\pm s^n a$ with $n \neq 0$.

Figure 3.5 is a representation of the quotient heteroclinic network Σ/Γ. Looking at figure 3.5 we can easily see that Σ/Γ is the union of three heteroclinic cycles, represented in figure 3.6, namely a heteroclinic cycle involving only the equivalence classes of the equilibria, a heteroclinic cycle involving all the equivalence classes, and a homoclinic cycle to the equivalence class of the periodic trajectories. We call these heteroclinic cycles the *quotient heteroclinic cycles.*

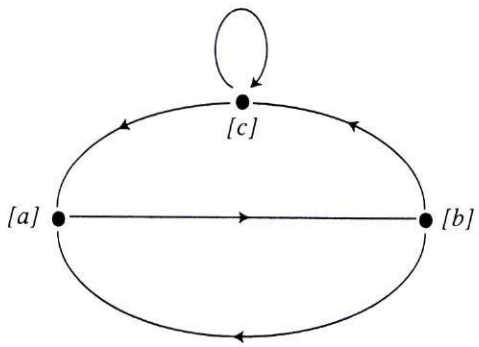

Figure 3.5: Quotient heteroclinic network Σ/Γ of the heteroclinic network Σ in Field's example.

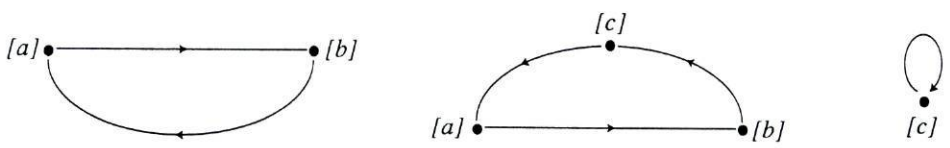

Figure 3.6: Quotient heteroclinic cycles of the quotient heteroclinic network Σ/Γ.

Instead of studying the local dynamics in the neighbourhood of the quotient network

we study the local dynamics in the neighbourhood of each of the quotient heteroclinic cycles. The heteroclinic cycles are the minimum paths in the network that can give rise to complex dynamics.

Our approach to characterize the local dynamics in the neighbourhood of the heteroclinic network Σ is to study the local dynamics in the neigbourhood of each of the quotient heteroclinic cycles and then compose those dynamics using a codification of the dynamics along the network Σ.

3.4 Overview of the rest of the thesis

In the next chapter, we start by constructing examples, each containing part of the complex behaviour that we observe in Field's example. We construct two four--dimensional systems with heteroclinic cycles topologically equivalent to quotient heteroclinic cycles in Σ/Γ. In both examples there is a flow invariant globally attracting three-sphere. In the flow restricted to the sphere there is a structurally stable heteroclinic cycle, with two saddle-foci in the example of section 4.1, and with four saddle-foci and a periodic trajectory in the example of section 4.2. In both examples we prove that, on the sphere, the two-dimensional invariant manifolds of the invariant saddles intersect transversely.

These examples are important for several reasons. They are simple examples with complex dynamics and easy to study analitically. They are a proof that what was conjectured in the case of Field's example can really exist. They are of great help in the study of the dynamics of more complex examples, as is the case of Field's example that we study here.

In section 5.1 we study the local dynamics in the neighbourhood of a generic heteroclinic cycle topologically equivalent to the quotient heteroclinic cycle in Σ/Γ involving the equivalence classes of equilibria and we find conditions for horseshoe dynamics. This establishes the existence of local horseshoe dynamics in one of the examples we construct. In section 5.2 we establish the existence of horseshoe dynamics in the neighbourhood of a generic homoclinic orbit topologically equivalent to the orbit homoclinic to the equivalence class of periodic trajectories in Σ/Γ.

In section 6.1 we define symbolic dynamics that codifies the dynamics along the network Σ, and finally in section 6.2 we define symbolic dynamics that codifies the dynamics in the neighbouhood of the network.

The approach of structuring the study of the local dynamics in the neighbourhood of the heteroclinic network Σ, not only makes it easier, but also has the advantage of allowing to say more than just that there is horseshoe dynamics in the neighbourhood of the network. We conclude that there is also horseshoe dynamics in the neighbourhood of the heteroclinic cycles in the network and so the final conclusion in section 6.2 is that in the neighbourhood of the network Σ there is a horseshoe of horseshoes.

We conclude that there is an infinity of periodic trajectories and a dense trajectory not only in the neighbourhood of the network Σ but also in the neighbourhood of the heteroclinic cycles in Σ.

Chapter 4

Construction of examples

The examples we construct in this chapter have each of them a feature of the complex dynamics of Field's example discussed in chapter 3, but are simpler. They are helpful in the study of the complex dynamics, of that and other examples, and are also interesting for their own sake, because

- they are simple examples with complicated dynamics,
- we can prove transverse intersection of two-dimensional complex invariant manifolds in many cases,
- they are constructive,
- the techniques used for putting them together can be used generally.

The goal is to define systems that are simple and easy to study, such that we can make a good geometrical and analytical description of their flow.

4.1 Example: heteroclinic cycle with two saddle-foci in $\mathbf{R}^4$

In this section we construct a family of systems in $\mathbf{R}^4$ with a structurally stable heteroclinic cycle involving two saddle-foci with a pair of complex eigenvalues and with the invariant manifolds of dimension ≥ 2 intersecting transversely.

We define *saddle-focus* as a saddle having at least one pair of complex eigenvalues.

We look for systems with a globally attracting invariant compact manifold where we can capture the dynamics. A good choice for that manifold is an invariant sphere.

As we want to have a heteroclinic cycle connecting two saddle-foci, the invariant sphere must be at least three-dimensional. So, we construct the examples in $\mathbf{R}^4$ with an invariant three-dimensional sphere.

The construction of the final system comprizes two essential steps. We start with a system whose flow restricted to the three-dimensional sphere has an asymptotically stable heteroclinic cycle between two saddle-foci connected by an invariant two-dimensional sphere. We then find symmetry-breaking terms that preserve the three-dimensional sphere while destroying the connecting two-dimensional sphere into a transverse intersection of the two-dimensional invariant manifolds. The final system, perturbed by the symmetry-breaking terms, possesses the desired dynamics.

We also analize the different dynamics for some symmetry-breaking terms that preserve the three-sphere.

4.1.1 Construction of the unperturbed system

We want to define a system in $\mathbf{R}^4$ satisfying:

(C1) There is a three-dimensional sphere, $\mathbf{S}^3_r$, that is invariant by the flow and globally attracting, in the sense that every trajectory with nonzero initial condition is asymptotic to the sphere in forward time.

(C2) On the invariant three-sphere, the system has an asymptotically stable heteroclinic cycle involving two saddle-foci, p_{w_-}, p_{w_+}. The invariant manifolds of the equilibria satisfy, on the invariant sphere, $W^s(p_{w_-}) = W^u(p_{w_+})$ and $W^s(p_{w_+}) = W^u(p_{w_-})$. One of the connections is one-dimensional, the other two-dimensional. The two-dimensional connection coincides with $\mathbf{D} - \{p_{w_-}, p_{w_+}\}$, with $\mathbf{D}$ a two-dimensional sphere.

(C3) The system has no equilibria other than the origin, p_{w_-} and p_{w_+}.

(C4) The system has two hyperbolic periodic trajectories, each in one connected component of $\mathbf{S}^3_r \backslash \mathbf{D}$. On the invariant sphere the periodic trajectories are repelling.

The construction consists in defining a vector field in $\mathbf{R}^3$ that lifts to $\mathbf{R}^4$ by an $SO(2)$--action. Thus the final system has $SO(2)$-symmetry in addition to properties (C1)-(C4).

We construct a three-dimensional system with a two-dimensional invariant globally attracting sphere, $\mathbf{S}^2_r$, which lifts to the three-sphere $\mathbf{S}^3_r$ by the $SO(2)$-action, and a heteroclinic cycle between two saddles with a one-dimensional connection that lifts by the $SO(2)$-action to a two-dimensional connection. We further require the existence of unstable foci that lift to the two repelling periodic trajectories. See figure 4.1.

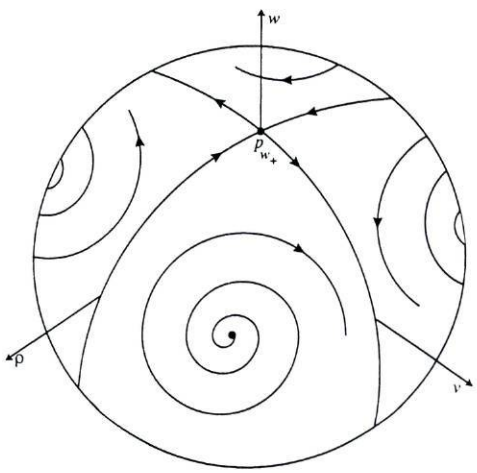

Figure 4.1: Dynamics of the three-dimensional system restricted to the two-sphere $\mathbf{S}^2_r$.

4.1.1.1 Basic example in $\mathbf{R}^3$

In this section we construct an example in $\mathbf{R}^3$ with the desired properties. The properties are easily satisfied in flow invariant spaces. Hence, the example will have some symmetry, since symmetric systems possess natural flow invariant sets, the fixed point spaces. Moreover, the symmetry makes the lifting to $\mathbf{R}^4$ easier.

We consider the compact Lie group G generated by the action of the following elements,

$$\begin{array}{rcl} (\rho, v, w) & \overset{\mathrm{d}}{\mapsto} & (\rho, -v, w), \\ (\rho, v, w) & \overset{\mathrm{q}}{\mapsto} & (-v, \rho, -w). \end{array} \tag{4.1}$$

The action of this symmetry group in $\mathbf{R}^3$ has symmetry planes,

$$\begin{array}{rcl} Fix(d) & = & \{(\rho, v, w) : v = 0\}, \\ Fix(dq^2) & = & \{(\rho, v, w) : \rho = 0\}, \end{array} \tag{4.2}$$

and symmetry axes,

$$\begin{aligned} Fix(q^2) &= \{(\rho, v, w) : \rho = 0,\ v = 0\}, \\ Fix(dq^3) &= \{(\rho, v, w) : \rho = v,\ w = 0\}, \\ Fix(dq) &= \{(\rho, v, w) : \rho = -v,\ w = 0\}. \end{aligned} \tag{4.3}$$

Theorem 14 *Consider the G-equivariant family of vector fields in $\mathbf{R}^3$ with equations given by*

$$\begin{aligned} \dot{\rho} &= \rho(\lambda - Rr^2) - \alpha\rho w + \beta\rho w^2, \\ \dot{v} &= v(\lambda - Rr^2) + \alpha v w + \beta v w^2, \\ \dot{w} &= w(\lambda - Rr^2) - \alpha(v^2 - \rho^2) - \beta w(\rho^2 + v^2), \end{aligned} \tag{4.4}$$

with $r^2 = \rho^2 + v^2 + w^2$.

For $\lambda > 0,\ R > 0,\ \beta < 0,\ \lambda\beta^2 < 8\alpha^2 R,\ |\lambda\beta| < |\alpha\sqrt{\lambda R}|$, and $\alpha \neq 0$ we have:

(a) The two-sphere of radius $r = \sqrt{\frac{\lambda}{R}}$, denoted by $\mathbf{S}^2_r$, is invariant by the flow of (4.4) and globally attracting, in the sense that every trajectory with nonzero initial condition is asymptotic to the sphere in forward time.

(b) On the invariant sphere, the system has an asymptotically stable heteroclinic cycle involving two saddles, p_{w_-} and p_{w_+}. On the invariant sphere, the invariant manifolds of p_{w_-} and p_{w_+} satisfy $W^s(p_{w_-}) = W^u(p_{w_+})$ and $W^s(p_{w_+}) = W^u(p_{w_-})$.

(c) Besides p_{w_-}, p_{w_+} and the origin, system (4.4) has four unstable foci.

(d) System (4.4) has no compact limit sets other than the ones mentioned above.

Moreover, any G-equivariant polynomial vector field of degree 3 in $\mathbf{R}^3$ with the properties above can be obtained from (4.4) by a linear change of coordinates.

Proof: It is trivial to see that system (4.4) is equivariant by the symmetry group G.

Sometimes it is easier to work with system (4.4) in spherical polar coordinates,

$$\begin{aligned} \dot{r} &= r(\lambda - Rr^2), \\ \dot{\theta} &= \alpha r \sin\theta\cos(2\phi) + \tfrac{\beta}{2} r^2 \sin(2\theta), \\ \dot{\phi} &= -\alpha r \cos\theta \sin(2\phi), \end{aligned} \tag{4.5}$$

and thus we use both coordinate systems.

We get (a) easily from the radial equation in (4.5). If $R > 0$ then the sphere of radius $r = \sqrt{\frac{\lambda}{R}}$ is invariant under the flow and, since $\lambda > 0$, it is globally attracting.

The intersection of the invariant sphere with the symmetry axes $Fix(dq^3)$ and $Fix(dq)$ gives the equilibrium points $p_{\rho+v+} = (\frac{r}{\sqrt{2}}, \frac{r}{\sqrt{2}}, 0)$, $p_{\rho-v-} = (-\frac{r}{\sqrt{2}}, -\frac{r}{\sqrt{2}}, 0)$, $p_{\rho+v-} = (\frac{r}{\sqrt{2}}, -\frac{r}{\sqrt{2}}, 0)$ and $p_{\rho-v+} = (-\frac{r}{\sqrt{2}}, \frac{r}{\sqrt{2}}, 0)$. We use $p_{\rho v}$ to refer to these equilibria.

The intersection of the invariant sphere with the symmetry axis $Fix(q^2)$ gives the equilibrium points $p_{w+} = (0, 0, r)$ and $p_{w-} = (0, 0, -r)$. We use p_w to refer to these equilibria.

To see that, for the parameter values that we are considering, there are no equilibria other than the aforementioned and the origin we simply evaluate the zeros of the equations for $\dot{\theta}$ and $\dot{\phi}$. We obtain either $\sin\theta = 0 = \sin(2\phi)$ or $\cos(2\phi) = 0 = \cos\theta$, which correspond to the equilibria p_w and $p_{\rho v}$, respectively.

The non-radial eigenvalues of the linearization of (4.4) at $p_{\rho v}$ are

$$\left(-\lambda\beta \pm \sqrt{\lambda^2\beta^2 - 8\lambda\alpha^2 R}\right)/2R.$$

Since $\lambda > 0$, $R > 0$, $\beta < 0$ and $\lambda\beta^2 < 8\alpha^2 R$, equilibria $p_{\rho v}$ are unstable foci. This proves (c).

The non-radial eigenvalues, in the $(1, 0, 0)$ and $(0, 1, 0)$ directions, of the linearization of (4.4), at p_{w+} are, respectively,

$$\left(\lambda\beta - \alpha\sqrt{\lambda R}\right)/R \quad \text{and} \quad \left(\lambda\beta + \alpha\sqrt{\lambda R}\right)/R,$$

and, at p_{w-} are, respectively,

$$\left(\lambda\beta + \alpha\sqrt{\lambda R}\right)/R \quad \text{and} \quad \left(\lambda\beta - \alpha\sqrt{\lambda R}\right)/R.$$

Since $\lambda > 0$, $R > 0$, $\beta < 0$ and $|\lambda\beta| < |\alpha\sqrt{\lambda R}|$, equilibria p_w are hyperbolic saddle points.

The heteroclinic cycle involving the equilibria p_w is the intersection of the invariant sphere with the symmetry planes. Thus, the heteroclinic cycle coincides with the union of the invariant circles given by the equations $\rho^2 + w^2 = \frac{\lambda}{R}$ and $v^2 + w^2 = \frac{\lambda}{R}$.

We know by the Poincaré-Bendixson theorem [20] that in the flow restricted to the invariant sphere, the ω-limit set of the unstable foci $p_{\rho v}$ can be either a closed trajectory or a heteroclinic loop in the heteroclinic cycle.

We will prove that there are no closed trajectories. We consider system (4.4) as a

perturbation with parameter β of the G-equivariant system

$$\begin{aligned} \dot{\rho} &= \rho(\lambda - Rr^2) - \alpha\rho w, \\ \dot{v} &= v(\lambda - Rr^2) + \alpha v w, \\ \dot{w} &= w(\lambda - Rr^2) - \alpha(v^2 - \rho^2), \end{aligned} \tag{4.6}$$

with $r^2 = \rho^2 + v^2 + w^2$. In spherical polar coordinates, we do $\beta = 0$ in (4.5).

In the dynamics of system (4.6) restricted to the invariant sphere there is the heteroclinic cycle between the saddle points p_w. The equilibria $p_{\rho v}$ are centres and the regions limited by the heteroclinic loops, as we are going to see, are filled with closed trajectories.

The heteroclinic cycle is, as we have already seen, a consequence of the G-symmetry.

Consider

$$f(\rho, v, w) = (\rho - v)^2 + w^2. \tag{4.7}$$

The Lie derivative of f with respect to the vector field v in (4.6), $L_v f$, is zero when $\lambda - Rr^2 = 0$. This means that trajectories of the flow of (4.6) on the invariant sphere move along the closed trajectories that are the intersection of the invariant sphere and the level surfaces of (4.7).

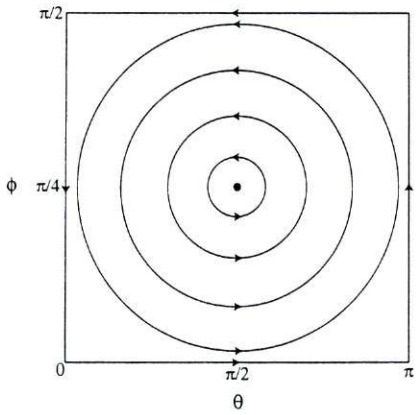

Figure 4.2: Flow of the unperturbed system (4.5,$\beta = 0$) for $\alpha > 0$.

Consider the invariant *fundamental domain* (see [15], chapter 6, section 2) in spherical polar coordinates $(\theta, \phi) \in [0, \pi] \times \left[0, \frac{\pi}{2}\right]$. For the unperturbed system (4.5, $\beta = 0$), the fundamental domain is filled with closed trajectories, see figure 4.2. We will show that for the perturbed system (4.5, $\beta \neq 0$) there is no closed trajectory in this region, and thus, that the unstable foci $p_{\rho v}$ are forward asymptotic to the heteroclinic loop on the boundary of the fundamental domain.

Let s be the segment $\theta = \frac{\pi}{2}$, $\phi \in \left(0, \frac{\pi}{2}\right)$. For $\phi \neq \frac{\pi}{4}$ the segment is transverse to the flow of (4.5) (see figure 4.3).

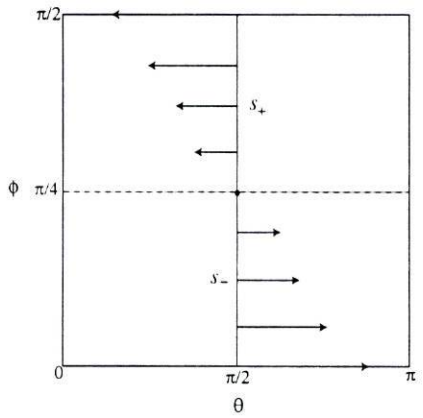

Figure 4.3: The invariant fundamental domain for (4.5) restricted to $r = \sqrt{\frac{\lambda}{R}}$ with $\alpha > 0$. For $\alpha < 0$, the arrows are reversed.

Let s_- be the segment defined by $\theta = \frac{\pi}{2}, \phi \in \left(0, \frac{\pi}{4}\right)$ and s_+ the segment defined by $\theta = \frac{\pi}{2}, \phi \in \left(\frac{\pi}{4}, \frac{\pi}{2}\right)$. We consider an initial condition $p_0 = (\frac{\pi}{2}, \phi_0)$ on the segment s_- and study the return of its trajectory by the flow of system (4.5) to s_-. If this has no fixed-points then there are no closed trajectories.

Note that, in the invariant fundamental domain, we have for the unperturbed system (4.5, $\beta = 0$) with $\alpha > 0$,

- $\dot{\theta} > 0$ and $\dot{\phi} < 0$, for $(\theta, \phi) \in \left(0, \frac{\pi}{2}\right) \times \left(0, \frac{\pi}{4}\right)$;
- $\dot{\theta} > 0$ and $\dot{\phi} > 0$, for $(\theta, \phi) \in \left(\frac{\pi}{2}, \pi\right) \times \left(0, \frac{\pi}{4}\right)$;
- $\dot{\theta} < 0$ and $\dot{\phi} > 0$, for $(\theta, \phi) \in \left(\frac{\pi}{2}, \pi\right) \times \left(\frac{\pi}{4}, \frac{\pi}{2}\right)$;
- $\dot{\theta} < 0$ and $\dot{\phi} < 0$, for $(\theta, \phi) \in \left(0, \frac{\pi}{2}\right) \times \left(\frac{\pi}{4}, \frac{\pi}{2}\right)$.

When $\beta \neq 0$ the perturbation of $\dot{\phi}$ is zero and the perturbation of $\dot{\theta}$ is negative for $\theta \in \left(0, \frac{\pi}{2}\right)$ (on the left of s) and positive for $\theta \in \left(\frac{\pi}{2}, \pi\right)$ (on the right of s).

Let γ_0 be the closed orbit that is the trajectory of p_0 by the flow of the unperturbed system, and γ_β the trajectory of p_0 by the flow of the perturbed system (4.5,$\beta \neq 0$). Let $p_1 = (\frac{\pi}{2}, \phi_1)$ be the first hit of γ_0 with s_+, see figure 4.4. By the above observations we conclude that the trajectory γ_β first hits the segment line s_+ in a point $p_2 = (\frac{\pi}{2}, \phi_2)$ such that $\phi_2 > \phi_1$, see figure 4.4.

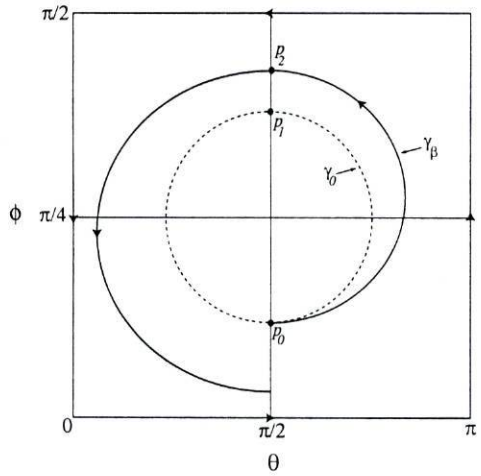

Figure 4.4: Flow of (4.5, $\beta = 0$) (dotted line) and (4.5, $\beta > 0$) (full line), for $\alpha > 0$.

By symmetry, we conclude that the value of the ϕ coordinate for the next hit with s_- of the trajectory of p_0 by the flow of the perturbed system (4.5, $\beta \neq 0$) is less than ϕ_0. This conclusion is independent of the initial condition p_0 we consider in s_-. Therefore there are no fixed points for the return map defined on s_-, and thus there are no closed orbits in the fundamental domain. By symmetry we obtain the same for the rest of the phase space.

This, besides proving that the heteroclinic cycle is the w-limit set of the unstable foci $p_{\rho v}$, proves that there are no other limit sets for the flow of (4.4) other than the heteroclinic cycle. This also proves the asymptotic stability of the heteroclinic cycle, that has also been confirmed by the stability criterion presented by Krupa and Melbourne in [34].

This completes the proof of assertions (b) and (d).

Figure 4.1 above represents a phase portrait for the flow of system (4.4) restricted to the invariant sphere when $\alpha > 0$. For $\alpha < 0$, the arrows on the heteroclinic connections are reversed.

Finally, we prove that, up to a linear change of coordinates, system (4.4) is the only G-equivariant vector field of degree 3 in $\mathbf{R}^3$ satisfying $(a) - (d)$.

It is an easy computation to see that a basis for the space of G-equivariant vector fields of degree 3 in $\mathbf{R}^3$ is given by

$$\begin{array}{llll} (\rho, v, 0), & (0, 0, w), & (\rho w, -vw, 0), & (0, 0, \rho^2 - v^2) \\ (\rho^3, v^3, 0), & (\rho v^2, \rho^2 v, 0), & (0, 0, w(\rho^2 + v^2). & \end{array} \tag{4.8}$$

One of the properties that we want to have is the flow invariance of the two-sphere of radius $r = \sqrt{\frac{\lambda}{R}}$. To force the flow of a vector field have such an invariant sphere we must demand that at each point of the sphere the scalar product of the vector field with a vector ortogonal to the sphere at that point is zero. By imposing this restriction we obtain a system that is linearly equivalent to system (4.4). □

4.1.1.2 Example in $\mathbf{R}^4$ obtained by rotation

Before stating the next theorem, we expand on the properties of (4.4) and the corresponding system in $\mathbf{R}^4$ we are looking for.

System (4.4) has the form

$$\begin{aligned} \dot{\rho} &= \rho F(\rho^2, v, w), \\ \dot{v} &= G_1(\rho^2, v, w), \\ \dot{w} &= G_2(\rho^2, v, w), \end{aligned} \tag{4.9}$$

with $F, G_1, G_2 : \mathbf{R}^3 \to \mathbf{R}$.

If we add the auxiliary equation $\dot{\varphi} = \gamma$, with constant $\gamma \in \mathbf{R}$ and interpret the coordinates (ρ, φ) as polar coordinates, then, in rectangular coordinates,

$$\begin{aligned} x &= \rho \cos\varphi, \\ y &= \rho \sin\varphi, \end{aligned} \tag{4.10}$$

with $\rho^2 = x^2 + y^2$, system (4.4) lifts to a system in $\mathbf{R}^4$ (system (4.16) in the next theorem). The rotation lifting the equations is well defined due to the action of dq^2.

The symmetries of system (4.16) come from the symmetries of system (4.4) and from the rotation used to perform the lift.

The action of d gives rise to the action

$$(x, y, v, w) \overset{\sigma}{\mapsto} (x, y, -v, w). \tag{4.11}$$

From the interpretation of φ as an angle, and the equation $\dot{\varphi} = 1$ we get the following action of $SO(2)$,

$$(x, y, v, w) \overset{\psi}{\mapsto} (x\cos\psi - y\sin\psi, x\sin\psi + y\cos\psi, v, w), \tag{4.12}$$

given by a phase shift $\varphi \mapsto \varphi + \psi$ in the angular coordinate φ.

This is easily seen if we interpret a $\mathbf{Z}_2$-equivariant equation in ρ as the radial coordinate in a polar coordinate system.

Let κ be the following element of $SO(2)$

$$(x, y, v, w) \overset{\kappa}{\mapsto} (-x, -y, v, w). \tag{4.13}$$

The symmetry group of system (4.16) below is isomorphic to $\mathbf{Z}_2(\sigma) \times SO(2) \cong O(2)$.

The action of $\mathbf{Z}_2(\sigma) \times SO(2)$ in $\mathbf{R}^4$ has the following spaces of symmetry,

$$Fix(\mathbf{Z}_2(\sigma)) = \{(x, y, v, w) : v = 0\}, \tag{4.14}$$

$$Fix(SO(2)) = \{(x, y, v, w) : x = 0,\ y = 0\}, \tag{4.15}$$

and

$$Fix(O(2)) = \{(x, y, v, w) : x = 0,\ y = 0,\ v = 0\}.$$

Theorem 15 *Consider the family of $\mathbf{Z}_2(\sigma) \times SO(2)$-equivariant vector fields in $\mathbf{R}^4$ with equations given by*

$$\begin{aligned} \dot{x} &= x(\lambda - Rr^2) - \alpha xw + \beta xw^2 - \gamma y, \\ \dot{y} &= y(\lambda - Rr^2) - \alpha yw + \beta yw^2 + \gamma x, \\ \dot{v} &= v(\lambda - Rr^2) + \alpha vw + \beta vw^2, \\ \dot{w} &= w(\lambda - Rr^2) - \alpha(v^2 - x^2 - y^2) - \beta w(x^2 + y^2 + v^2), \end{aligned} \tag{4.16}$$

with $r^2 = x^2 + y^2 + v^2 + w^2$.

For $\lambda > 0$, $R > 0$, $\beta < 0$, $\lambda\beta^2 < 8\alpha^2 R$, $|\lambda\beta| < |\alpha\sqrt{\lambda R}|$, $\alpha \neq 0$ and $\gamma \in \mathbf{R}$ system (4.16) satisfies conditions (C1)-(C4)in section 4.1.1.

Proof: To prove the result we look at how system (4.4) lifts to system (4.16).

The two-sphere of radius $r = \sqrt{\frac{\lambda}{R}}$, denoted by $\mathbf{S}^2_r$, lifts to the three-sphere of radius $r = \sqrt{\frac{\lambda}{R}}$, denoted by $\mathbf{S}^3_r$ which is invariant by the flow of (4.16) and globally attracting.

Restricted to the sphere, the only compact flow invariant limit sets are a heteroclinic cycle and two hyperbolic periodic trajectories. The periodic trajectories arise from the rotation of the equilibria $p_{\rho v}$ of system(4.4) and are given by

$$x^2 + y^2 = \frac{\lambda}{2R},\ v = \pm\sqrt{\frac{\lambda}{2R}},\ w = 0.$$

As the equilibria $p_{\rho v}$ of (4.4) are repelling in the non-radial directions, on the invariant three-sphere $\mathbf{S}_r^3$ the periodic trajectories of (4.16) are repelling.

The heteroclinic cycle of (4.4) in $\mathbf{S}_r^2$ lifts to a heteroclinic cycle of (4.16) in $\mathbf{S}_r^3$ involving the equilibria $p_{w_+} = (0,0,0,\sqrt{\frac{\lambda}{R}})$ and $p_{w_-} = (0,0,0,-\sqrt{\frac{\lambda}{R}})$ which correspond to the intersection of the invariant three-sphere $\mathbf{S}_r^3$ with the axis $Fix(O(2))$.

By construction, in $\mathbf{S}_r^3$ the stable manifold of p_{w_-} and the unstable manifold of p_{w_+} coincide as do the unstable manifold of p_{w_-} and the stable manifold of p_{w_+}.

The circle $\rho^2 + w^2 = \frac{\lambda}{R}$, invariant under the flow of (4.4), gives rise to a two-sphere of radius $r = \sqrt{\frac{\lambda}{R}}$, invariant under the flow of (4.16), that we denote by $\mathbf{D}$. The two-sphere $\mathbf{D}$ corresponds to the intersection of the hyperplane $Fix(\mathbf{Z}_2(\sigma))$ with $\mathbf{S}_r^3$.

We note that, the rotation that we perform to lift the three-dimensional system (4.4) to system (4.16) does not alter the real part of the eigenvalues.

If $\alpha > 0$, we have that $\mathbf{D} \setminus \{p_{w_-}, p_{w_+}\}$ coincides with the invariant manifolds $W^u(p_{w_-}) \cap \mathbf{S}_r^3$ and $W^s(p_{w_+}) \cap \mathbf{S}_r^3$, see figure 4.5. If $\alpha < 0$, we have that $\mathbf{D} \setminus \{p_{w_-}, p_{w_+}\}$ coincides with the invariant manifolds $W^u(p_{w_+}) \cap \mathbf{S}_r^3$ and $W^s(p_{w_-}) \cap \mathbf{S}_r^3$.

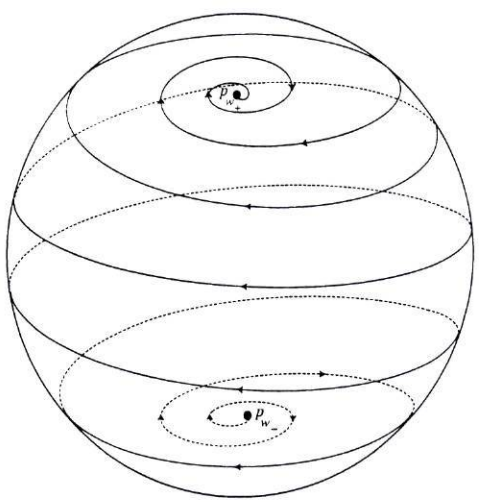

Figure 4.5: Invariant two-sphere $\mathbf{D}$ on $\mathbf{S}_r^3$ that coincides with the two-dimensional heteroclinic connection from p_{w_-} to p_{w_+}, when $\alpha > 0$. (If $\alpha < 0$ the arrows are reversed.)

The one-dimensional connection in the invariant circle $v^2 + w^2 = \frac{\lambda}{R}$ in the flow of (4.4) remains invariant and corresponds to the intersection of $Fix(SO(2))$ with $\mathbf{S}_r^3$, see figure 4.6.

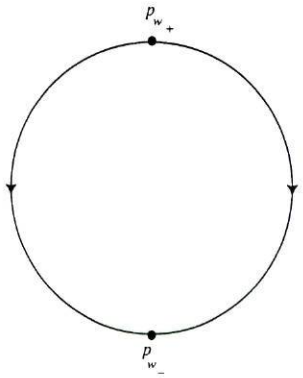

Figure 4.6: The one-dimensional connection from p_{w_+} to p_{w_-} on the invariant circle that is the intersection of of $Fix(SO(2))$ with $\mathbf{S}^3_r$.

The heteroclinic cycle is asymptotically stable since the heteroclinic cycle in the three--dimensional system is asymptotically stable and asymptotic stability is preserved by the rotation. Since the lift by the rotation does not alter the real part of the eigenvalues of the equilibria, the stability criterion of Krupa and Melbourne in [34] still applies.

This ends the proof of (C1)-(C4). □

4.1.2 Useful third-order perturbations

Our aim is to perturb (4.16) in such a way that the two-dimensional manifolds of the equilibria p_{w_-}, p_{w_+} intersect transversely instead of coinciding in $\mathbf{D} - \{p_{w_-}, p_{w_+}\}$. This can be achieved by perturbing the system in such a way that the invariance of $\mathbf{D}$ is broken.

We are interested in the symmetry-breaking perturbations of system (4.16) that preserve the invariance of the three-sphere $\mathbf{S}^3_r$. These are of two types: those that preserve the invariance of the two-sphere $\mathbf{D}$ and those that do not. We distinguish them in different subsections.

Lemma 16 *Consider a family of vector fields in* $\mathbf{R}^4$ *whose flow leaves the three-sphere invariant and globally attracting. The third-order perturbing terms that maintain the invariance and global attraction of the sphere are a linear combination of the following,*

$$
\begin{array}{llll}
(x^2y, -x^3, 0, 0), & (x^2v, 0, -x^3, 0), & (x^2w, 0, 0, -x^3), & (xyv, -x^2v, 0, 0), \\
(xyv, 0, -x^2y, 0), & (0, x^2v, -x^2y, 0), & (xyw, -x^2w, 0, 0), & (xyw, 0, 0, -x^2y), \\
(0, x^2w, 0, -x^2y), & (xvw, 0, -x^2w, 0), & (xvw, 0, 0, -x^2v), & (0, 0, x^2w, -x^2v), \\
(y^3, -xy^2, 0, 0), & (y^2v, -xyv, 0, 0), & (y^2v, 0, -xy^2, 0), & (0, xyv, -xy^2, 0), \\
(y^2w, -xyw, 0, 0), & (y^2w, 0, 0, -xy^2), & (0, xyw, 0, -xy^2), & (yv^2, -xv^2, 0, 0), \\
(yv^2, 0, -xyv, 0), & (0, xv^2, -xyv, 0), & (yw^2, -xw^2, 0, 0), & (yw^2, 0, 0, -xyw), \\
(0, xw^2, 0, -xyw), & (yvw, -xvw, 0, 0), & (yvw, 0, -xyw, 0), & (yvw, 0, 0, -xyv), \\
(0, xvw, -xyw, 0), & (0, xvw, 0, -xyv), & (0, 0, xyw, -xyv), & (v^3, 0, -xv^2, 0), \\
(v^2w, 0, -xvw, 0), & (v^2w, 0, 0, -xv^2), & (0, 0, xvw, -xv^2), & (vw^2, 0, -xw^2, 0), \\
(vw^2, 0, 0, -xvw), & (0, 0, xw^2, -xvw), & (w^3, 0, 0, -xw^2), & (0, y^2v, -y^3, 0), \\
(0, y^2w, 0, -y^3), & (0, yvw, -y^2w, 0), & (0, yvw, 0, -y^2v), & (0, 0, y^2w, -y^2v), \\
(0, v^3, -yv^2, 0), & (0, v^2w, -yvw, 0), & (0, v^2w, 0, -yv^2), & (0, 0, yvw, -yv^2), \\
(0, vw^2, -yw^2, 0), & (0, vw^2, 0, -yvw), & (0, 0, yw^2, -yvw), & (0, w^3, 0, -yw^2), \\
(0, 0, v^2w, -v^3), & (0, 0, w^3, -vw^2), & (xy^2, -x^2y, 0, 0), & (xv^2, 0, -x^2v, 0), \\
(xw^2, 0, 0, -x^2w), & (0, yv^2, -y^2v, 0), & (0, yw^2, 0, -y^2w), & (0, 0, vw^2, -v^2w).
\end{array}
\tag{4.17}
$$

Proof: The proof consists in a sequence of calculations which we merely describe here. We compute the generic third-order perturbing term by considering all linear combinations of monomials of degree three on the variables x, y, v and w. From these, we select those that are tangent to the three-sphere by finding the coefficients of the generic linear combinations which are orthogonal to a basis of the vector space orthogonal to the three-sphere. □

As we have already mentioned our main aim is to perturb (4.16) keeping $\mathbf{S}_r^3$ invariant and breaking the invariance of $\mathbf{D}$ to obtain the transverse intersection of the two--dimensional manifolds of the equilibria p_{w_-}, p_{w_+}.

We also analize, in section 4.1.3.2, the only $SO(2)$-equivariant perturbation and, in section 4.1.4, perturbations that break the symmetry to $\mathbf{Z}_2(\sigma)$ or the trivial symmetry. We note that the behaviour we obtain in sections 4.1.3.2 and 4.1.4 is the same as that for an $O(2)$-equivariant system with a homoclinic cycle when perturbed with the same type of symmetry breaking perturbations (see theorem 1.1 in Chossat and Field [8]).

In [8], Chossat and Field present a new technique for the geometric analysis of the effect of symmetry-breaking perturbations on $O(2)$-equivariant systems with a homoclinic cycle between equilibria on the same $O(2)$-orbit. The technique in [8] seems to be generalizable to $O(2)$-equivariant systems with a heteroclinic cycle as that of the example we construct in section 4.1.1.2.

4.1.3 Third-order perturbations that destroy the invariance of the two-sphere D

The sphere $\mathbf{D}$ is the two-dimensional manifold arising from the intersection of $Fix(\mathbf{Z}_2(\sigma))$ with the three-sphere $\mathbf{S}_r^3$. Thus, a necessary condition for a perturbation that leaves the three-sphere invariant, to break the invariance of $\mathbf{D}$ is to break the invariance of the hyperplane of symmetry $Fix(\mathbf{Z}_2(\sigma))$.

The perturbations that break the invariance of the hyperplane of symmetry $Fix(\mathbf{Z}_2(\sigma))$, break the $\mathbf{Z}_2(\sigma)$-equivariance.

It is clear that breaking the invariance of the two-sphere is necessary for the existence of a transverse intersection of the manifolds in the perturbed system. It is not sufficient as the manifolds could intersect non-transversely in an invariant manifold other than the two-sphere. We claim this does not happen generically. This could happen, for instance, if the invariant hyperplane $Fix(\mathbf{Z}_2(\sigma))$ perturbed into another invariant three-manifold whose intersection with the three-sphere would be the image of the two-sphere under the perturbation.

Lemma 17 *A third-order perturbation of (4.16) that breaks the invariance of the hyperplane $Fix(\mathbf{Z}_2(\sigma))$ while preserving the invariance of the three-sphere consists of*

a linear combination of the $SO(2)$-equivariant term,

$$(0, 0, w^3, -vw^2), \tag{4.18}$$

the $\mathbf{Z}_2(\kappa)$-equivariant terms,

$$\begin{array}{llll} (xvw, 0, -x^2w, 0), & (yvw, 0, -xyw, 0), & (0, xvw, -xyw, 0), & (0, yvw, -y^2w, 0), \\ (0, 0, x^2w, -x^2v), & (0, 0, xyw, -xyv), & (0, 0, y^2w, -y^2v), & \end{array} \tag{4.19}$$

the $\mathbf{Z}_2(\sigma\kappa)$-equivariant terms,

$$(0, 0, xw^2, -xvw), \quad (0, 0, yw^2, -yvw), \tag{4.20}$$

and the terms with trivial isotropy subgroup,

$$\begin{array}{llll} (x^2v, 0, -x^3, 0), & (y^2v, 0, -xy^2, 0), & (vw^2, 0, -xw^2, 0), & (xyv, 0, -x^2y, 0), \\ (0, x^2v, -x^2y, 0), & (0, y^2v, -y^3, 0), & (0, vw^2, -yw^2, 0), & (0, xyv, -xy^2, 0). \end{array} \tag{4.21}$$

Proof: A necessary condition to break the invariance of the hyperplane $Fix(\mathbf{Z}_2(\sigma))$ is to break the equivariance of the vector field by the $\mathbf{Z}_2(\sigma)$-action.

Hence, we determine the perturbing terms that break the invariance of the hyperplane $Fix(\mathbf{Z}_2(\sigma))$ and preserve the invariance of the three-sphere among the perturbing terms that break the $\mathbf{Z}_2(\sigma)$-equivariance and satisfy lemma 16 by direct computation. □

Note that almost all the perturbations in lemma 17 preserve the invariance of the hyperplane $Fix(SO(2))$, and thus the one-dimensional connection in that plane, even when the $SO(2)$-symmetry is broken.

Among the perturbations in lemma 17 we distinguish between $SO(2)$- and non-$SO(2)$--equivariant perturbations.

The fundamental difference between these two types of perturbations is the following: consider a codimension one section, Δ that contains the plane $Fix(SO(2))$ and is transverse to the direction of rotation. The intersection of Δ with the three-dimensional sphere is the two-dimensional sphere $\mathbf{S}^2_r$. Define a first return map R on that two--sphere for the flow of the unperturbed system (4.16) defined in section 4.1.1.2. This first return map R is a discretization of the flow of the three-dimensional system (4.4) defined in section 4.1.1.1, that lifts to system (4.16) by the rotation. Make a perturbation that breaks the invariance of the plane $Fix(\mathbf{Z}_2(\sigma))$. The first return map of the perturbation on $\mathbf{S}^2_r$ breaks the one-dimensional connection between the fixed points p_w on the plane $Fix(\mathbf{Z}_2(\sigma))$. There can be the two following different situations:

(1) the invariant manifolds of the fixed points p_w no longer intersect, and we obtain two attracting periodic orbits on the two-sphere,

(2) the manifolds keep intersecting transversely at infinitely many points and we have what is called a homoclinic tangle.

In the first case the perturbed first return map can be immersed in a three-dimensional flow, but in the second case it cannot.

The perturbed first return map R for the $SO(2)$-equivariant perturbation, can be seen as immersed in the flow of the corresponding "unrotated" perturbed system in $\mathbf{R}^3$. A first return map for a $SO(2)$-equivariant perturbation must be in the situation where the invariant manifolds do not intersect and there are two attracting periodic trajectories. In this case we have an attracting 2-torus invariant by the flow of the perturbed system in $\mathbf{R}^4$, as we prove in section 4.1.3.2.

On the other hand, in the situation where the rotational symmetry is broken we cannot have an invariant 2-torus, and this is the situation where the invariant manifolds may intersect transversely along one-dimensional orbits.

4.1.3.1 Dynamics after $SO(2)$-breaking perturbations

Among the perturbations that break the $SO(2)$-equivariance most preserve the invariance of the plane $Fix(SO(2))$. This implies the persistence of the one-dimensional connection between the equilibria p_w since the connection takes place in the intersection of the plane $Fix(SO(2))$ with the invariant three-sphere.

Among the $SO(2)$-breaking perturbations that preserve the invariance of the plane $Fix(SO(2))$, we choose the following $\mathbf{Z}_2(\sigma\kappa)$-equivariant perturbation,

$$\begin{aligned}
\dot{x} &= x(\lambda - Rr^2) - \alpha xw + \beta xw^2 - \gamma y, \\
\dot{y} &= y(\lambda - Rr^2) - \alpha yw + \beta yw^2 + \gamma x, \\
\dot{v} &= v(\lambda - Rr^2) + \alpha vw + \beta vw^2 + \delta xw^2, \\
\dot{w} &= w(\lambda - Rr^2) - \alpha(v^2 - x^2 - y^2) - \beta w(x^2 + y^2 + v^2) - \delta xvw,
\end{aligned} \tag{4.22}$$

with $r^2 = x^2 + y^2 + v^2 + w^2$.

Note that there are no perturbing terms in the x and y components of the vector field and that the perturbing terms in the v and w components are zero when $w = 0$; this simplifies the computations.

Figure 4.7 represents the time series for the variable v for the flow of the unperturbed system (4.16), for trajectories with initial condition $v > 0$. Note that the trajectories remain in the region $v > 0$. For initial conditions $v < 0$ we get the same type of behaviour but the trajectories stay at $v < 0$. This means that the trajectories in the flow of system (4.16) with initial conditions on the invariant three-sphere, lying on a side of the two-sphere, remain on that same side of the two-sphere, as was to be expected since the two-sphere is invariant by the flow of (4.16).

Figure 4.8 represents the time series for the variable v for the flow of the perturbed system (4.22), for trajectories with initial condition $v > 0$. For initial conditions $v < 0$ we also get a time series with irregular transitions and irregular transition times between $v > 0$ and $v < 0$. This means that for trajectories in the flow of system (4.22) there are irregular transitions between one side and the other side of the two-sphere.

Figures 4.9 and 4.10 are the time series for the variable w for the flow of systems (4.16) and (4.22), respectively.

In figure 4.9 we observe the flow jumping from one equilibrium to the other, each time staying longer near each equilibrium, that is, the return times increase monotonically and very fast. Comparing the two time series we observe, for the same values of the common parameters, that the perturbed flow keeps jumping from one equilibrium to the other, but seems to do it at irregular time intervals and the return times no longer grow.

These time series provide numerical evidence to the fact that the invariant manifolds of the equilibria p_w with dimension ≥ 2 intersect transversely.

The projections in some coordinate planes of trajectories in the unperturbed and perturbed systems are also elucidatory (see figures 4.11, 4.13, 4.15, 4.12, 4.14 and 4.16).

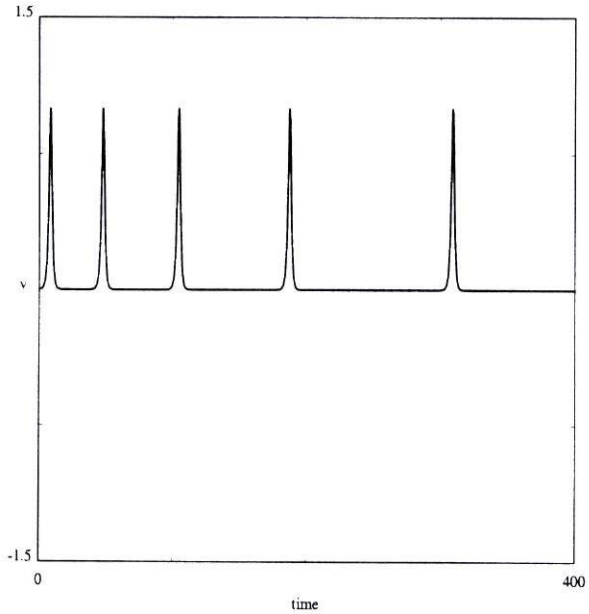

Figure 4.7: Time series for v for the flow of the unperturbed system (4.16) when $\lambda = 1,\ R = 1,\ \alpha = 1,\ \beta = -0.1,\ \gamma = 1$ and initial condition $v > 0$ (if $v < 0$ we get the same picture but symmetric with symmetry axis $v = 0$.

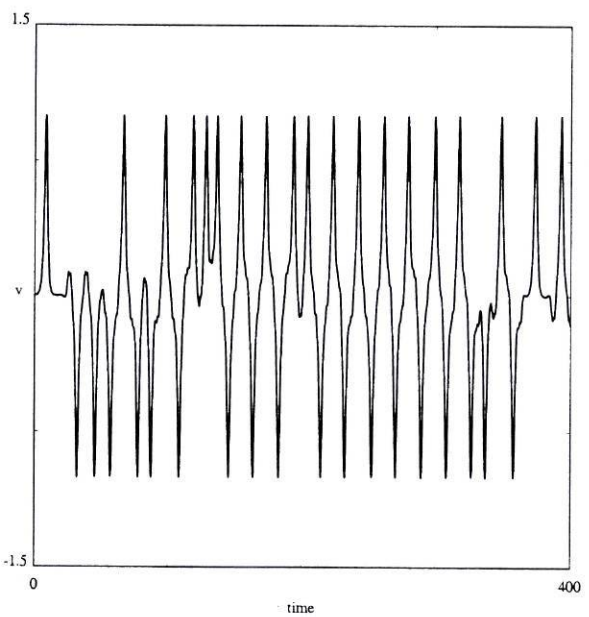

Figure 4.8: Time series for v for the flow of the perturbed system (4.22) when $\lambda = 1,\ R = 1,\ \alpha = 1,\ \beta = -0.1,\ \gamma = 1, \delta = 0.3$ and initial condition $v > 0$ (For initial conditions $v < 0$ we also get time series with irregular and random transitions).

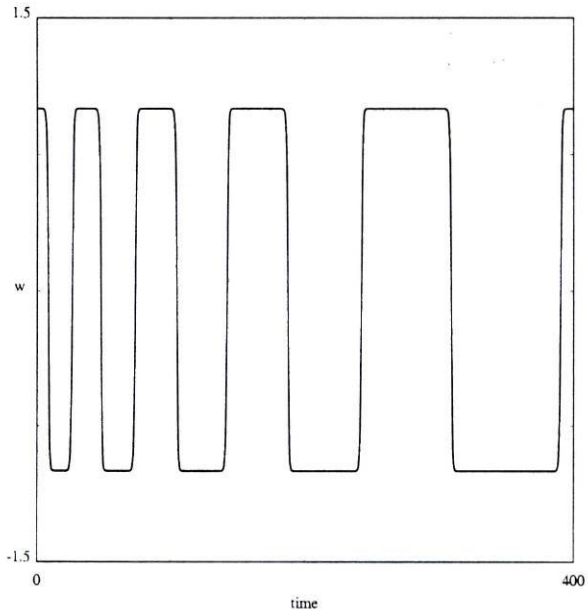

Figure 4.9: Time series for w for the flow of the unperturbed system (4.16) when $\lambda = 1,\ R = 1,\ \alpha = 1,\ \beta = -0.1,\ \gamma = 1.$

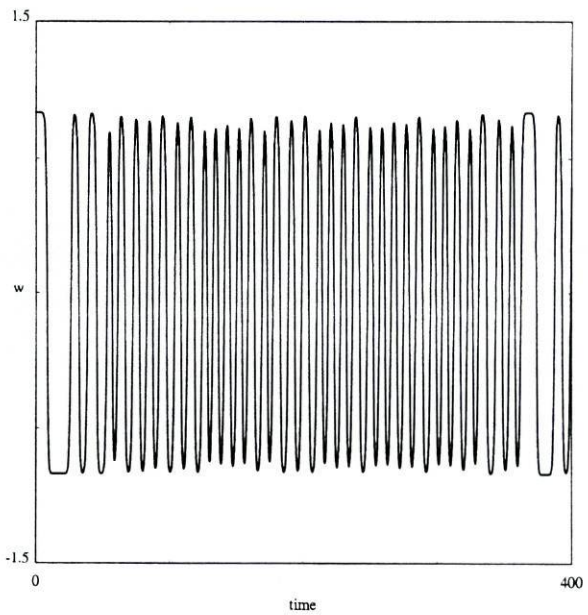

Figure 4.10: Time series for w for the flow of the perturbed system (4.22) when $\lambda = 1,\ R = 1,\ \alpha = 1,\ \beta = -0.1,\ \gamma = 1, \delta = 0.3.$

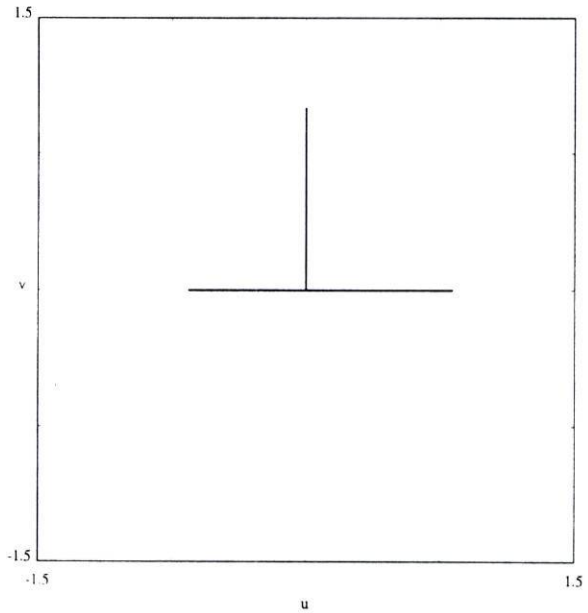

Figure 4.11: Projection in the (x, v)-plane of the trajectory with initial condition $(x, y, v, w) = (0.001, 0.001, 0.001, 1)$, for the flow of the unperturbed system (4.16) when $\lambda = 1,\ R = 1,\ \alpha = 1,\ \beta = -0.1,\ \gamma = 1$. For the same initial condition, but with $v = -0.001$ the projection is symmetric.

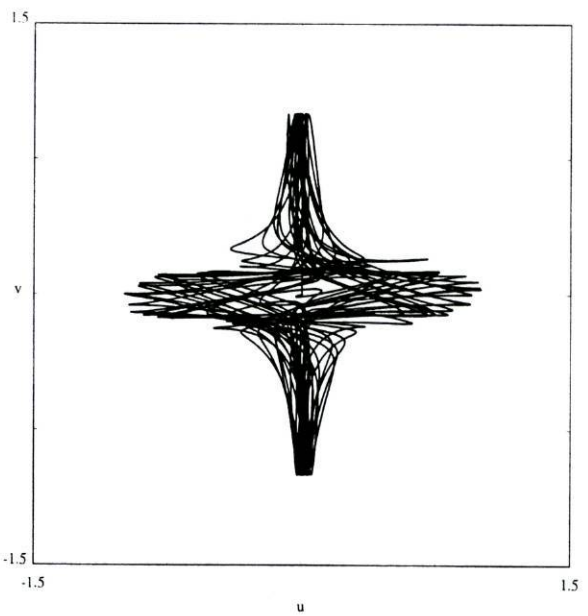

Figure 4.12: Projection in the (x, v)-plane of the trajectory with initial condition $(x, y, v, w) = (0.001, 0.001, 0.001, 1)$, for the flow of the perturbed system (4.22) when $\lambda = 1,\ R = 1,\ \alpha = 1,\ \beta = -0.1,\ \gamma = 1, \delta = 0.3$.

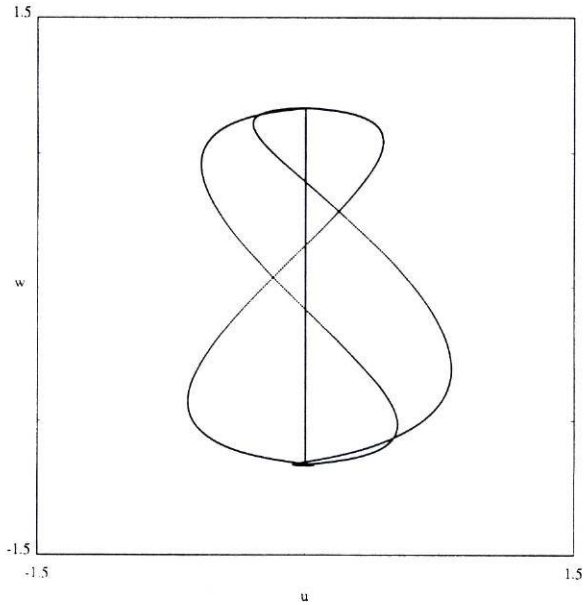

Figure 4.13: Projection in the (x, w)-plane of the trajectory with initial condition $(x, y, v, w) = (0.001, 0.001, 0.001, 1)$, for the flow of the unperturbed system (4.16) when $\lambda = 1,\ R = 1,\ \alpha = 1,\ \beta = -0.1,\ \gamma = 1$. For the same initial condition, but with $v = -0.001$ the projection is the same.

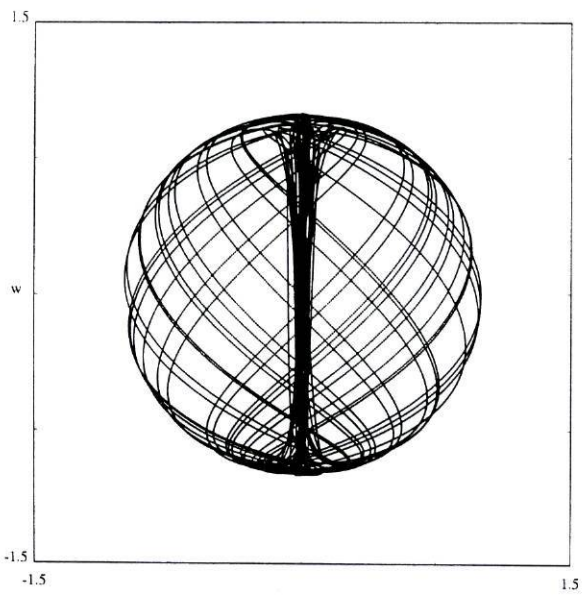

Figure 4.14: Projection in the (x, w)-plane of the trajectory with initial condition $(x, y, v, w) = (0.001, 0.001, 0.001, 1)$, for the flow of the perturbed system (4.22) when $\lambda = 1,\ R = 1,\ \alpha = 1,\ \beta = -0.1,\ \gamma = 1, \delta = 0.3$.

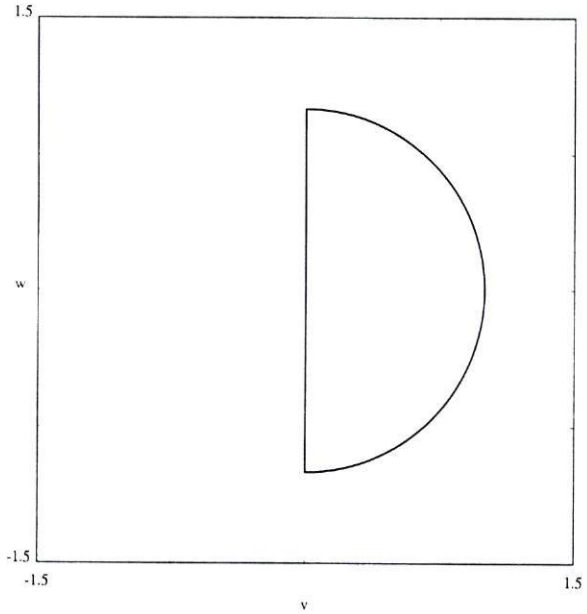

Figure 4.15: Projection in the (v, w)-plane of the trajectory with initial condition $(x, y, v, w) = (0.001, 0.001, 0.001, 1)$, for the flow of the unperturbed system (4.16) when $\lambda = 1$, $R = 1$, $\alpha = 1$, $\beta = -0.1$, $\gamma = 1$. For the same initial condition, but with $v = -0.001$ the projection is symmetric.

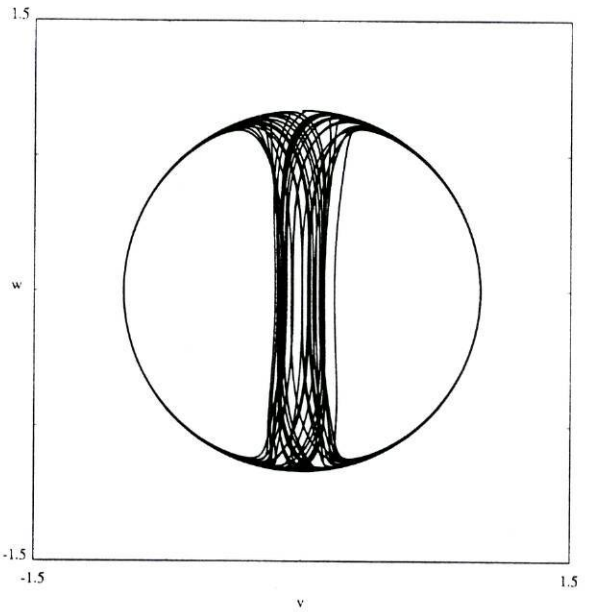

Figure 4.16: Projection in the (v, w)-plane of the trajectory with initial condition $(x, y, v, w) = (0.001, 0.001, 0.001, 1)$, for the flow of the perturbed system (4.22) when $\lambda = 1$, $R = 1$, $\alpha = 1$, $\beta = -0.1$, $\gamma = 1, \delta = 0.3$.

Theorem 18 *For $\lambda > 0$, $R > 0$, $\beta < 0$, $\lambda\beta^2 < 8\alpha^2 R$, $|\lambda\beta| < |\alpha\sqrt{\lambda R}|$, $\alpha \neq 0$, $\gamma \in \mathbf{R}$ and $\delta \in \mathbf{R}$, system (4.22) is such that*

(C1) There is a three-dimensional sphere, $\mathbf{S}^3_r$, that is invariant by the flow and globally attracting, in the sense that every trajectory with nonzero initial condition is asymptotic to the sphere in forward time.

(C3) The system has no equilibria other than the origin and the saddle-foci p_{w-}, p_{w+}.

(C5) In the restriction to the invariant sphere, system (4.22) has a stable heteroclinic cycle involving the saddle-foci p_{w+} and p_{w-}, and the two-dimensional manifolds of the equilibria intersect transversely along one-dimensional orbits.

(C6) On the invariant sphere, the system has two hyperbolic periodic trajectories, each in one connected component of $\mathbf{S}^3_r \backslash \mathbf{D}$. If $|\delta| < -2\beta$, on the invariant sphere, the periodic trajectories are repelling.

Proof: System (4.22) is a perturbation of system (4.16) with third-order linear terms as in lemma 16, thus the three-sphere remains invariant and globally attracting, and (C1) is verified.

We write the equations of system (4.22) in spherical polar coordinates,

$$\begin{aligned} \dot{r} &= r(\lambda - Rr^2), \\ \dot{\theta} &= \alpha r \sin\theta \cos(2\phi) + \tfrac{\beta}{2} r^2 \sin(2\theta) + \tfrac{\delta}{4} r^2 \sin(2\theta)\sin(2\phi)\cos\varphi, \\ \dot{\phi} &= -\alpha r \cos\theta \sin(2\phi) - \delta r^2 (\cos\theta)^2 (\sin\phi)^2 \cos\varphi, \\ \dot{\varphi} &= \gamma. \end{aligned} \tag{4.23}$$

From the equation for $\dot{\varphi}$ we get $\varphi(t) = \gamma t$, $t \in \mathbf{R}$. We replace φ by γt in the other equations, ignore the equation for $\dot{\varphi}$ and consider the reduced system,

$$\begin{aligned} \dot{r} &= r(\lambda - Rr^2), \\ \dot{\theta} &= \alpha r \sin\theta \cos(2\phi) + \tfrac{\beta}{2} r^2 \sin(2\theta) + \tfrac{\delta}{4} r^2 \sin(2\theta)\sin(2\phi)\cos(\gamma t), \\ \dot{\phi} &= -\alpha r \cos\theta \sin(2\phi) - \delta r^2 (\cos\theta)^2 (\sin\phi)^2 \cos(\gamma t). \end{aligned} \tag{4.24}$$

The equations for $\dot{\theta}$ and $\dot{\phi}$ of system (4.24) are time dependent, nevertheless they are time periodic with period $2\pi/\gamma$. So, we can see system (4.23) as a lift of system (4.24) by a rotation. System (4.24) is a nonautonomous perturbation of system (4.5).

The zeros of the perturbed system (4.24, $\delta \neq 0$) are given by either $\sin\theta = 0 = \sin(2\phi)$, or $\cos(2\phi) = 0 = \cos\theta$, which correspond, respectively, to the equilibria p_w and $p_{\rho v}$ of the unperturbed system (4.24, $\delta = 0$).

The non-radial eigenvalues at $p_{\rho v}$ are

$$\left(-2\lambda\beta - \delta\lambda\cos(\gamma t) \pm \sqrt{\{2\lambda\beta + \delta\lambda\cos(\gamma t)\} - 32\lambda\alpha^2 R}\right)/4R.$$

For the parameter values we are considering and $|\delta| < -2\beta$, equilibria $p_{\rho v}$ are unstable foci.

The equilibria $p_{\rho v}$ lift to two periodic trajectories in the flow of system (4.22) and are given by the same equations of the periodic trajectories in the unperturbed system (4.16). In fact, since the perturbing terms are zero when $w = 0$, the dynamics in the hyperplane $\{(x, y, v, w) \ : \ w = 0\}$ remains unchanged in the perturbed system (4.22).

This proves (C3) and (C6).

The linearization of the perturbed system (4.24, $\delta \neq 0$) at p_w has the same eigenvalues as the linearization of the unperturbed system (4.24, $\delta = 0$).

In the next proposition we prove that in the restriction to the three-sphere the two--dimensional invariant manifolds of the equilibria p_w intersect transversely. This ends the proof of (C5). □

Proposition 19 *In the conditions of theorem 18, consider the restriction of the perturbed system (4.22) to the invariant three-sphere* $\mathbf{S}^3_r$ *of radius* $r = \sqrt{\frac{\lambda}{R}}$. *Then the two-dimensional invariant manifolds of* p_{w_-} *and* p_{w_+} *intersect transversely.*

Proof:

We will prove that in the flow of system (4.22) restricted to the invariant three-sphere $\mathbf{S}^3_r$ the two-dimensional manifolds intersect transversely, by proving that in the flow of system (4.24) restricted to the invariant two-sphere $\mathbf{S}^2_r$ of radius $r = \sqrt{\frac{\lambda}{R}}$ the correspondent invariant manifolds intersect transversely.

We use Melnikov's method, which is a tool for finding the transverse intersection of stable and unstable manifolds given a time-periodic perturbation. It decides whether the invariant manifolds intersect by calculating the distance between them. The measure of that distance is given by the Melnikov function. The existence of simple zeros of the Melnikov function implies that the invariant manifolds intersect transversely. See [20], section 4.5.

We compute the Melnikov function for the perturbed heteroclinic connections in (4.24) by considering its restriction to the invariant two-sphere $\mathbf{S}^2_r$:

$$\begin{aligned} \dot{\theta} &= \alpha r \sin\theta\cos(2\phi) + \tfrac{\beta}{2} r^2 \sin(2\theta) + \tfrac{\delta}{4} r^2 \sin(2\theta)\sin(2\phi)\cos(\gamma t), \\ \dot{\phi} &= -\alpha r \cos\theta \sin(2\phi) - \delta r^2 \cos^2\theta \sin^2\phi \cos(\gamma t). \end{aligned} \tag{4.25}$$

Until the end of this section, we fix $r = \sqrt{\frac{\lambda}{R}}$.

System (4.25) has the form,

$$\begin{aligned} \dot{\theta} &= f_1(\theta,\phi) + \delta g_1(\theta,\phi,t), \\ \dot{\phi} &= f_2(\theta,\phi) + \delta g_2(\theta,\phi,t), \end{aligned} \tag{4.26}$$

with

$$\begin{aligned} f_1(\theta,\phi) &= \alpha r \sin\theta\cos(2\phi) + \tfrac{\beta}{2} r^2 \sin(2\theta), \\ f_2(\theta,\phi) &= -\alpha r \cos\theta \sin(2\phi), \\ g_1(\theta,\phi,t) &= \tfrac{1}{4} r^2 \sin(2\theta)\sin(2\phi)\cos(\gamma t), \\ g_2(\theta,\phi,t) &= -r^2 \cos^2\theta \sin^2\phi \cos(\gamma t), \end{aligned} \tag{4.27}$$

where g_1 and g_2 are periodic in t with period $\frac{2\pi}{\gamma}$.

We consider (4.25) as a time-periodic perturbation of $\dot{\theta} = f_1(\theta,\phi)$, $\dot{\phi} = f_2(\theta,\phi)$. As the unperturbed system is non-Hamiltonian the Melnikov function is given by,

$$M(t_0) = \int_{-\infty}^{\infty} f(q_0(t)) \wedge g(q_0(t), t+t_0)\ exp\left(-\int_0^t traceDf(q_0(s))ds\right) dt,$$

with $q_0(t)$ a parametrization of the unperturbed heteroclinic orbit, $f = (f_1, f_2)$, $g = (g_1, g_2)$, ([20], section 4.5).

The unperturbed heteroclinic connection in the flow of (4.22, $\delta = 0$) which when perturbed produces a transverse intersection is in $x^2 + y^2 + w^2 = \frac{\lambda}{R}$ and $v = 0$. Thus, in spherical polar coordinates, it corresponds to the heteroclinic connections given by $\phi = \frac{\pi}{2}$ and $\phi = \frac{3\pi}{2}$ in (4.25). Let $q_0(t) = (\theta(t), \frac{\pi}{2})$ or $q_0(t) = (\theta(t), \frac{3\pi}{2})$.

We have,

$$\begin{aligned} f_1(q_0(t)) &= -\alpha r \sin\theta(t) + \tfrac{\beta}{2} r^2 \sin(2\theta(t)), \\ f_2(q_0(t)) &= 0, \\ g_1(q_0(t), t+t_0) &= 0, \\ g_2(q_0(t), t+t_0) &= -r^2 \cos^2\theta(t) \cos(\gamma t + \gamma t_0), \end{aligned} \tag{4.28}$$

then,

$$\begin{aligned} f(q_0(t)) \wedge g(q_0(t), t+t_0) &= f_1(q_0(t)) g_2(q_0(t), t+t_0) - f_2(q_0(t)) g_1(q_0(t), t+t_0) = \\ &= \left(-\alpha r \sin\theta(t) + \tfrac{\beta}{2} r^2 \sin(2\theta(t))\right)\left(-r^2 \cos^2\theta(t) \cos(\gamma t + \gamma t_0)\right), \end{aligned}$$

and

$$traceDf(q_0(t)) = \alpha r\cos(\theta(t)) + \beta r^2\cos(2\theta(t)).$$

For $\phi = \frac{\pi}{2}$ or $\phi = \frac{3\pi}{2}$ we have the following equation for $\dot{\theta}$,

$$\dot{\theta} \;=\; r\sin\theta(t)(-\alpha + \beta r\cos\theta(t)). \tag{4.29}$$

We obtain the Melnikov function,

$$M(t_0) = \int_{-\infty}^{\infty}\cos(\gamma t + \gamma t_0)E(t)dt, \tag{4.30}$$

with

$$E(t) = r^2\cos^2\theta(t)\left(\alpha r\sin\theta(t) - \frac{\beta}{2}r^2\sin(2\theta(t))\right)e^{\left[-\int_0^t \alpha r\cos(\theta(s))+\beta r^2\cos(2\theta(s))ds\right]}.$$

The convergence of $M(t_0)$ is proved in lemma 20 below. In order to prove the transverse intersection of the invariant manifolds it only remains to prove that $M(t_0)$ has simple zeros. Rewrite $M(t_0)$ as:

$$M(t_0) = \int_{-\infty}^{\infty}\cos(\gamma t)\cos(\gamma t_0)E(t)dt - \int_{-\infty}^{\infty}\sin(\gamma t)\sin(\gamma t_0)E(t)dt.$$

Let $C = \int_{-\infty}^{\infty}\cos(\gamma t)E(t)dt$, and $S = \int_{-\infty}^{\infty}\sin(\gamma t)E(t)dt$, then

$$M(t_0) \;=\; \cos(\gamma t_0)C - \sin(\gamma t_0)S \tag{4.31}$$

From (4.31), the Melnikov function has infinitely many zeros provided

$$\tan(\gamma t_0) \;=\; \tfrac{C}{S}, \qquad t_0 \in \mathbf{R}. \tag{4.32}$$

Note that from the proof of lemma 20 below, we can also conclude that C and S converge.

The zeros t_0' of the Melnikov function are simple if $\frac{dM}{dt_0}(t_0') \neq 0$. We have from (4.31),

$$\tfrac{dM}{dt_0}(t_0) \;=\; -\gamma\sin(\gamma t_0)C - \gamma\cos(\gamma t_0)S \tag{4.33}$$

Thus the zeros of the Melnikov function are simple provided

$$\tan(\gamma t_0) \;\neq\; -\tfrac{S}{C}, \qquad t_0 \in \mathbf{R}, \tag{4.34}$$

which is trivially verified, since the zeros of the Melnikov function satisfy (4.32). □

Lemma 20 *The Melnikov integral*

$$M(t_0) = \int_{-\infty}^{\infty} f(t)e^{-g(t)}dt,$$

with

$$f(t) = \left(-\alpha r \sin\theta(t) + \frac{\beta}{2}r^2 \sin(2\theta(t))\right)\left(-r^2\cos^2\theta(t)\cos(\gamma t + \gamma t_0)\right),$$

and

$$g(t) = \int_0^t \alpha r\cos(\theta(s)) + \beta r^2\cos(2\theta(s))ds,$$

converges.

Proof: In order to prove that $M(t_0)$ converges, and since $f(t)$ is bounded, it is sufficient to prove that $\int_{-\infty}^{\infty} e^{-g(t)}dt$ converges.

We take $\alpha > 0$. Recall that,

$$\dot{\theta} = r\sin\theta\left(-\alpha + \beta r\cos\theta\right). \tag{4.35}$$

We are studying the perturbation of the heteroclinic connection in the plane $\{(\rho, v, w) : v = 0\}$. Remember from the study of the eigenvalues of the equilibria p_w, in the proof of theorem 14 that, when $\alpha > 0$, the heteroclinic connection is from p_{w_-} to p_{w_+}.

Thus, we have $\lim_{t\to+\infty}\theta(t) = 0$, $\lim_{t\to-\infty}\theta(t) = \pi$ and $\theta(t) \in [0, \pi], \forall t \in \mathbf{R}$. For the parameter values we are considering, we have $\alpha > |\beta r|$, and thus $-\alpha + \beta r\cos\theta < 0$, and $\dot{\theta} < 0$ for $\theta \in]0, \pi[$.

We do the variable change $u = \theta(s)$ and get

$$g(t) = \int_{\theta(0)}^{\theta(t)} \alpha r\cos(u) + \beta r^2\cos(2u)\frac{du}{\dot{\theta}}.$$

Computations with Maple give

$$g(t) = -A\ln J(u)\Big]_{\theta(0)}^{\theta(t)},$$

with $A = \frac{1}{(\alpha-\beta r)(\alpha+\beta r)}$, and

$$J(u) = \frac{\left(1+\tan^2(\frac{u}{2})\right)^{2(\alpha^2-\beta^2r^2)}\left(\tan(\frac{u}{2})\right)^{(\alpha+\beta r)^2}}{\left((\alpha-\beta r)+(\alpha+\beta r)\tan^2(\frac{u}{2})\right)^{(3\alpha^2-\beta^2r^2)}}.$$

Since $\alpha > |\beta r|$, we have $A > 0$. We have

$$e^{-g(t)} = J(\theta(0))^{-A} J(\theta(t))^{A}. \tag{4.36}$$

To prove that $\int_{-\infty}^{\infty} e^{-g(t)}dt$ converges, it is thus sufficient to prove the convergence of $\int_{-\infty}^{\infty} J(\theta(t))^{A}dt$.

For the parameter values we are considering we have by lemma 21 below,

$$0 \leq J(\theta(t)) < \frac{1}{(\alpha+\beta r)^{(3\alpha^2-\beta^2r^2)}} \left(\frac{\sin(\theta(t))}{2}\right)^{(\alpha+\beta r)^2}.$$

Thus, we conclude

$$J(\theta(t))^{A} < \left(\frac{1}{(\alpha+\beta r)^{(3\alpha^2-\beta^2r^2)}}\right)^{A} \left(\frac{\sin(\theta(t))}{2}\right)^{B}, \tag{4.37}$$

with $0 < B = \frac{\alpha+\beta r}{\alpha-\beta r} < 1$.

Thus, to prove that $\int_{-\infty}^{\infty} J(\theta(t))^{A}dt$ converges we only need to prove that

$$\int_{-\infty}^{\infty} \left(\frac{\sin\theta(t)}{2}\right)^{B} dt \tag{4.38}$$

converges.

By arguments above, (4.38) is equal to

$$\int_0^{\pi} \frac{\left(\frac{\sin\theta}{2}\right)^{B}}{r\sin\theta(\alpha-\beta r\cos\theta)}d\theta. \tag{4.39}$$

For $\theta \in]0, \pi[$, we have,

$$\frac{\left(\frac{\sin\theta}{2}\right)^{B}}{r\sin\theta\,(\alpha-\beta r\cos\theta)} = \frac{1}{2^{B}r\,(\sin\theta)^{1-B}\,(\alpha-\beta r\cos\theta)},$$

with $0 < 1 - B < 1$.

Since $\alpha > 0$, $\beta < 0$ and $\alpha > |\beta r|$, we have $\alpha - \beta r\cos\theta > 0$. It remains to prove that,

$$\int_0^{\pi} \frac{1}{(\sin\theta)^{1-B}\,(\alpha-\beta r\cos\theta)}d\theta$$

converges, which is easily seen since $\frac{1}{\alpha-\beta r\cos\theta}$ is bounded, and

$$\int_0^{\pi} \frac{1}{(\sin\theta)^{1-B}}d\theta$$

converges, by comparison with $\int_0^{\pi} \frac{1}{\theta^{1-B}}d\theta$. □

Lemma 21 *Let*

$$J(u) = \frac{\left(1+\tan^2(\frac{u}{2})\right)^{2(\alpha^2-\beta^2r^2)}\left(\tan(\frac{u}{2})\right)^{(\alpha+\beta r)^2}}{\left((\alpha-\beta r)+(\alpha+\beta r)\tan^2(\frac{u}{2})\right)^{(3\alpha^2-\beta^2r^2)}}.$$

For the parameter values we are considering we have

$$0 \le J(u) < \frac{1}{(\alpha+\beta r)^{(3\alpha^2-\beta^2r^2)}}\left(\frac{\sin(u)}{2}\right)^{(\alpha+\beta r)^2}.$$

Proof: Since $0 < \alpha+\beta r < \alpha-\beta r$ and $3\alpha^2-\beta^2r^2 > 0$, we have

$$\begin{aligned} 0 \le J(u) &< \frac{\left(1+\tan^2(\frac{u}{2})\right)^{2(\alpha^2-\beta^2r^2)}\left(\tan(\frac{u}{2})\right)^{(\alpha+\beta r)^2}}{\left((\alpha+\beta r)\left(1+\tan^2(\frac{u}{2})\right)\right)^{(3\alpha^2-\beta^2r^2)}} = \\ &= \frac{1}{(\alpha+\beta r)^{(3\alpha^2-\beta^2r^2)}}\frac{\left(\tan(\frac{u}{2})\right)^{(\alpha+\beta r)^2}}{\left(1+\tan^2(\frac{u}{2})\right)^{(\alpha^2+\beta^2r^2)}}. \end{aligned} \tag{4.40}$$

Since $(\alpha+\beta r)^2 < \alpha^2+\beta^2r^2$ and $1+\tan^2(\frac{u}{2}) \ge 1$, we have

$$\begin{aligned} J(u) &< \frac{1}{(\alpha+\beta r)^{(3\alpha^2-\beta^2r^2)}}\left(\frac{\tan(\frac{u}{2})}{1+\tan^2(\frac{u}{2})}\right)^{(\alpha+\beta r)^2} = \\ &= \frac{1}{(\alpha+\beta r)^{(3\alpha^2-\beta^2r^2)}}\left(\sin\left(\frac{u}{2}\right)\cos\left(\frac{u}{2}\right)\right)^{(\alpha+\beta r)^2} \\ &= \frac{1}{(\alpha+\beta r)^{(3\alpha^2-\beta^2r^2)}}\left(\frac{\sin(u)}{2}\right)^{(\alpha+\beta r)^2}. \end{aligned} \tag{4.41}$$

□

4.1.3.2 Dynamics after $SO(2)$-equivariant perturbations

Among the perturbations that preserve the globally attracting three-sphere and break the invariance of the two-sphere there is only one that preserves the $SO(2)$-equivariance, namely,

$$\begin{aligned}
\dot{x} &= x(\lambda - Rr^2) - \alpha xw + \beta xw^2 - \gamma y, \\
\dot{y} &= y(\lambda - Rr^2) - \alpha yw + \beta yw^2 + \gamma x, \\
\dot{v} &= v(\lambda - Rr^2) + \alpha vw + \beta vw^2 + \tau w^3, \\
\dot{w} &= w(\lambda - Rr^2) - \alpha(v^2 - x^2 - y^2) - \beta w(x^2 + y^2 + v^2) - \tau vw^2,
\end{aligned} \tag{4.42}$$

with $r^2 = x^2 + y^2 + v^2 + w^2$.

System (4.42) can be seen as the lift by the rotation around $Fix(dq^2)$ of the following perturbation with parameter τ of system (4.4),

$$\begin{aligned}
\dot{\rho} &= \rho(\lambda - Rr^2) - \alpha\rho w + \beta\rho w^2, \\
\dot{v} &= v(\lambda - Rr^2) + \alpha vw + \beta vw^2 + \tau w^3, \\
\dot{w} &= w(\lambda - Rr^2) - \alpha(v^2 - \rho^2) - \beta w(\rho^2 + v^2) - \tau vw^2,
\end{aligned} \tag{4.43}$$

with $r^2 = \rho^2 + v^2 + w^2$.

Thus, the dynamics of the perturbation (4.42) can be understand by studying the dynamics of the three-dimensional perturbed system (4.43).

Theorem 22 *For $\lambda > 0$, $R > 0$, $\beta < 0$, $\lambda\beta^2 < 8\alpha^2 R$, $|\lambda\beta| < |\alpha\sqrt{\lambda R}|$, $\alpha \neq 0$, and for $\tau^2 > -\frac{\lambda\beta^2}{\frac{1}{4}\alpha^2 R} - \frac{4}{\beta^2}$, system (4.42) satisfies*

(C1) There is a three-dimensional sphere, $\mathbf{S}^3_r$, that is invariant by the flow and globally attracting, in the sense that every trajectory with nonzero initial condition is asymptotic to the sphere in forward time.

(C3) The only equilibria are the origin, and two saddles p_{w_-} and p_{w_+}.

(C4) The system has two hyperbolic periodic trajectories, each in one connected component of $\mathbf{S}^3_r \backslash \mathbf{D}$. On the invariant sphere the periodic trajectories are repelling.

(C7) Restricted to the invariant sphere the flow of system (4.42) has an attracting invariant two-torus close to the heteroclinic cycle in the flow of system (4.16).

Proof: The flow of the perturbed system (4.42) leaves the three-sphere $\mathbf{S}^3_r$ invariant and globally attracting as it is a perturbation tangent to the sphere, by lemma 16.

The persistence of the two hyperbolic repelling periodic trajectories, with equations

$$x^2 + y^2 = -\frac{\lambda}{2R}, \; v = \pm\sqrt{\frac{\lambda}{2R}}, \qquad \text{and} \qquad w = 0,$$

is a result of the persistence of equilibria $p_{\rho v}$, and their stability, in the flow of the three-dimensional perturbed system (4.43). If $\tau^2 > -\frac{\lambda\beta^2}{\frac{1}{4}\alpha^2 R} - \frac{4}{\beta^2}$, the only equilibria of system (4.43) besides $p_{\rho v}$ and the origin, are two saddle points $p^\tau_{w_-}$ and $p^\tau_{w_+}$ on the two-sphere of radius $r = \sqrt{\frac{\lambda}{R}}$ with, respectively, $w < 0$ and $w > 0$, that are perturbations of the equilibria p_{w_-} and p_{w_+} of the unperturbed system and are given by $(0, -\frac{\tau w^2}{\alpha+\beta w}, w)$.

This proves (C1), (C3) and (C4).

To prove (C7) we show that the flow of system (4.43) has two hyperbolic attracting periodic trajectories on the two-sphere $\mathbf{S}^2_r$ that lift to an attracting two-torus on the three-sphere $\mathbf{S}^3_r$.

In $Fix(dq^2)$, the one-dimensional connection between the equilibria p_{w_-} and p_{w_+} persists as a one-dimensional connection between the equilibria $p^\tau_{w_-}$ and $p^\tau_{w_+}$ in the flow of the three-dimensional perturbed system (4.43), since the perturbation remains equivariant by the action of dq^2.

However, as the perturbation breaks the invariance of the plane $Fix(d)$, the most generic situation is for the one-dimensional connection between the equilibria p_{w_-} and p_{w_+} in this plane to be broken.

We prove that the connection is really broken. We give a geometrical proof based on the value of the sign of the v and w components of the vector fields restricted to the two-sphere $\mathbf{S}^2_r$.

The equations of system (4.43) restricted to the two-sphere $\mathbf{S}^2_r$ simplify to

$$\begin{aligned} \dot{\rho} &= -\alpha\rho w + \beta\rho w^2, \\ \dot{v} &= \alpha v w + \beta v w^2 + \tau w^3, \\ \dot{w} &= -\alpha(v^2 - \rho^2) - \beta w(\rho^2 + v^2) - \tau v w^2, \end{aligned} \tag{4.44}$$

with $\rho^2 + v^2 + w^2 = \frac{\lambda}{R}$.

We first note that we can, in this study of the sign of $\dot{v}$ and $\dot{w}$, ignore the ρ component of the vector fields: the equation for $\dot{v}$ does not depend on the variable ρ, and the

equation for $\dot{w}$ can be equivalently written independently of ρ,

$$\dot{w} = \alpha(\tfrac{\lambda}{R} - 2v^2 - w^2) + \beta w(w^2 - \tfrac{\lambda}{R}) - \tau w^2 v. \tag{4.45}$$

Thus we reduce our study to a vector field in the (v, w)-plane with equations,

$$\begin{aligned} \dot{v} &= \alpha vw + \beta v w^2 + \tau w^3, \\ \dot{w} &= \alpha(\tfrac{\lambda}{R} - 2v^2 - w^2) + \beta w(w^2 - \tfrac{\lambda}{R}) - \tau w^2 v. \end{aligned} \tag{4.46}$$

with $v^2 + w^2 \leq \frac{\lambda}{R}$.

We consider $\alpha > 0$ (the case $\alpha < 0$ is analogous).

In the unperturbed case, that is when $\tau = 0$, we have, in the restriction of the vector field to $Fix(dq^2)$, that p_{w_+} is a source and p_{w_-} is a sink. We have that $\dot{v}$ is zero when either $v = 0$ or $w = 0$, and $\dot{v}$ assumes negative values in the second and fourth quadrants of the (v, w)-plane and assumes positive values in the first and third quadrants.

Let $v_s = \sqrt{\frac{\lambda}{R}}$, and $v_{w=0} = \sqrt{\frac{(\beta w - \alpha)(w^2 - \frac{\lambda}{R})}{2\alpha}}$. The equation of $\dot{w}$ is zero for $\pm v_{w=0}$, takes negative values in

$$[-v_s, -v_{w=0}) \cup (v_{w=0}, v_s],$$

and takes positive values in

$$(-v_{w=0}, v_{w=0}).$$

We have then a vector field as the one in figure 4.17. Observing figure 4.17 we can understand the reason why in the unperturbed case the unstable manifold of p_{w_-} coincides with the invariant axis $Fix(d) = \{(\rho, v, w) : v = 0\}$: the unstable manifold of p_{w_-} when infinitesimaly close to p_{w_-} must be in the region of the (v, w)-plane where $\dot{w} > 0$. In this region we have $\dot{v} > 0$ when $v < 0$, $\dot{v} = 0$ when $v = 0$, and $\dot{v} < 0$ when $v > 0$. We conclude that if we consider an initial condition in the unstable manifold of p_{w_-} and infinitesimally close to p_{w_-}, iterating forward, the trajectory will intersect $v = 0$ after some time. As $v = 0$ is an invariant axis, we conclude that the unstable manifold of p_{w_-} must be within that axis and coincide in it with the stable manifold of p_{w_+}.

We now consider the perturbed situation when $\tau > 0$. The case $\tau < 0$ is analogous.

The dynamics restricted to $Fix(dq^2)$ is topologically equivalent to the nonperturbed situation, that is $p^\tau_{w_+}$ is a source and $p^\tau_{w_-}$ is a sink.

Let $v_{v=0} = -\frac{\tau w^2}{\alpha + \beta w}$. The equation of $\dot{v}$ is zero for $\pm v_{v=0}$ or $w = 0$. The sign of $\dot{v}$, is negative in $[-v_s, v_{v=0})$ when $w > 0$ and in $(v_{v=0}, v_s]$ when $w < 0$.

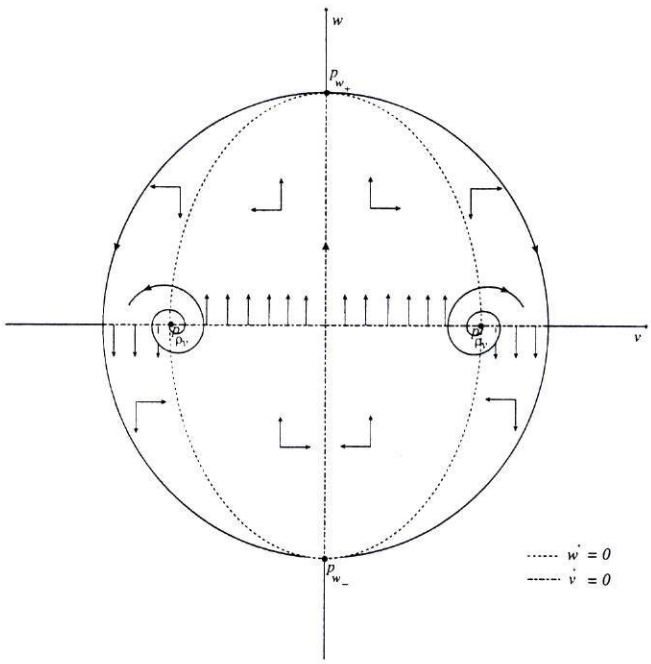

Figure 4.17: Sketch, when $\alpha > 0$, of the restriction to the plane (v, w) of the unperturbed vector field (4.43, $\tau = 0$) restricted to the two-sphere $\mathbf{S}^2_r$.

The sign of $\dot{v}$ is positive in $(v_{v=0}, v_s]$ when $w > 0$ and in $[-v_s, v_{v=0})$ when $w < 0$.

Let

$$v_{w=0_\pm} = \frac{\tau w^2 \pm \sqrt{\tau^2 w^4 + 8\alpha(\beta w - \alpha)(w^2 - \frac{\lambda}{R})}}{-4\alpha}.$$

The equation of $\dot{w}$ is zero in $v_{w=0}$. In $\left[-v_s, v_{w=0_-}\right) \cup \left(v_{w=0_+}, v_s\right]$, $\dot{w}$ takes negative values, and in $\left(v_{w=0_-}, v_{w=0_+}\right)$, takes positive values. We thus have a vector field as in figure 4.18.

Figure 4.18 helps understand the unstable manifold of $p^\tau_{w_-}$. As in the unperturbed case the unstable manifold of $p^\tau_{w_-}$ when infinitesimaly close to $p^\tau_{w_-}$ must be in the region of the (v, w)-plane where $\dot{w} > 0$. Observing the figure we conclude it must be the region where $\dot{w} > 0$ and $\dot{v} > 0$, region E in figure 4.18.

If we consider an initial condition in the unstable manifold of $p^\tau_{w_-}$ and infinitesimaly close to $p^\tau_{w_-}$, then, when we iterate it forward, the trajectory will stay in region E and infinitesimaly close to the curve $\dot{v} = 0$ until it intersects $\dot{v} = 0$ in $(0, 0)$. In $(0, 0)$ we have $\dot{v} = 0$ and $\dot{w} > 0$, thus the manifold will be in region A, see figure 4.18.

In region A, $\dot{v}$ is positive, so the trajectory will go far away from the equilibrium $p^\tau_{w_+}$ and enter region B. In region B, $\dot{v} > 0$ and $\dot{w} < 0$, so the trajectory will enter region

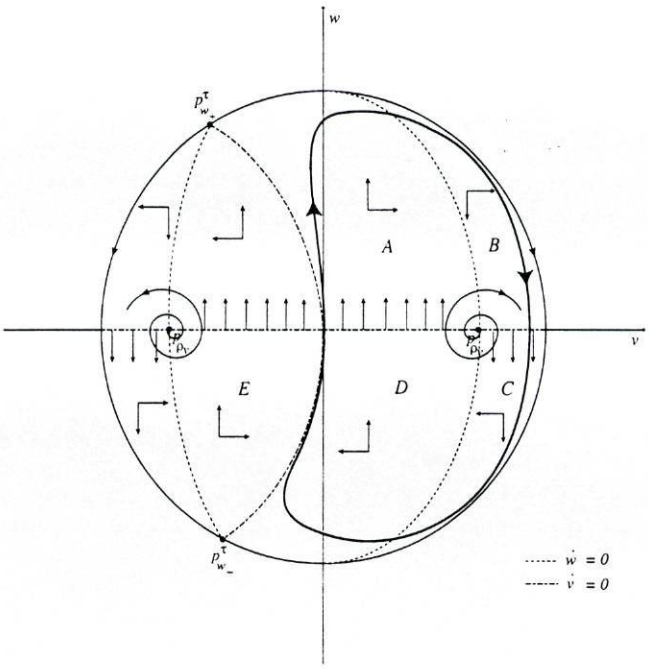

Figure 4.18: Sketch, when $\alpha > 0$ and $\tau > 0$, of the restriction to the plane (v, w) of the perturbed vector field (4.43, $\tau \neq 0$) restricted to the two-sphere $\mathbf{S}^2_r$. The attracting periodic trajectory is represented by the bold solid curve.

C, after that region D, until it enters again in region A.

The trajectory will sucessively pass through the last four mentioned regions in the given order. We can thus conclude that the one-dimensional connection in $Fix(d)$ between the equilibria p_{w_-}, p_{w_+} is broken. Since the unstable manifold of $p^\tau_{w_-}$ cannot accumulate in the equilibria $p_{\rho v}$, as $p_{\rho v}$ is repelling, by Poincaré-Bendixon's Theorem (Theorem 1.8.1 in [20]), there must be an attracting hyperbolic periodic trajectory where the unstable manifolds of $p^\tau_{w_-}$ and of $p_{\rho v}$ accumulate, see figure 4.18.

In the restriction to the two-sphere $\mathbf{S}^2_r$, that is when we consider the variable ρ, there are two (symmetric) connections that are broken, and thus we get two symmetric attracting hyperbolic periodic trajectories.

In the case $\tau < 0$, the dynamics is equivalent but the connection is broken in a symmetric way, i.e., the flow is the image in a mirror of that in figure 4.18.

In the case $\alpha < 0$, we get the same kind of behaviour, with the difference that in the restriction to $Fix(dq^2)$, $p^\tau_{w_+}$ is a sink and $p^\tau_{w_-}$ is a source.

The periodic trajectories in the three-dimensional system lift by the $SO(2)$-symmetry

to a two-torus in the four-dimensional system. The two-torus is normally hyperbolic and attracting. □

The numerical evidence that the dynamics restricted to the torus is quasi-periodic is given by the projections in figures 4.19, 4.20, 4.21, and the time series in figures 4.22, 4.23, 4.24.

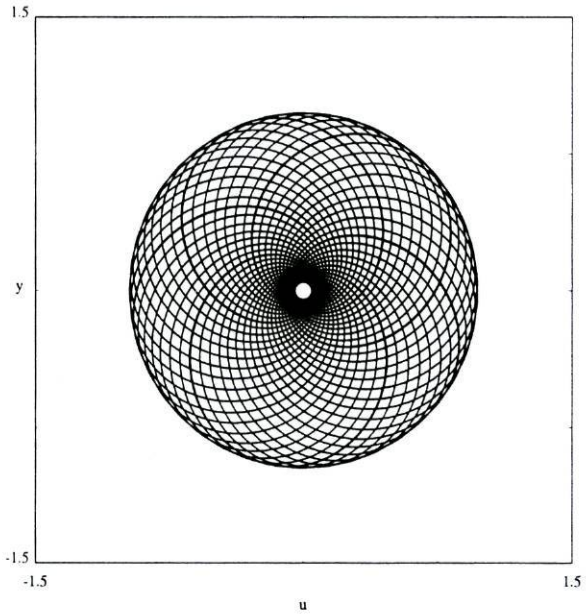

Figure 4.19: Projection in the (x, y)-plane of a trajectory on the two-torus, when $\lambda = 1,\ R = 1,\ \alpha = 1, \beta = -0.1,\ \gamma = 1,\ \tau = 0.5$.

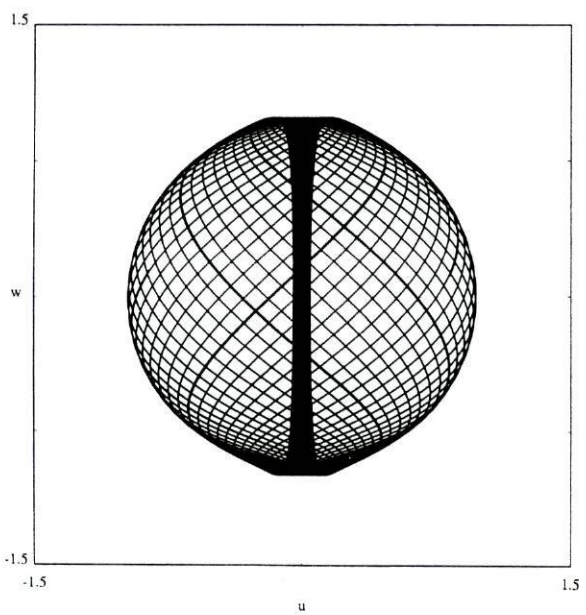

Figure 4.20: Projection in the (x, w)-plane of a trajectory on the two-torus, when $\lambda = 1,\ R = 1,\ \alpha = 1, \beta = -0.1,\ \gamma = 1,\ \tau = 0.5$.

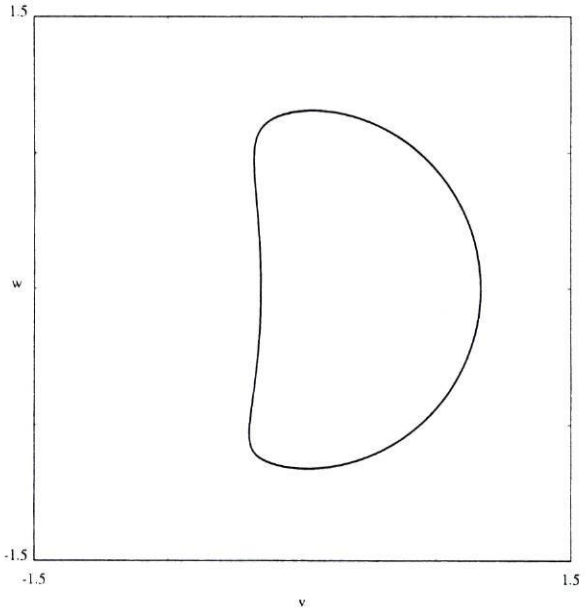

Figure 4.21: Projection in the (v, w)-plane of a trajectory on the two-torus, when $\lambda = 1,\ R = 1,\ \alpha = 1, \beta = -0.1,\ \gamma = 1,\ \tau = 0.5$.

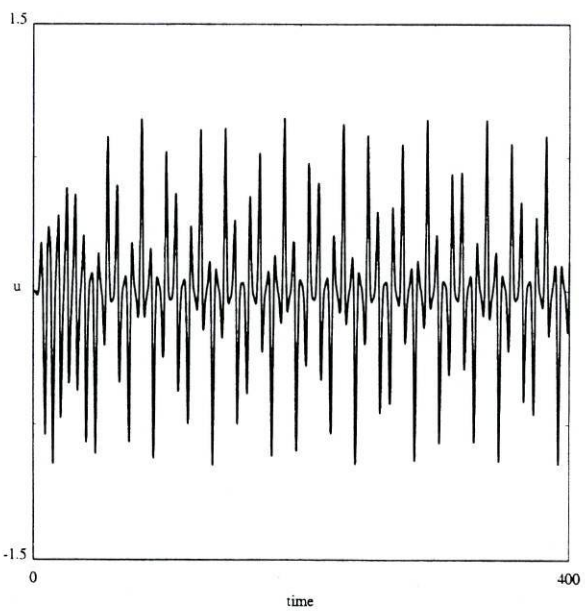

Figure 4.22: Time series for x for a trajectory with initial condition near the origin, when $\lambda = 1,\ R = 1, \alpha = 1, \beta = -0.1,\ \gamma = 1,\ \tau = 0.5$.

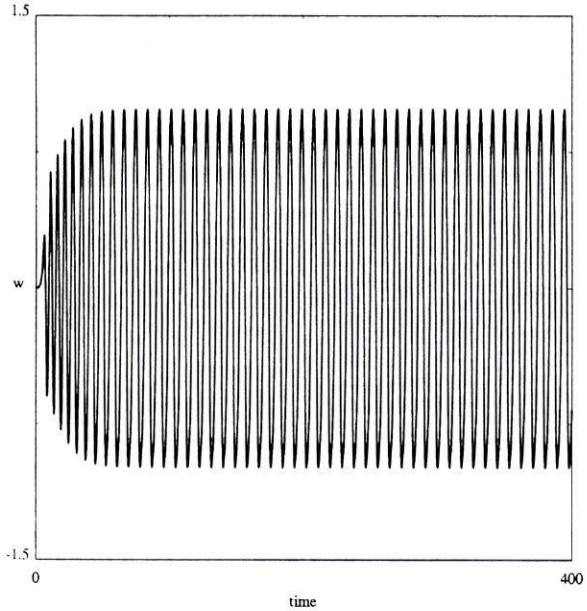

Figure 4.23: Time series for v for a trajectory with initial condition near the origin, when $\lambda = 1,\ R = 1, \alpha = 1, \beta = -0.1,\ \gamma = 1,\ \tau = 0.5$.

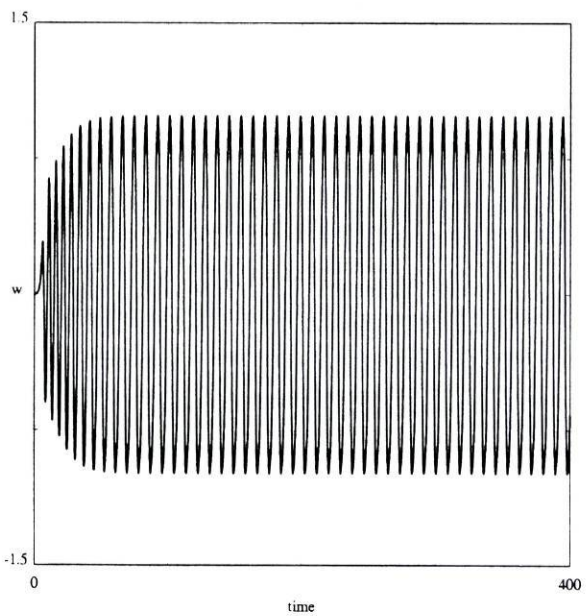

Figure 4.24: Time series for w for a trajectory with initial condition near the origin, when $\lambda = 1,\ R = 1, \alpha = 1, \beta = -0.1,\ \gamma = 1,\ \tau = 0.5$.

Now consider the following perturbation of system (4.42)

$$\begin{aligned}
\dot{x} &= x(\lambda - Rr^2) - \alpha xw + \beta xw^2 - \gamma y + \delta xv^2, \\
\dot{y} &= y(\lambda - Rr^2) - \alpha yw + \beta yw^2 + \gamma x + \nu yv^2, \\
\dot{v} &= v(\lambda - Rr^2) + \alpha vw + \beta vw^2 - \delta x^2 v - \nu y^2 v + \tau w^3, \\
\dot{w} &= w(\lambda - Rr^2) - \alpha(v^2 - x^2 - y^2) - \beta w(x^2 + y^2 + v^2) - \tau vw^2,
\end{aligned} \tag{4.47}$$

with $r^2 = x^2 + y^2 + v^2 + w^2$.

We observe numerically, using Dstool and AUTO, that as the absolute value of the parameters δ and ν increases the invariant 2-torus approaches one of the repelling periodic trajectories and then collapses into it.

When $\nu = \delta$, system (4.47) can be seen as the lift by the rotation around the plane $Fix(dq^2)$ of the three-dimensional system,

$$\begin{aligned}
\dot{\rho} &= \rho(\lambda - Rr^2) - \alpha\rho w + \beta\rho w^2 + \delta\rho v^2, \\
\dot{v} &= v(\lambda - Rr^2) + \alpha vw + \beta vw^2 + \tau w^3 - \delta\rho^2 v, \\
\dot{w} &= w(\lambda - Rr^2) - \alpha(v^2 - \rho^2) - \beta w(\rho^2 + v^2) - \tau vw^2,
\end{aligned} \tag{4.48}$$

with $r^2 = \rho^2 + v^2 + w^2$.

System (4.48) is a perturbation of system (4.43).

If system (4.48) has a Hopf bifurcation, then system (4.47) has a bifurcation from a periodic trajectory to a 2-torus.

For $\nu = \delta$, numerical simulations with AUTO revealead that for positive values of τ the equilibrium with negative v-coordinate has a subcritical Hopf bifurcation for negative values of δ and the equilibrium with positive v-coordinate has a Hopf bifurcation for positive values of δ, see figure 4.25. For negative values of τ the same happens but with opposite signs.

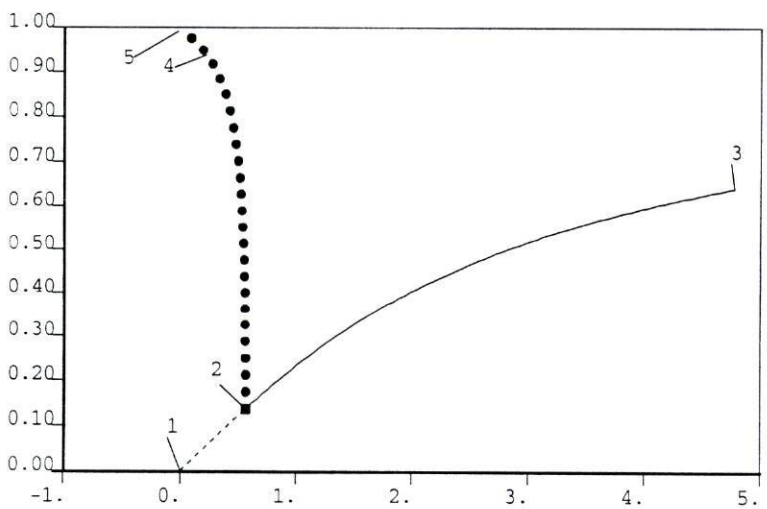

Figure 4.25: Projection in the (δ, w)-plane of the bifurcation diagram of the equilibria $(\sqrt{-\frac{\lambda}{2R}}, \sqrt{\frac{\lambda}{2R}}, 0)$ with $\nu = \delta > 0$, when $\lambda = 1,\ R = -1,\ \alpha = 1, \beta = -0.1,\ \gamma = 1,\ \tau = 0.5$. Dashed and solid curves represent, respectively, unstable and stable equilibria. Solid circles represent stable periodic trajectories. Label 2 identifies the subcritical Hopf bifurcation.

4.1.4 Third-order perturbations that preserve the invariance of the two-sphere D

Among the perturbations of system (4.16) that do not break the invariance of the hyperplane $Fix(\mathbf{Z}_2(\sigma))$ and thus that do not break the invariance of the two-sphere we can distinguish two different situations, one where the plane $Fix(SO(2))$ remains invariant and the case where it does not. In both cases the perturbations can either have $\mathbf{Z}_2(\sigma)$-symmetry or trivial symmetry.

The dynamics when $Fix(SO(2))$ is preserved is topologically equivalent to that of the unperturbed case. In the situation where $Fix(SO(2))$ is no longer invariant there will be, generically, two attracting periodic trajectories close to the heteroclinic cycle of system (4.16).

Note that, when the invariance of $Fix(SO(2))$ is broken, generically the one-dimensional connection between the equilibria p_{w_-}, p_{w_+} in that plane will be broken.

As the two-sphere in the hyperplane $Fix(\mathbf{Z}_2(\sigma))$ remains invariant, we still have the two-dimensional connection between the equilibria p_{w_-}, p_{w_+}. Thus we have two periodic trajectories on the three-sphere, one for $v < 0$ that attracts all the trajectories on the three-sphere with initial condition with $v < 0$, and one for $v > 0$ that attracts all the trajectories on the three-sphere with initial condition with $v > 0$.

Lemma 23 *A third-order perturbation of system (4.16) that preserves the invariance of the two-sphere* **D** *and breaks the invariance of* $Fix(SO(2))$ *is a linear combination of the following terms,*

$$\begin{array}{llll} (v^3,0,-xv^2,0), & (v^2w,0,0,-xv^2), & (v^2w,0,-xvw,0), & (w^3,0,0,-xw^2), \\ (vw^2,0,0,-xvw), & (0,v^3,-yv^2,0), & (0,v^2w,0,-yv^2), & (0,w^3,0,-yw^2), \\ (0,v^2w,-yvw,0), & (0,vw^2,0,-yvw). & & \end{array} \tag{4.49}$$

Proof: Direct calculation, as in lemma 17. □

4.2 Example: heteroclinic network with equilibria and a periodic trajectory

In this section we construct a family of systems in $\mathbf{R}^4$ with a globally attracting invariant three-sphere, where there is a structurally stable heteroclinic network of a group orbit of heteroclinic cycles involving four saddle-foci and a periodic trajectory. In the restriction to the three-sphere, the two-dimensional invariant manifold of the periodic trajectory intersects transversely the two-dimensional invariant manifolds of the equilibria.

As in the last section, the goal is to define systems that are simple and easy to study. The construction process is similar to that of the previous section in that we start by defining a family of systems such that, in the restriction to the invariant three-sphere the two-dimensional invariant manifold of the periodic trajectory coincides with the two-dimensional invariant manifolds of the equilibria, and then we perturb so as to get transverse intersection of those manifolds.

4.2.1 Construction of the unperturbed system

We use the designation *of type* m, n to specify that an equilibrium has m-dimensional stable manifold and n-dimensional unstable manifold.

In this section we define a system in $\mathbf{R}^4$ satisfying:

(D1) There is a three-dimensional sphere, $\mathbf{S}^3_r$, that is invariant by the flow and globally attracting, in the sense that every trajectory with nonzero initial condition is asymptotic to the sphere in forward time.

(D2) On the invariant sphere, the system has an asymptotically stable heteroclinic network involving two saddle-foci of type 2, 1, denoted by p_{v_-}, p_{v_+} ; two saddle-foci of type 1, 2, denoted by p_{w_-}, p_{w_+} ; and a hyperbolic periodic trajectory, denoted by c. The invariant manifolds of the equilibria and of the periodic trajectory satisfy, on the invariant sphere, $W^u(p_{w_-}) \cup W^u(p_{w_+}) = W^s(c)$, $W^u(c) = W^s(p_{v_-}) \cup W^s(p_{v_+})$, and $W^u(p_{v_-}) \cup W^u(p_{v_+}) = W^s(p_{w_-}) \cup W^s(p_{w_+})$. The connections from p_{v_-} and p_{v_+} to p_{w_-} and p_{w_+} are one-dimensional. The connections from p_{w_-} and p_{w_+} to c coincide with $\mathbf{D}_1 - \{p_{w_-}, p_{w_+}, c\}$, with $\mathbf{D}_1$ a two-dimensional sphere. The connections from c to p_{v_-} and p_{v_+} coincide with $\mathbf{D}_2 - \{p_{v_-}, p_{v_+}, c\}$, with $\mathbf{D}_2$ a two-dimensional sphere.

(D3) The system has no equilibria other than the origin and the four saddle-foci p_{v_-}, p_{v_+}, p_{w_-} and p_{w_+}.

(D4) In addition to the periodic trajectory c there are four hyperbolic periodic trajectories, each in one connected component of $\mathbf{S}^3_r \setminus (\mathbf{D}_1 \cup \mathbf{D}_2)$. On the invariant sphere, the four periodic trajectories are repelling.

As in the previous section we start by defining a vector field in $\mathbf{R}^3$ that lifts into $\mathbf{R}^4$ by an $SO(2)$-action. Thus, in addition to satisfying properties (D1-D4), the final system is $SO(2)$-equivariant.

4.2.1.1 Basic example in $\mathbf{R}^3$

As in the construction of the example in section 4.1.1.1, we require the three-dimensional system to have properties and symmetry adequate to be lifted to a system in $\mathbf{R}^4$ satisfying (D1-D4). Here we consider a compact Lie group G that is a finite subgroup of $O(3)$ generated by

$$p = \begin{bmatrix} 0 & 1 & 0 \\ 0 & 0 & 1 \\ 1 & 0 & 0 \end{bmatrix},$$

and

$$r_x = \begin{bmatrix} -1 & 0 & 0 \\ 0 & 1 & 0 \\ 0 & 0 & 1 \end{bmatrix}.$$

The subgroup G consists of cyclic permutations of the coordinate axes and reflections in the coordinate planes.

The fixed-point subspaces are the coordinate axes,

$$\begin{aligned} Fix(pr_\rho p^2 r_\rho p^2) &= \{(\rho, v, w) : v = 0, w = 0\}, \\ Fix(r_\rho p r_\rho p^2) &= \{(\rho, v, w) : \rho = 0, w = 0\}, \\ Fix(r_\rho p^2 r_\rho p) &= \{(\rho, v, w) : \rho = 0, v = 0\}, \end{aligned} \tag{4.50}$$

the axes,

$$\begin{aligned} Fix(p) &= \{(\rho, v, w) : w = v = \rho\}, \\ Fix(r_\rho p^2 r_\rho p^2) &= \{(\rho, v, w) : w = -v = \rho\}, \\ Fix(r_\rho p r_\rho p) &= \{(\rho, v, w) : -w = v = \rho\}, \\ Fix(r_\rho p r_\rho) &= \{(\rho, v, w) : -w = -v = \rho\}, \end{aligned} \tag{4.51}$$

and the coordinate planes,

$$\begin{aligned} Fix(r_\rho) &= \{(\rho, v, w) : \rho = 0\}, \\ Fix(p^2 r_\rho p) &= \{(\rho, v, w) : v = 0\}, \\ Fix(p r_\rho p^2) &= \{(\rho, v, w) : w = 0\}. \end{aligned} \tag{4.52}$$

In [21], Guckenheimer and Holmes show that there is an open set U of topologically equivalent vector fields in the space of C^r vector fields on $\mathbf{R}3$ that are G-equivariant such that each vector field in U has a heteroclinic cycle that is an attractor. The result is proved by analysing the dynamics of the third-order G-equivariant normal form and proving that it is structurally stable.

Inspired by the results in [21] we study in the next theorem a fifth-order perturbation of the normal form studied in [21].

Theorem 24 *Consider the family of G-equivariant vector fields in $\mathbf{R}^3$ with equations given by*

$$\begin{aligned} \dot{\rho} &= \rho\left(\lambda + \alpha\rho^2 + \beta v^2 + \gamma w^2 + \delta(v^4 - \rho^2 w^2)\right), \\ \dot{v} &= v\left(\lambda + \alpha v^2 + \beta w^2 + \gamma \rho^2 + \delta(w^4 - \rho^2 v^2)\right), \\ \dot{w} &= w\left(\lambda + \alpha w^2 + \beta \rho^2 + \gamma v^2 + \delta(\rho^4 - v^2 w^2)\right). \end{aligned} \tag{4.53}$$

For $\lambda > 0$, $\beta + \gamma = 2\alpha$, $\beta < \alpha < \gamma < 0$ and $\delta < 0$ we have:

(a) The two-sphere of radius $\sqrt{-\frac{\lambda}{\alpha}}$, denoted by $\mathbf{S}^2_r$, is invariant by the flow of (4.53) and globally attracting, in the sense that every trajectory with nonzero initial condition is asymptotic to the sphere in forward time.

(b) On the invariant sphere, the system has an asymptotically stable heteroclinic network connecting the equilibria, $p_\rho = (\pm\sqrt{-\frac{\lambda}{\alpha}}, 0, 0)$, $p_v = (0, \pm\sqrt{-\frac{\lambda}{\alpha}}, 0)$, and $p_w = (0, 0, \pm\sqrt{-\frac{\lambda}{\alpha}})$.

(c) Besides the equilibria in (b) and the origin, system (4.53) has eight unstable foci.

Proof: It is trivial to see that system (4.53) is G-equivariant.

The existence of the invariant globally attracting sphere S^2_r is easily derived from the equation of the radial component in spherical polar coordinates,

$$\dot{r} = r\left(\lambda + \alpha r^2 + (-2\alpha + \beta + \gamma) r^2 \sin^2(\theta)(\sin^2(\theta)\sin^2(\phi)\cos^2(\phi) + \cos^2(\theta))\right). \tag{4.54}$$

Since $-2\alpha + \beta + \gamma = 0$, (4.54) reduces to,

$$\dot{r} = r(\lambda + \alpha r^2). \tag{4.55}$$

Since $\lambda > 0$ and $\alpha < 0$, we have that S_r^2 is invariant and globally atractting. This proves (a).

The intersection of the invariant sphere with the coordinate axes gives the equilibria $p_\rho = (\pm\sqrt{-\frac{\lambda}{\alpha}}, 0, 0)$, $p_v = (0, \pm\sqrt{-\frac{\lambda}{\alpha}}, 0)$, and $p_w = (0, 0, \pm\sqrt{-\frac{\lambda}{\alpha}})$.

The intersection of the invariant sphere with the remaining symmetry axes produce the eight equilibria $p_{\rho vw} = (\pm\sqrt{-\frac{\lambda}{3\alpha}}, \pm\sqrt{-\frac{\lambda}{3\alpha}}, \pm\sqrt{-\frac{\lambda}{3\alpha}})$.

It is an immediate computation to show that, for the parameter values we are considering, there are no other equilibria.

To complete the proof of (c) we show that the equilibria $p_{\rho vw}$ are unstable foci: the non-radial eigenvalues of the linearization of (4.53) at these points are two complex conjugate eigenvalues with real part given by $(-\delta\lambda^2/3\alpha^2)$. This is positive since we are considering $\delta < 0$.

There are three invariant circles which correspond to the intersection of the invariant sphere with the invariant coordinate planes. The union of these circles is a heteroclinic network connecting the equilibria p_ρ, p_v and p_w, see figure 4.26.

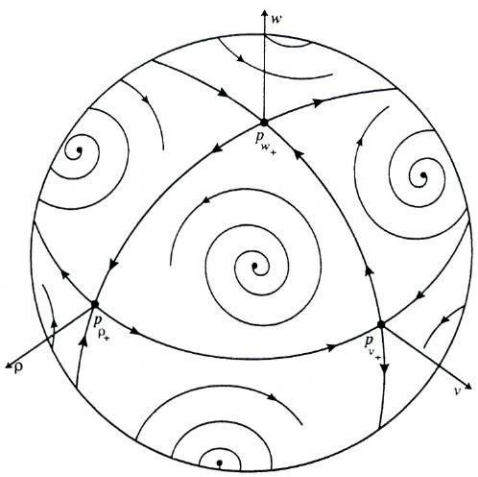

Figure 4.26: Dynamics of the three-dimensional system (4.53) restricted to the invariant two-sphere $\mathbf{S}_r^2$.

The eigenvalues of the equilibria in the heteroclinic network are -2λ in the radial direction, $\frac{\lambda(\alpha-\gamma)}{\alpha} > 0$ in the direction of $(0,1,0)$ for p_ρ, of $(0,0,1)$ for p_v, and of $(1,0,0)$

for p_w, and $\frac{\lambda(\alpha^2-\alpha\beta+\lambda\delta)}{\alpha^2} < 0$ in the direction of $(0,0,1)$ for p_ρ, of $(1,0,0)$ for p_v, and of $(0,1,0)$ for p_w.

The stability criterion in Krupa and Melbourne [34] applies to the heteroclinic network as it is the G-orbit of the heteroclinic cycles in it. Applying the criterion in [34] we conclude that the heteroclinic network is asymptotically stable. □

4.2.1.2 Example in $\mathbf{R}^4$ obtained by rotation

System (4.53) has the form

$$\begin{aligned} \dot{\rho} &= \rho F(\rho^2, v^2, w^2), \\ \dot{v} &= vG(\rho^2, v^2, w^2), \\ \dot{w} &= wH(\rho^2, v^2, w^2), \end{aligned} \tag{4.56}$$

with $F, G, H : \mathbf{R}^3 \to \mathbf{R}$.

As in the example in section 4.1.1.2, adding the auxiliary equation $\dot{\varphi} = \eta$, $\eta \in \mathbf{R}$ and interpreting the coordinates (ρ, φ) as polar coordinates, system (4.53) lifts to a system in $\mathbf{R}^4$ ((4.62) in the next theorem).

The symmetries of system (4.62) come from the symmetries of system (4.53) and from the rotation used to perform the lift. These are generated by the actions of

$$\begin{aligned} (x, y, v, w) &\overset{r_v}{\mapsto} (x, y, -v, w), \\ (x, y, v, w) &\overset{r_w}{\mapsto} (x, y, v, -w), \end{aligned} \tag{4.57}$$

and the $SO(2)$-action

$$(x, y, v, w) \overset{\varphi}{\mapsto} (x\cos\varphi - y\sin\varphi, x\sin\varphi + y\cos\varphi, v, w). \tag{4.58}$$

There are the symmetry axes,

$$\begin{aligned} Fix(\mathbf{Z}_2(r_v) \times SO(2)) &= \{(x, y, v, w) : x = y = v = 0\}, \\ Fix(\mathbf{Z}_2(r_w) \times SO(2)) &= \{(x, y, v, w) : x = y = w = 0\}, \end{aligned} \tag{4.59}$$

the symmetry planes,

$$\begin{aligned} Fix(r_v r_w) &= \{(x, y, v, w) : v = w = 0\}, \\ Fix(SO(2)) &= \{(x, y, v, w) : x = y = 0\}, \end{aligned} \tag{4.60}$$

and the symmetry hyperplanes,

$$\begin{aligned} Fix(r_v) &= \{(x, y, v, w) : v = 0\}, \\ Fix(r_w) &= \{(x, y, v, w) : w = 0\}. \end{aligned} \tag{4.61}$$

Theorem 25 *Consider the family of vector fields in* $\mathbf{R}^4$ *with equations given by*

$$\begin{aligned}
\dot{x} &= x\left(\lambda+\alpha\left(x^2+y^2\right)+\beta v^2+\gamma w^2+\delta\left(v^4-(x^2+y^2)w^2\right)\right)-\eta y,\\
\dot{y} &= y\left(\lambda+\alpha\left(x^2+y^2\right)+\beta v^2+\gamma w^2+\delta\left(v^4-(x^2+y^2)w^2\right)\right)+\eta x,\\
\dot{v} &= v\left(\lambda+\alpha v^2+\beta w^2+\gamma(x^2+y^2)+\delta\left(w^4-(x^2+y^2)v^2\right)\right),\\
\dot{w} &= w\left(\lambda+\alpha w^2+\beta(x^2+y^2)+\gamma v^2+\delta\left((x^2+y^2)^2-v^2w^2\right)\right).
\end{aligned} \tag{4.62}$$

For $\lambda>0$, $\beta+\gamma=2\alpha$, $\beta<\alpha<\gamma<0$, $\delta<0$ *and* $\eta\in\mathbf{R}$, *system (4.62) satisfies (D1)-(D4).*

Proof: To prove the theorem we look at how system (4.53) lifts to system (4.62), using the $SO(2)$-symmetry.

The two-sphere of radius $r=\sqrt{-\frac{\lambda}{\alpha}}$ lifts to a three-sphere with the same radius, denoted by $\mathbf{S}^3_r$, that is invariant by the flow of (4.62) and globally attracting.

In the flow restricted to the sphere the invariant sets are a heteroclinic network and four repelling periodic trajectories. The periodic trajectories arise from the rotation of the unstable foci $p_{\rho vw}$ in the flow of system (4.53) and have equations

$$x^2+y^2=-\frac{\lambda}{3\alpha},\qquad v=\pm\sqrt{-\frac{\lambda}{3\alpha}},\qquad w=\pm\sqrt{-\frac{\lambda}{3\alpha}}.$$

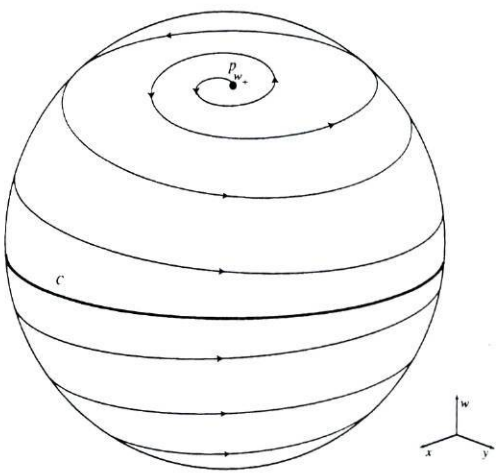

Figure 4.27: The invariant manifolds $W^u(p_{w_-})$ and $W^u(p_{w_+})$ coincide with the invariant manifold $W^s(c)$ on $\mathbf{D}_1-\{(p_{w_-},p_{w_+},c\}$, with $\mathbf{D}_1$ the invariant two-sphere that is the intersection of $Fix(r_v)$ with $\mathbf{S}^3_r$.

As the equilibria $p_{\rho vw}$ are repelling in the non-radial directions, the periodic trajectories are repelling in the restriction to the invariant three-sphere $\mathbf{S}^3_r$.

The saddles p_ρ give rise to a hyperbolic periodic trajectory, denoted by c, with equations

$$x^2 + y^2 = -\frac{\lambda}{\alpha}, \qquad v = 0, \qquad w = 0.$$

The heteroclinic network in $\mathbf{S}_r^2$ lifts to a heteroclinic network in $\mathbf{S}_r^3$ involving the periodic trajectory c and the saddles $p_v = (0, 0, \pm\sqrt{-\frac{\lambda}{\alpha}}, 0)$, $p_w = (0, 0, 0, \pm\sqrt{-\frac{\lambda}{\alpha}})$.

By construction, in the restriction to $\mathbf{S}_r^3$ we have, $W^u(p_{w_-}) \cup W^u(p_{w_+}) = W^s(c)$, $W^u(c) = W^s(p_{v_-}) \cup W^s(p_{v_+})$, and $W^u(p_{v_-}) \cup W^u(p_{v_+}) = W^s(p_{w_-}) \cup W^s(p_{w_+})$. See figures 4.27, 4.28 and 4.29, respectively.

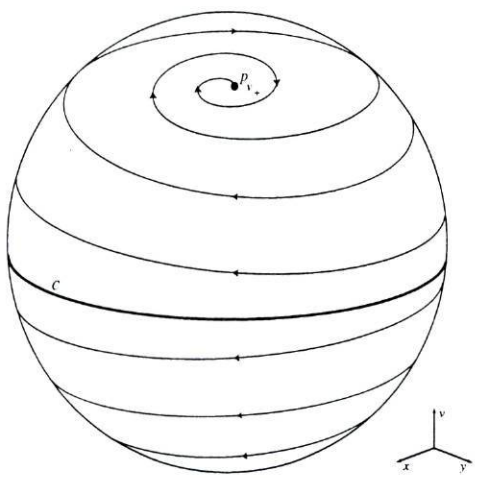

Figure 4.28: The invariant manifolds $W^s(p_{v_-})$ and $W^s(p_{v_+})$ coincide with the invariant manifold $W^u(c)$ on $\mathbf{D}_2 - \{(p_{v_-}, p_{v_+}, c\}$, with $\mathbf{D}_2$ the invariant two-sphere that is the intersection of $Fix(r_w)$ with $\mathbf{S}_r^3$.

The rotation of the invariant circle $\rho^2 + w^2 = -\frac{\lambda}{\alpha}$ in the flow of (4.53) gives rise to an invariant two-sphere of radius $r = \sqrt{-\frac{\lambda}{\alpha}}$ in the hyperplane $Fix(r_v)$, that we denote by $\mathbf{D}_1$. The equilibria p_w, the periodic trajectory c and the intersection of their two--dimensional manifolds restricted to $\mathbf{S}_r^3$ coincide with the sphere $\mathbf{D}_1$, see figure 4.27.

The rotation of the invariant circle $\rho^2 + v^2 = -\frac{\lambda}{\alpha}$ in the flow of (4.53) gives rise to an invariant two-sphere of radius $r = \sqrt{-\frac{\lambda}{\alpha}}$ in the hyperplane $Fix(r_w)$, that we denote by $\mathbf{D}_2$. The equilibria p_v, the periodic trajectory c and the intersection of their two--dimensional manifolds restricted to $\mathbf{S}_r^3$ coincide with the sphere $\mathbf{D}_2$, see figure 4.28.

The invariant two-spheres $\mathbf{D}_1$ and $\mathbf{D}_2$ intersect each other on the periodic trajectory c, and $\mathbf{S}_r^3 \setminus (\mathbf{D}_1 \cup \mathbf{D}_2)$ has four connected components.

The one-dimensional connections from equilibria p_v to equilibria p_w on the invariant circle $v^2 + w^2 = \frac{\lambda}{R}$ remain and correspond to the intersection of $Fix(SO(2))$ with $\mathbf{S}^3_r$, see figure 4.29.

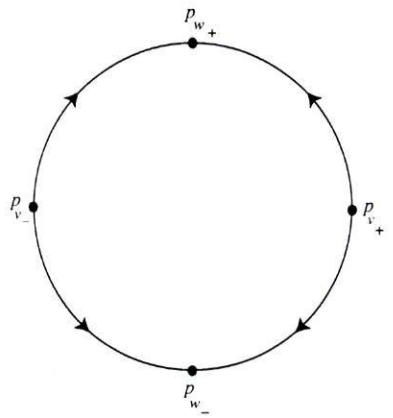

Figure 4.29: The one-dimensional connections from equilibria p_v to equilibria p_w on the invariant circle that is the intersection of of $Fix(SO(2))$ with $\mathbf{S}^3_r$.

The periodic trajectory c is, as we have already noticed, the group orbit of the saddles p_ρ by the $SO(2)$-action, i.e., it is a relative equilibrium. *Relative equilibria* are group orbits that are invariant under the flow of an equivariant vector field (see Krupa [32]).

In [32], Krupa shows that near a relative equilibrium the vector field can be decomposed as the sum of two equivariant vector fields: one tangent and the other normal to the group orbit. He shows that the asymptotic dynamics of the vector field can be determined by the asymptotic dynamics of the normal vector field modulo drifts along the group orbit.

In our particular case this means that the asymptotic stability of the periodic trajectory c is given by the asymptotic stability of the equilibria p_ρ. Then, the asymptotic stability of the heteroclinic network in $\mathbf{S}^3_r$ follows from the asymptotic stability of the heteroclinic network in $\mathbf{S}^2_r$, since the same stability criterion applies (see [34] and theorem 2.10 in [37]).

This ends the proof. □

4.2.2 $SO(2)$-breaking perturbation

We want to perturb system (4.62) preserving properties (D1)-(D4) but with the two--dimensional invariant manifolds intersecting transversely instead of coinciding in the restriction to the three-sphere. That is, we want to look for a perturbation that keeps the invariance of the globally attracting three-sphere, destroys the invariance of the two invariant two-spheres $\mathbf{D}_1$ and $\mathbf{D}_2$ in the hyperplanes $Fix(r_v)$ and $Fix(r_w)$, respectively, preserving the equilibria, the hyperbolic periodic trajectory and the repelling periodic trajectories.

Necessary conditions for this are that the perturbation be zero in the x and y components; the perturbing term in $\dot{v}$ contain the variable w and be nonzero when $v = 0$; the perturbing term in $\dot{w}$ contain the variable v and be nonzero when $w = 0$. Taking into account lemma 16 in section 4.1.2, the third order perturbing terms that satisfy these conditions are $(0, 0, x^2w, -x^2v)$, $(0, 0, xyw, -xyv)$ and $(0, 0, y^2w, -y^2v)$. Note that these are not sufficient conditions since no linear combination of these terms preserves the invariance of the repelling periodic trajectories. This problem is overcome by multiplying the third-order perturbations by the norm of (x, y), obtaining a perturbation of order five:

$$\begin{aligned}
\dot{x} &= x\left(\lambda + \alpha\left(x^2+y^2\right) + \beta v^2 + \gamma w^2 + \delta\left(v^4 - (x^2+y^2)w^2\right)\right) - \eta y,\\
\dot{y} &= y\left(\lambda + \alpha\left(x^2+y^2\right) + \beta v^2 + \gamma w^2 + \delta\left(v^4 - (x^2+y^2)w^2\right)\right) + \eta x,\\
\dot{v} &= v\left(\lambda + \alpha v^2 + \beta w^2 + \gamma(x^2+y^2) + \delta\left(w^4 - (x^2+y^2)v^2\right)\right) + \xi xyw\left(\lambda + 3\alpha(x^2+y^2)\right),\\
\dot{w} &= w\left(\lambda + \alpha w^2 + \beta(x^2+y^2) + \gamma v^2 + \delta\left((x^2+y^2)^2 - v^2w^2\right)\right) - \xi xyv\left(\lambda + 3\alpha(x^2+y^2)\right).
\end{aligned} \tag{4.63}$$

Figures 4.30 and 4.31 represent the projection in the (v, w)-plane of trajectories in the flow of the unperturbed system (4.62) and perturbed system (4.63), respectively.

The origin corresponds to the projection of the periodic trajectory c, the intersections of the axes $w = 0$ and $v = 0$ with the circle are, respectively, the equilibria $p_{v_\pm}$ and $p_{w_\pm}$.

In Figure 4.30, the line segments on the axes $w = 0$ and $v = 0$, inside the circle, correspond to the projection of the two-spheres D_1 and D_2.

Figure 4.30 represents the projection of four trajectories in the flow of the unperturbed system (4.62), each with initial conditions on the invariant three-sphere lying on one of the four connected components of $\mathbf{S}^3_r \setminus (D_1 \cup D_2)$. We observe that trajectories with initial conditions on the invariant three-sphere lying on one of the connected components of $\mathbf{S}^3_r \setminus (D_1 \cup D_2)$ remain on that same component.

Figure 4.31 represents just one trajectory in the flow of the perturbed system (4.63). We observe that the trajectory goes through each of the four connected components of $\mathbf{S}^3_r \setminus (D_1 \cup D_2)$.

Looking at the time series in figures 4.33 and 4.35 we can see that the transitions between the connected components of $\mathbf{S}^3_r \setminus (D_1 \cup D_2)$ are irregular and at irregular transition times.

The comparison of the time series in figures 4.32 and 4.33, and 4.34 and 4.35 is also elucidatory.

Figures 4.36 and 4.37 are the time series for the variable x for the flow of systems (4.62) and (4.63), respectively.

In figure 4.36, we observe the flow jumping sucessively from one equilibrium to the periodic trajectory, and form the periodic trajectory to another equilibrium, each time staying longer near each equilibrium and the periodic trajectory. The return times increase monotonically and very fast.

For the same values of the commom parameters, the perturbed flow keeps jumping sucessively from one equilibrium to the periodic trajectory, and form the periodic trajectory to another equilibrium, but seems to do it at irregular time intervals and the return times no longer grow.

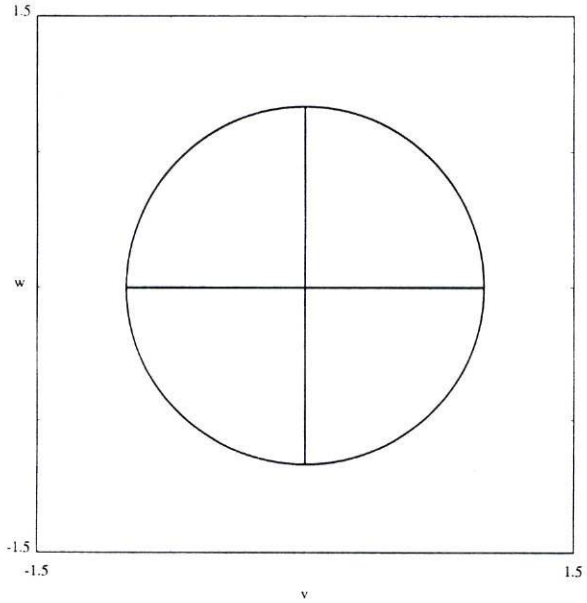

Figure 4.30: Projection in the (v, w)-plane of the four trajectories with initial conditions $(0.001, 0.001, 0.001, 1)$, $(0.001, 0.001, -0.001, 1)$, $(0.001, 0.001, 0.001, -1)$ and $(0.001, 0.001, -0.001, -1)$, for the flow of the unperturbed system (4.62) when $\lambda = 0.33333333$, $\alpha = -0.33333333$, $\beta = -0.5$, $\gamma = -0.16666667$ and $\delta = 0 - 0.05$.

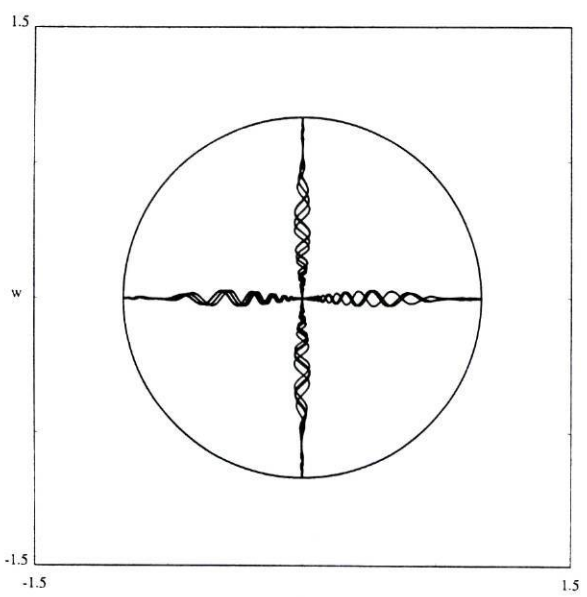

Figure 4.31: Projection in the (v, w)-plane of the trajectory with initial condition $(0.001, 0.001, 0.001, 1)$, for the flow of the perturbed system (4.63) when $\lambda = 0.33333333$, $\alpha = -0.33333333$, $\beta = -0.5$, $\gamma = -0.16666667$, $\delta = 0 - 0.05$ and $\xi = -1$.

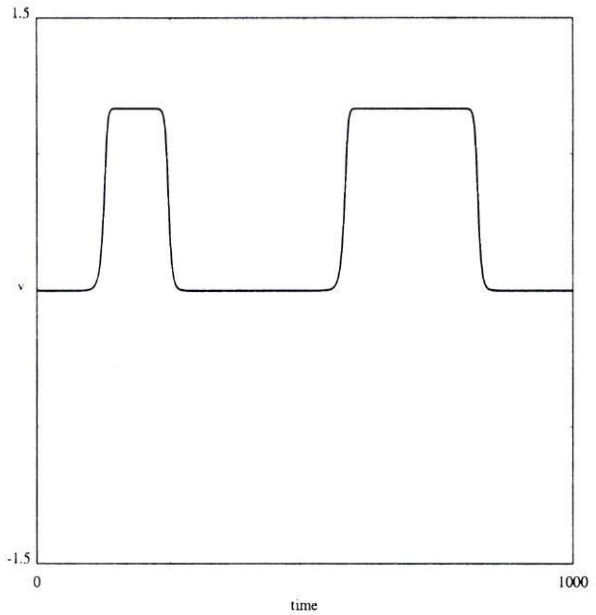

Figure 4.32: Time series for v for a trajectory with initial condition $(0.001, 0.001, 0.001, 1)$, for the flow of the unperturbed system (4.62) when $\lambda = 0.33333333$, $\alpha = -0.33333333$, $\beta = -0.5$, $\gamma = -0.16666667$ and $\delta = 0 - 0.05$.

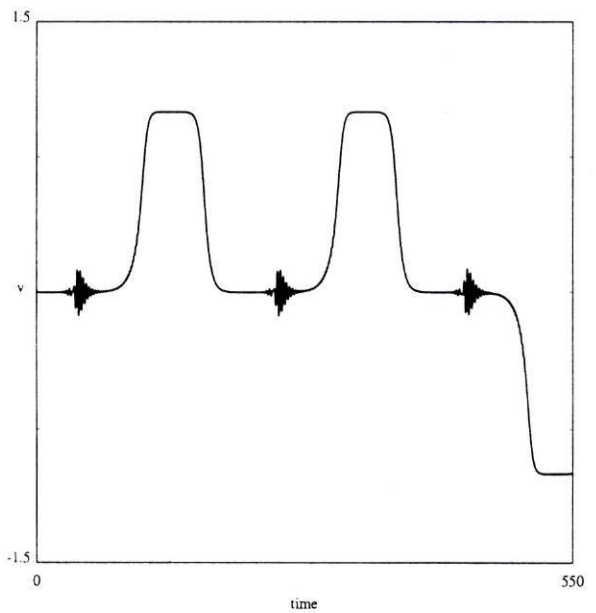

Figure 4.33: Time series for v for a trajectory with initial condition $(0.001, 0.001, 0.001, 1)$, for the flow of the perturbed system (4.63) when $\lambda = 0.33333333$, $\alpha = -0.33333333$, $\beta = -0.5$, $\gamma = -0.16666667$, $\delta = 0 - 0.05$ and $\xi = -1$.

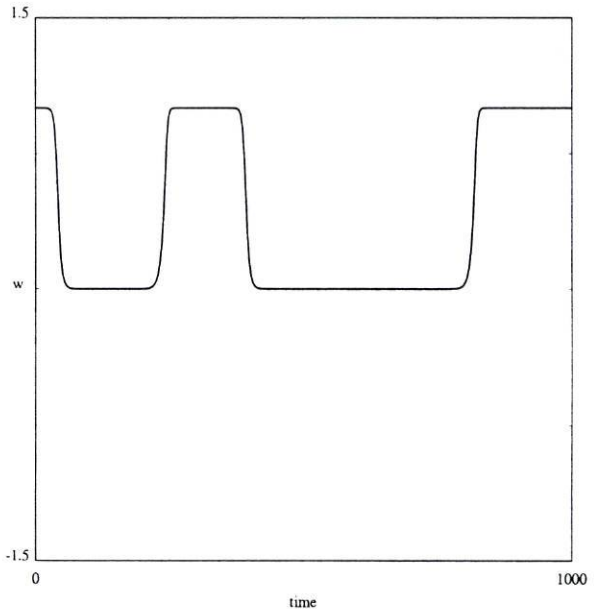

Figure 4.34: Time series for w for a trajectory initial condition $(0.001, 0.001, 0.001, 1)$, for the flow of the unperturbed system (4.62) when $\lambda = 0.33333333$, $\alpha = -0.33333333$, $\beta = -0.5$, $\gamma = -0.16666667$ and $\delta = 0 - 0.05$.

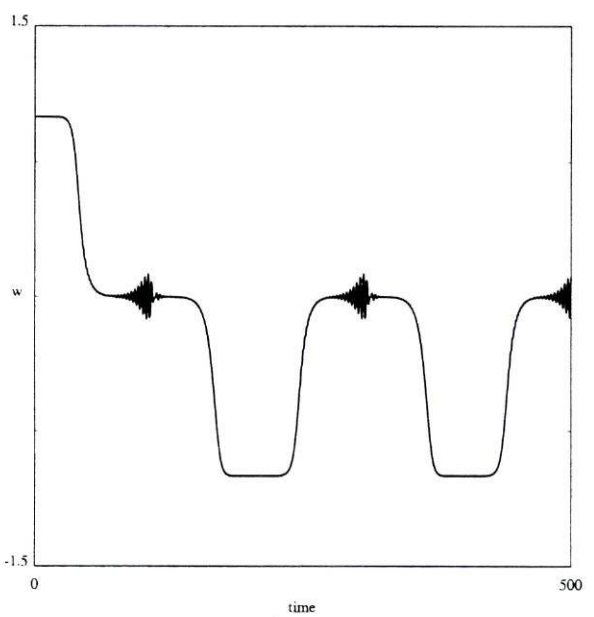

Figure 4.35: Time series for w for a trajectory with initial condition $(0.001, 0.001, 0.001, 1)$, for the flow of the perturbed system (4.63) when $\lambda = 0.33333333$, $\alpha = -0.33333333$, $\beta = -0.5$, $\gamma = -0.16666667$, $\delta = 0 - 0.05$ and $\xi = -1$.

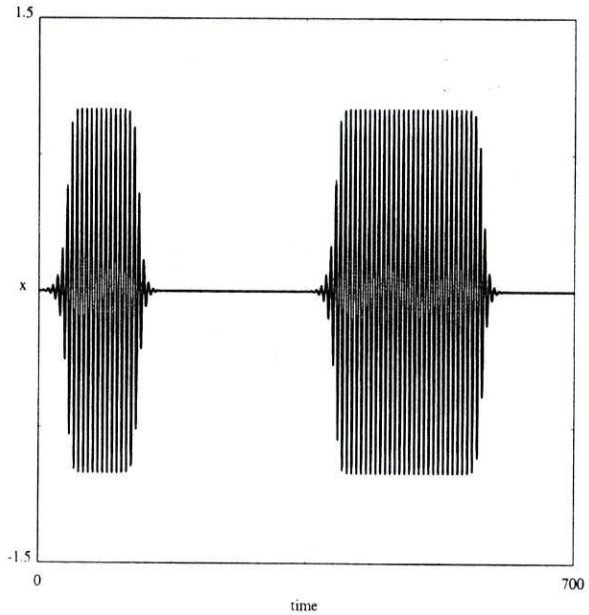

Figure 4.36: Time series for x for a trajectory with initial condition $(0.001, 0.001, 0.001, 1)$, for the flow of the unperturbed system (4.62) when $\lambda = 0.33333333$, $\alpha = -0.33333333$, $\beta = -0.5$, $\gamma = -0.16666667$ and $\delta = 0 - 0.05$.

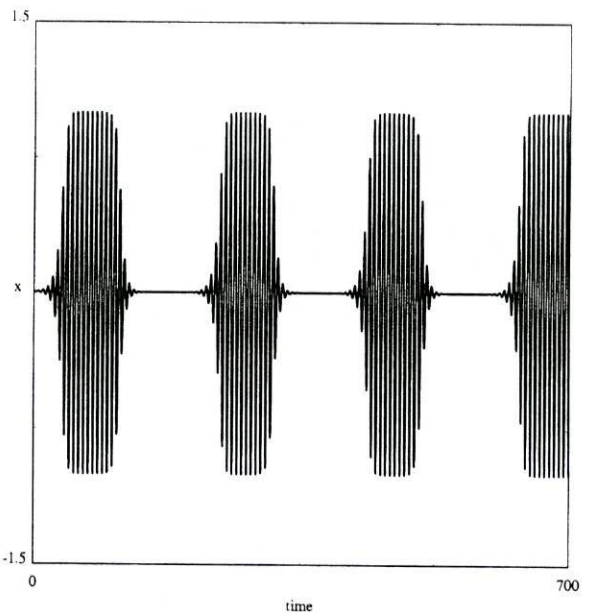

Figure 4.37: Time series for x for a trajectory with initial condition $(0.001, 0.001, 0.001, 1)$, for the flow of the perturbed system (4.63) when $\lambda = 0.33333333$, $\alpha = -0.33333333$, $\beta = -0.5$, $\gamma = -0.16666667$, $\delta = 0 - 0.05$ and $\xi = -1$.

Theorem 26 *For $\lambda > 0$, $\beta + \gamma = 2\alpha$, $\beta < \alpha < \gamma < 0$, $\delta < 0$, $\eta \in \mathbf{R}$ and for values of ξ sufficiently small and such that $|\xi| < \frac{-\alpha\beta+\alpha\gamma+\delta\lambda}{2\lambda\alpha}$ and $\xi^2 < \frac{(\gamma-\beta)(2\delta\lambda-\alpha\beta+\alpha\gamma)}{4\alpha\lambda^2}$ system (4.63) satisfies*

(D1) There is a three-dimensional sphere, $\mathbf{S}^3_r$, that is invariant by the flow and globally attracting, in the sense that every trajectory with nonzero initial condition is asymptotic to the sphere in forward time.

(D3) The only equilibria are the origin and the four saddle-foci $p_{\pm v}$ and $p_{\pm w}$. On the invariant sphere, $p_{\pm v}$ are of type $2,1$ and $p_{\pm w}$ are of type $1,2$.

(D5) In the restriction to the invariant sphere, system (4.63) has a structurally stable heteroclinic network involving the four saddle-foci $p_{\pm v}$ and $p_{\pm w}$, and the periodic trajectory c. When $\alpha(\beta - \alpha) + \delta\lambda > 0$ the two dimensional manifolds of the periodic trajectory intersect transversely the two-dimensional manifolds of the saddle-foci $p_{\pm v}$ and $p_{\pm w}$.

(D) In addition to the periodic trajectory c, the system has four hyperbolic periodic trajectories each in one connected component of $\mathbf{S}^3_r \setminus (\mathbf{D}_1 \cup \mathbf{D}_2)$. On the invariant sphere, the four periodic trajectories are repelling.

Proof: System (4.63) is a fifth-order perturbation of system (4.62) that is tangent to the three-sphere, thus the three-sphere remains invariant and globally attracting, and (D1) is verified.

We consider the equations of system (4.63) in spherical polar coordinates,

$$\begin{aligned}
\dot{r} &= r(\lambda + \alpha r^2),\\
\dot{\theta} &= \tfrac{r^2}{2}\sin(2\theta)\left[(\alpha-\beta)(1-2\cos^2(\phi)) + \delta r^2(\cos^2(\theta)\cos^2(\phi) - \sin^2(\theta)\sin^4(\phi))\right] +\\
&\quad + \tfrac{\xi}{4} r^2 \sin^2(\theta)\sin(\phi)\sin(2\phi)\sin(2\varphi)(\lambda + 3\alpha r^2\sin^2(\theta)\sin^2(\phi)),\\
\dot{\phi} &= \tfrac{r^2}{2}\sin(2\phi)\left[(\beta-\alpha)(1-3\cos^2(\theta)) + \delta r^2(-1+\sin^2(\theta)(1+\cos^2(\phi)))\right] -\\
&\quad - \tfrac{\xi}{4} r^2 \sin(2\theta)\sin^3(\phi)\sin(2\varphi)(\lambda + 3\alpha r^2\sin^2(\theta)\sin^2(\phi)),\\
\dot{\varphi} &= \eta.
\end{aligned} \tag{4.64}$$

From the equation for $\dot{\varphi}$ we get $\varphi(t) = \eta t$, $t \in \mathbf{R}$. Following the proof of theorem 18

in section 4.1.3.1, we replace φ by ηt and consider the reduced system,

$$\begin{aligned}
\dot{r} &= r(\lambda + \alpha r^2), \\
\dot{\theta} &= \tfrac{r^2}{2}\sin(2\theta)\left[(\alpha - \beta)(1 - 2\cos^2(\phi)) + \delta r^2(\cos^2(\theta)\cos^2(\phi) - \sin^2(\theta)\sin^4(\phi))\right] + \\
&\quad + \tfrac{\xi}{4} r^2 \sin^2(\theta)\sin(\phi)\sin(2\phi)\sin(2\eta t)(\lambda + 3\alpha r^2 \sin^2(\theta)\sin^2(\phi)), \\
\dot{\phi} &= \tfrac{r^2}{2}\sin(2\phi)\left[(\beta - \alpha)(1 - 3\cos^2(\theta)) + \delta r^2(-1 + \sin^2(\theta)(1 + \cos^2(\phi)))\right] - \\
&\quad - \tfrac{\xi}{4} r^2 \sin(2\theta)\sin^3(\phi)\sin(2\eta t)(\lambda + 3\alpha r^2 \sin^2(\theta)\sin^2(\phi)).
\end{aligned} \tag{4.65}$$

Note that although the equations for $\dot{\theta}$ and $\dot{\phi}$ in (4.65) are time dependent, they are time-periodic with period $\frac{2\pi}{\eta}$. Thus system (4.64) can be seen as the lift by the rotation of system (4.65).

System (4.65) with $\xi = 0$ represents the equations of the three-dimensional unperturbed system (4.53) in spherical polar coordinates. System (4.65) with $\xi \neq 0$ is a nonautonomous perturbation.

The equilibria of the unperturbed system, p_ρ, p_v, p_w, and $p_{\rho vw}$, persist for $\xi \neq 0$. We show that, for ξ sufficiently small, there are no other equilibria.

System (4.65) has the same number of zeros for $\xi = 0$ and $\xi \neq 0$ if and only if, for $r^2 = -\frac{\lambda}{\alpha}$, the two curves $\dot{\theta} = 0$ and $\dot{\phi} = 0$ intersect at the same number of points for $\xi = 0$ and $\xi \neq 0$. Since the Jacobian matrix of $(\dot{\theta}, \dot{\phi})$ for $\xi = 0$ at the intersection points is nondegenerate, we have that the curves intersect transversely at those points. We can thus conclude that, for $\xi \neq 0$ and sufficiently small, there are no other intersection points and thus there are no other equilibria of (4.65).

The non-radial eigenvalues of the linearization of (4.65) at p_ρ are

$$\frac{\left(\delta\lambda \pm \sqrt{(\delta\lambda - \alpha\beta + \alpha\gamma)^2 - 4\xi^2 \sin^2(2\varphi)\alpha^2\lambda^2}\right)\lambda}{2\alpha^2}.$$

For the parameter values we are considering, equilibria p_ρ are saddles in the restriction of the flow of (4.65) to the invariant two-sphere, and lift by the rotation to the hyperbolic periodic trajectory c in the flow of system (4.63).

The equilibria $p_{\rho vw}$ lift to four periodic trajectories in the flow of system (4.63) and are given by the same equations as the periodic trajectories in the four-dimensional unperturbed system (4.62).

The non-radial eigenvalues of the linearization of (4.65) at $p_{\rho vw}$ are

$$\frac{\left(-\delta\lambda \pm \sqrt{(-\alpha\beta + \alpha\gamma + \delta\lambda)(-3(-\alpha\beta + \alpha\gamma + \delta\lambda) + 2\lambda\xi\alpha\sin(2\varphi))}\right)\lambda}{3\alpha^2}.$$

For the parameter values we are considering, equilibria $p_{\rho vw}$ are unstable foci.

This proves (D3) and (D6).

Finally, we prove that in the flow of system (4.63) restricted to the invariant three--sphere, the two-dimensional invariant manifolds of the periodic trajectory and of the equilibria intersect transversely. This implies that the two-dimensional manifold connecting the periodic trajectory to the equilibria breaks to a transverse intersection, that is, into heteroclinic connections that arise in the transverse intersection of the invariant manifolds. Specifically, we prove that the two-dimensional heteroclinic connection from p_{w_-} to c and the two-dimensional heteroclinic connection from p_{w_+} to c in the two-dimensional sphere $x^2+y^2+w^2=\frac{-\lambda}{\alpha}$, $v=0$ break into transverse heteroclinic connections. Analogously, the two-dimensional heteroclinic connection from c to p_{v_-} and the two-dimensional heteroclinic connection from c to p_{v_+} in the two-dimensional sphere $x^2+y^2+v^2=\frac{-\lambda}{\alpha}$, $w=0$ break into transverse heteroclinic connections.

Using the same approach as in section 4.1.3.1, we prove this by equivalently proving the tranversal intersection of the corresponding invariant manifolds in the flow of system (4.65), and to do this we apply Melnikov's method ([20], section 4.5). Melnikov's method was initially defined for a system with a homoclinic saddle connection. But it naturally generalizes to the case of more than one saddle connection, that is, to the heteroclinic case (see Bertozzi [6]).

Instead of working with system (4.65), we consider its restriction to the invariant two-sphere $\mathbf{S}^2_r$ of radius $r=\sqrt{-\frac{\lambda}{\alpha}}$,

$$\begin{aligned}
\dot{\theta} &= \tfrac{r^2}{2}\sin(2\theta)\left[(\alpha-\beta)(1-2\cos^2(\phi))+\delta r^2(\cos^2(\theta)\cos^2(\phi)-\sin^2(\theta)\sin^4(\phi))\right]+\\
&\quad +\tfrac{\xi}{4}r^2\sin^2(\theta)\sin(\phi)\sin(2\phi)\sin(2\eta t)(\lambda+3\alpha r^2\sin^2(\theta)\sin^2(\phi)),\\
\dot{\phi} &= \tfrac{r^2}{2}\sin(2\phi)\left[(\beta-\alpha)(1-3\cos^2(\theta))+\delta r^2(-1+\sin^2(\theta)(1+\cos^2(\phi)))\right]-\\
&\quad -\tfrac{\xi}{4}r^2\sin(2\theta)\sin^3(\phi)\sin(2\eta t)(\lambda+3\alpha r^2\sin^2(\theta)\sin^2(\phi)),
\end{aligned} \tag{4.66}$$

with $r=\sqrt{-\frac{\lambda}{\alpha}}$.

From now on and until the end of this section we fix $r=\sqrt{-\frac{\lambda}{\alpha}}$. System (4.66) has the form,

$$\begin{aligned}
\tfrac{d\theta}{dt} &= f_1(\theta,\phi)+\xi g_1(\theta,\phi,t),\\
\tfrac{d\phi}{dt} &= f_2(\theta,\phi)+\xi g_2(\theta,\phi,t),
\end{aligned} \tag{4.67}$$

with

$$\begin{aligned} f_1(\theta,\phi) &= \tfrac{r^2}{2}\sin(2\theta)\left[(\alpha-\beta)(1-2\cos^2(\phi))+\delta r^2(\cos^2(\theta)\cos^2(\phi)-\sin^2(\theta)\sin^4(\phi))\right], \\ f_2(\theta,\phi) &= \tfrac{r^2}{2}\sin(2\phi)\left[(\beta-\alpha)(1-3\cos^2(\theta))+\delta r^2(-1+\sin^2(\theta)(1+\cos^2(\phi)))\right], \\ g_1(\theta,\phi,t) &= \tfrac{r^2}{4}\sin^2(\theta)\sin(\phi)\sin(2\phi)\sin(2\eta t)(\lambda+3\alpha r^2\sin^2(\theta)\sin^2(\phi)), \\ g_2(\theta,\phi,t) &= -\tfrac{r^2}{4}\sin(2\theta)\sin^3(\phi)\sin(2\eta t)(\lambda+3\alpha r^2\sin^2(\theta)\sin^2(\phi)), \end{aligned} \tag{4.68}$$

where g_1 and g_2 are periodic in t with period $\frac{2\pi}{\eta}$.

The unperturbed system is non-Hamiltonian, so the Melnikov function is given by,

$$M(t_0)=\int_{-\infty}^{\infty} f(q_0(t))\wedge g(q_0(t),t+t_0)exp\left(-\int_0^t traceDf(q_0(s))ds\right)dt,$$

with $q_0(t)$ a parametrization of the unperturbed heteroclinic connection, $f=(f_1,f_2)$, $g=(g_1,g_2)$, ([20], section 4.5).

First, we prove that the two unperturbed two-dimensional heteroclinic connections in $Fix(r_v)\cap \mathbf{S}^3_r$, that is, in $x^2+y^2+w^2=-\frac{\lambda}{\alpha}$ with $v=0$, perturb to transverse heteroclinic connections. In spherical polar coordinates the corresponding heteroclinic connections in the flow of system (4.66) are given by $q_0(t)=(\theta(t),\phi)$ with $\theta(t)\in]0,\frac{\pi}{2}[$ or $\theta(t)\in]\frac{\pi}{2},\pi[$ and with $\phi=\frac{\pi}{2}$ or $\phi=\frac{3\pi}{2}$.

For $\phi=\frac{\pi}{2}$ we have,

$$\begin{aligned} f_1(q_0(t)) &= \tfrac{r^2}{2}\sin(2\theta(t))\left(\alpha-\beta-\delta r^2\sin^2(\theta(t))\right), \\ f_2(q_0(t)) &= 0, \\ g_1(q_0(t),t+t_0) &= 0, \\ g_2(q_0(t),t+t_0) &= -\tfrac{r^2}{4}\sin(2\theta(t))\sin(2\eta(t+t_0))(\lambda+3\alpha r^2\sin^2(\theta(t))), \end{aligned} \tag{4.69}$$

then,

$$\begin{aligned} f(q_0(t))\wedge g(q_0(t),t+t_0) &= f_1(q_0(t))g_2(q_0(t),t+t_0)-f_2(q_0(t))g_1(q_0(t),t+t_0)= \\ &= -\tfrac{r^4}{8}\sin^2(2\theta(t))\sin(2\eta(t+t_0)) \\ &\qquad (\alpha-\beta-\delta r^2\sin^2(\theta(t)))(\lambda+3\alpha r^2\sin^2(\theta(t))), \end{aligned} \tag{4.70}$$

and

$$trace\left[Df(q_0(t))\right]=r^2\left((\beta-\alpha)\cos^2(\theta(t))+\delta r^2\cos^2(2\theta(t))\right).$$

For $\phi=\frac{\pi}{2}$ we have the following equation for $\dot{\theta}$,

$$\dot{\theta} = \tfrac{r^2}{2}\sin(2\theta(t))\left(\alpha-\beta-\delta r^2\sin^2(\theta(t))\right). \tag{4.71}$$

For $\phi=\frac{\pi}{2}$, we obtain the Melnikov function,

$$M(t_0)=\textstyle\int_{-\infty}^{\infty}\sin(2\eta(t+t_0))E(t)dt, \tag{4.72}$$

with

$$E(t) = -\frac{r^4}{8}\sin^2(2\theta(t))(\alpha-\beta-\delta r^2\sin^2(\theta(t)))(\lambda+3\alpha r^2\sin^2(\theta(t)))e^{\left[-\int_0^t r^2((\beta-\alpha)\cos^2(\theta(s))+\delta r^2\cos^2(2\theta(s)))\right]}.$$

In the case $\phi = \frac{3\pi}{2}$ we obtain the same Melnikov function up to a minus sign, so the conclusions below also apply.

Since the integral in (4.72) converges both for $\theta(t) \in]0, \frac{\pi}{2}[$ and for $\theta(t) \in]\frac{\pi}{2}, \pi[$, see lemma 27 below, in both cases $M(t_0)$ can be written as:

$$M(t_0) = \int_{-\infty}^{\infty} \sin(2\eta t)\cos(2\eta t_0)E(t)dt + \int_{-\infty}^{\infty} \cos(2\eta t)\sin(2\eta t_0)E(t)dt.$$

Let $S = \int_{-\infty}^{\infty} \sin(2\eta t)E(t)dt$ and $C = \int_{-\infty}^{\infty} \cos(2\eta t)E(t)dt$, then

$$M(t_0) \;=\; \cos(2\eta t_0)S + \sin(2\eta t_0)C \tag{4.73}$$

From (4.73), the Melnikov function has infinitely many zeros given by

$$\tan(2\eta t_0) \;=\; -\frac{C}{S}, \qquad t_0 \in \mathbf{R}. \tag{4.74}$$

The zeros t_0' of the Melnikov function are simple if $\frac{dM}{dt_0}(t_0') \neq 0$. We have from (4.73),

$$\frac{dM}{dt_0}(t_0) \;=\; -2\eta\sin(2\eta(t_0))S + 2\eta\cos(2\eta(t_0))C \tag{4.75}$$

Thus the zeros t_0' of the Melnikov function are simple provided

$$\tan(2\eta t_0') \;\neq\; \frac{S}{C}, \qquad t_0 \in \mathbf{R}, \tag{4.76}$$

which is trivially verified, since the zeros t_0' of $M(t_0)$ satisfy (4.74).

This proves that the heteroclinic connections given by $q_0(t) = (\theta(t), \phi)$ with $\theta(t) \in]0, \frac{\pi}{2}[$ or $\theta(t) \in]\frac{\pi}{2}, \pi[$ and with $\phi = \frac{\pi}{2}$ or $\phi = \frac{3\pi}{2}$ break into transverse heteroclinic connections and thus that the two heteroclinic connections in $Fix(r_v) \cap \mathbf{S}_r^3$, from p_{w_-} to c and from p_{w_+} to c, break into transverse heteroclinic connections.

Finally, we prove that the two unperturbed two-dimensional heteroclinic connections in $Fix(r_w) \cap \mathbf{S}_r^3$, that is, in $x^2 + y^2 + v^2 = -\frac{\lambda}{\alpha}$ with $w = 0$, perturb to transverse heteroclinic connections. In spherical polar coordinates the corresponding heteroclinic connections in the flow of system (4.66) are given by $q_0(t) = (\theta, \phi(t))$ with $\phi(t) \in]0, \frac{\pi}{2}[$ or $\phi(t) \in]\frac{\pi}{2}, \pi[$ and with $\theta = \frac{\pi}{2}$ or $\theta = \frac{3\pi}{2}$.

We have, for $\theta = \frac{\pi}{2}$ or $\theta = \frac{3\pi}{2}$,

$$\begin{aligned} f_1(q_0(t)) &= 0, \\ f_2(q_0(t)) &= \tfrac{r^2}{2}\sin(2\phi(t))\left(\beta - \alpha + \delta r^2\cos^2(\phi(t))\right), \\ g_1(q_0(t), t+t_0) &= \tfrac{r^2}{4}\sin(\phi(t))\sin(2\phi(t))\sin(2\eta(t+t_0))(\lambda + 3\alpha r^2\sin^2(\phi(t))), \\ g_2(q_0(t), t+t_0) &= 0, \end{aligned} \tag{4.77}$$

then,

$$\begin{aligned} f(q_0(t)) \wedge g(q_0(t), t+t_0) &= f_1(q_0(t))g_2(q_0(t), t+t_0) - f_2(q_0(t))g_1(q_0(t), t+t_0) = \\ &= -\tfrac{r^4}{8}\sin(\phi(t))\sin^2(2\phi(t))\sin(2\eta(t+t_0))(\beta - \alpha + \delta r^2\cos^2(\phi(t)))(\lambda + 3\alpha r^2\sin^2(\phi(t))), \end{aligned} \tag{4.78}$$

and

$$trace\left[Df(q_0(t))\right] = \delta r^4\left((\sin^2(\phi) - \cos^2(\phi))^2 - \sin^2(\phi)\cos^2(\phi)\right).$$

For $\theta = \frac{\pi}{2}$ or $\theta = \frac{3\pi}{2}$ we have the following equation for $\dot{\phi}$,

$$\dot{\phi} = \tfrac{r^2}{2}\sin(2\phi(t))\left(\beta - \alpha + \delta r^2\cos^2(\phi(t))\right). \tag{4.79}$$

We obtain the Melnikov function,

$$M(t_0) = \int_{-\infty}^{\infty}\sin(2\eta(t+t_0))E(t)dt,$$

with

$$E(t) = f(t)e^{\left[-\int_0^t \delta r^4\left((\sin^2(\phi(s))-\cos^2(\phi(s)))^2-\sin^2(\phi(s))\cos^2(\phi(s))\right)ds\right]},$$

and

$$f(t) = -\frac{r^4}{8}\sin(\phi(t))\sin^2(2\phi(t))(\beta - \alpha + \delta r^2\cos^2(\phi(t)))(\lambda + 3\alpha r^2\sin^2(\phi(t))).$$

Since the Melnikov integral converges both for $\phi(t) \in]0, \frac{\pi}{2}[$ and for $\phi(t) \in]\frac{\pi}{2}, \pi[$, by lemma 28 below, in both cases it can be written as,

$$M(t_0) = \int_{-\infty}^{\infty}\sin(2\eta t)\cos(2\eta t_0)E(t)dt + \int_{-\infty}^{\infty}\cos(2\eta t)\sin(2\eta t_0)E(t)dt,$$

and the proof follows as in the previous case. We conclude that the heteroclinic connections given by $q_0(t) = (\theta, \phi(t))$ with $\phi(t) \in]0, \frac{\pi}{2}[$ or $\phi(t) \in]\frac{\pi}{2}, \pi[$ and with $\theta = \frac{\pi}{2}$ or $\theta = \frac{3\pi}{2}$ break into transverse heteroclinic connections and thus that the two heteroclinic connections in $Fix(r_w) \cap \mathbf{S}^3_r$, from c to p_{v_-} and from c to p_{v_+}, break into transverse heteroclinic connections. □

Lemma 27 *The Melnikov integral*

$$M(t_0) = \int_{-\infty}^{\infty} \sin(2\eta(t+t_0)) f(t) e^{-g(t)} dt,$$

with

$$f(t) = -\frac{r^4}{8} \sin^2(2\theta(t))(\alpha - \beta - \delta r^2 \sin^2(\theta(t)))(\lambda + 3\alpha r^2 \sin^2(\theta(t))),$$

and

$$g(t) = \int_0^t r^2 \left((\beta - \alpha)\cos^2(\theta(s)) + \delta r^2 \cos^2(2\theta(s))\right) ds,$$

converges both for $\theta(t) \in]0, \frac{\pi}{2}[$ *and for* $\theta(t) \in]\frac{\pi}{2}, \pi[$.

Proof: In order to prove that $M(t_0)$ converges, and since $\sin(2\eta(t+t_0))$ is bounded, it is sufficient to prove that

$$\int_{-\infty}^{\infty} f(t) e^{-g(t)} dt$$

converges.

We first compute $e^{-g(t)} = e^{-\int_0^t r^2\left((\beta-\alpha)\cos^2(\theta(s))+\delta r^2\cos^2(2\theta(s))\right)ds}$.

Recall that,

$$\dot{\theta} = \frac{r^2}{2} \sin(2\theta(t)) \left(\alpha - \beta - \delta r^2 \sin^2(\theta(t))\right). \tag{4.80}$$

We do the variable change $u = \theta(s)$ and get

$$g(t) = \int_{\theta(0)}^{\theta(t)} r^2 \left((\beta - \alpha)\cos^2(u) + \delta r^2 \cos^2(2u)\right) \frac{du}{\dot{\theta}}.$$

Computations with Maple give

$$g(t) = \ln J(u) \Big]_{\theta(0)}^{\theta(t)},$$

with

$$J(u) = \frac{\left(\tan^2(\frac{u}{2}) - 1\right)^{\frac{-\delta r^2}{(\alpha-\beta)-\delta r^2}} \left(\alpha - \beta + 2(\alpha - \beta - 2\delta r^2)\tan^2(\frac{u}{2}) + (\alpha - \beta)\tan^4(\frac{u}{2})\right)^{\frac{5(\alpha-\beta)^2+\delta r^2(5(\beta-\alpha)+\delta r^2)}{2(\alpha-\beta)^2-2\delta r^2(\alpha-\beta)}}}{\left(\tan(\frac{u}{2})\right)^{\frac{(\alpha-\beta)^2-\delta r^2(2(\alpha-\beta)-\delta r^2)}{(\alpha-\beta)^2-\delta r^2(\alpha-\beta)}} \left(1+\tan^2(\frac{u}{2})\right)^{\frac{4(\alpha-\beta)-4\delta r^2}{(\alpha-\beta)-\delta r^2}}},$$

and we have

$$e^{-g(t)} = J(\theta(0)) J(\theta(t))^{-1}. \tag{4.81}$$

To prove that $\int_{-\infty}^{\infty} f(t) e^{-g(t)} dt$ converges, it is sufficient to prove that

$$\int_{-\infty}^{\infty} f(t) J(\theta(t))^{-1} dt \tag{4.82}$$

converges.

One of the heteroclinic connections that we are considering corresponds to $\theta(t) \in]0, \pi/2[, \forall t \in \mathbf{R}$ and the other to $\theta(t) \in]\pi/2, \pi[, \forall t \in \mathbf{R}$. Since we are considering parameter values such that $\alpha - \beta > 0$ and $\delta < 0$, we have $\dot{\theta} > 0$ for $\theta \in]0, \pi/2[$, and $\dot{\theta} < 0$ for $\theta \in]\pi/2, \pi[$. For the connection in $\theta(t) \in [0, \pi/2]$, we have $\lim_{t\to-\infty} \theta(t) = 0$, $\lim_{t\to+\infty} \theta(t) = \pi/2$. For the connection in $\theta(t) \in [\pi/2, \pi]$, we have $\lim_{t\to-\infty} \theta(t) = \pi$, $\lim_{t\to+\infty} \theta(t) = \pi/2$.

By the arguments above, for the heteroclinic connection in $\theta(t) \in [0, \pi/2], \forall t \in \mathbf{R}$, (4.82) is equal to

$$\int_0^{\frac{\pi}{2}} \frac{-\frac{r^4}{8}\sin^2(2\theta)(\alpha-\beta-\delta r^2\sin^2(\theta))(\lambda+3\alpha r^2\sin^2(\theta))}{\frac{r^2}{2}\sin(2\theta)\big(\alpha-\beta-\delta r^2\sin^2(\theta)\big)J(\theta)}d\theta =$$

$$= \int_0^{\frac{\pi}{2}} \frac{-\frac{r^4}{8}\sin^2(2\theta)(\alpha-\beta-\delta r^2\sin^2(\theta))(\lambda+3\alpha r^2\sin^2(\theta))\big(\tan(\frac{\theta}{2})\big)^{\frac{(\alpha-\beta)^2-\delta r^2(2(\alpha-\beta)-\delta r^2)}{(\alpha-\beta)^2-\delta r^2(\alpha-\beta)}}\big(1+\tan^2(\frac{\theta}{2})\big)^{\frac{4(\alpha-\beta)-4\delta r^2}{(\alpha-\beta)-\delta r^2}}}{\frac{r^2}{2}\sin(2\theta)\big(\alpha-\beta-\delta r^2\sin^2(\theta)\big)\big(\tan^2(\frac{\theta}{2})-1\big)^{\frac{-\delta r^2}{(\alpha-\beta)-\delta r^2}}\big(\alpha-\beta+2(\alpha-\beta-2\delta r^2)\tan^2(\frac{\theta}{2})+(\alpha-\beta)\tan^4(\frac{\theta}{2})\big)^{\frac{5(\alpha-\beta)^2+\delta r^2(5(\beta-\alpha)+\delta r^2)}{2(\alpha-\beta)^2-2\delta r^2(\alpha-\beta)}}}d\theta =$$

$$= \int_0^{\frac{\pi}{2}} \frac{-\frac{r^2}{4}\sin(2\theta)(\lambda+3\alpha r^2\sin^2(\theta))\big(\tan(\frac{\theta}{2})\big)^{\frac{(\alpha-\beta)^2-\delta r^2(2(\alpha-\beta)-\delta r^2)}{(\alpha-\beta)^2-\delta r^2(\alpha-\beta)}}\big(1+\tan^2(\frac{\theta}{2})\big)^{\frac{4(\alpha-\beta)-4\delta r^2}{(\alpha-\beta)-\delta r^2}}}{\big(\tan^2(\frac{\theta}{2})-1\big)^{\frac{-\delta r^2}{(\alpha-\beta)-\delta r^2}}\big(\alpha-\beta+2(\alpha-\beta-2\delta r^2)\tan^2(\frac{\theta}{2})+(\alpha-\beta)\tan^4(\frac{\theta}{2})\big)^{\frac{5(\alpha-\beta)^2+\delta r^2(5(\beta-\alpha)+\delta r^2)}{2(\alpha-\beta)^2-2\delta r^2(\alpha-\beta)}}}d\theta$$

$$= \int_0^{\frac{\pi}{2}} I(\theta)d\theta$$

We prove that $\int_0^{\frac{\pi}{2}} I(\theta)d\theta$ converges by proving that $I(\theta)$ is bounded in $[0, \frac{\pi}{2}]$. For the parameter values we are working with, the exponents in $I(\theta)$ are all positive, the numerator in $I(\theta)$ is bounded in $[0, \frac{\pi}{2}]$ and

$$\left(\alpha-\beta+2(\alpha-\beta-2\delta r^2)\tan^2(\frac{\theta}{2})+(\alpha-\beta)\tan^4(\frac{\theta}{2})\right)^{\frac{5(\alpha-\beta)^2+\delta r^2(5(\beta-\alpha)+\delta r^2)}{2(\alpha-\beta)^2-2\delta r^2(\alpha-\beta)}} > 0.$$

It only remains to see that $I(\theta)$ is bounded when $\theta = \frac{\pi}{2}$, that is, when $\big(\tan^2(\frac{\theta}{2})-1\big)^{\frac{-\delta r^2}{(\alpha-\beta)-\delta r^2}}$ is zero.

We have that

$$\begin{aligned} &\lim_{\theta\to\frac{\pi}{2}} \frac{\sin(2\theta)}{\big(\tan^2(\frac{\theta}{2})-1\big)^{\frac{-\delta r^2}{(\alpha-\beta)-\delta r^2}}} = \\ &\lim_{\theta\to\frac{\pi}{2}} -4\sin(\frac{\theta}{2})(\cos(\frac{\theta}{2}))^{(2\frac{-\delta r^2}{(\alpha-\beta)-\delta r^2}+1)}(1-\cos^2(\frac{\theta}{2}))^{(1-\frac{-\delta r^2}{(\alpha-\beta)-\delta r^2})}, \end{aligned} \tag{4.83}$$

which is zero, since $0 < \frac{-\delta r^2}{(\alpha-\beta)-\delta r^2} < 1$.

This completes the proof for the heteroclinic connection in $\theta(t) \in [0, \pi/2], \forall t \in \mathbf{R}$. For the heteroclinic connection in $\theta(t) \in [\pi/2, \pi], \forall t \in \mathbf{R}$ the proof is analogous. □

Lemma 28 *The Melnikov integral*

$$M(t_0) = \int_{-\infty}^{\infty} \sin(2\eta(t+t_0)) f(t) e^{-g(t)} dt,$$

with

$$f(t) = -\frac{r^4}{8} \sin(\phi(t)) \sin^2(2\phi(t))(\beta - \alpha + \delta r^2 \cos^2(\phi(t)))(\lambda + 3\alpha r^2 \sin^2(\phi(t))),$$

and

$$g(t) = \int_0^t \delta r^4 \left((\sin^2(\phi(s)) - \cos^2(\phi(s)))^2 - \sin^2(\phi(s)) \cos^2(\phi(s)) \right) ds,$$

converges both for $\phi(t) \in]0, \frac{\pi}{2}[$ *and for* $\phi(t) \in]\frac{\pi}{2}, \pi[$.

Proof: In order to prove that $M(t_0)$ converges, and since $\sin(2\eta(t+t_0))$ is bounded, it is sufficient to prove that

$$\int_{-\infty}^{\infty} f(t) e^{-g(t)} dt$$

converges.

We first compute $e^{-g(t)} = e^{-\int_0^t \delta r^4 \left((\sin^2(\phi(s)) - \cos^2(\phi(s)))^2 - \sin^2(\phi(s)) \cos^2(\phi(s)) \right) ds}$.

Recall that,

$$\dot{\phi} = \frac{r^2}{2} \sin(2\phi(t)) \left(\beta - \alpha + \delta r^2 \cos^2(\phi(t)) \right). \tag{4.84}$$

We do the variable change $u = \phi(s)$ and get

$$g(t) = \int_{\phi(0)}^{\phi(t)} \delta r^4 \left((\sin^2(u) - \cos^2(u))^2 - \sin^2(u) \cos^2(u) \right) \frac{du}{\dot{\phi}}.$$

Computations with Maple give

$$g(t) = \ln J(u) \Big]_{\phi(0)}^{\phi(t)},$$

with

$$J(u) = \frac{\left((\beta - \alpha - \delta r^2) + 2(\beta - \alpha - \delta r^2) \tan^2(\frac{u}{2}) + (\beta - \alpha + \delta r^2) \tan^4(\frac{u}{2}) \right)^{\frac{5(\alpha-\beta)^2 + \delta r^2 (5(\beta-\alpha) + \delta r^2)}{2(\beta-\alpha)(\beta-\alpha+\delta r^2)}} (\tan(\frac{u}{2}))^{\frac{\delta r^2}{\beta - \alpha + \delta r^2}}}{(1 + \tan^2(\frac{u}{2}))^5 (1 - \tan^2(\frac{u}{2}))^{\frac{\delta r^2 (\beta - \alpha + \delta r^2)}{(\beta-\alpha)(\beta-\alpha+\delta r^2)}}},$$

and we have

$$e^{-g(t)} = J(\phi(0)) J(\phi(t))^{-1}. \tag{4.85}$$

To prove that $\int_{-\infty}^{\infty} f(t)e^{-g(t)}dt$ converges, it is sufficient to prove that

$$\int_{-\infty}^{\infty} f(t)J(\phi(t))^{-1}dt \tag{4.86}$$

converges.

One of the heteroclinic connections that we are considering corresponds to $\phi(t) \in]0, \pi/2[, \forall t \in \mathbf{R}$ and the other to $\phi(t) \in]\pi/2, \pi[, \forall t \in \mathbf{R}$. Since we are considering parameter values such that $\beta - \alpha < 0$ and $\delta < 0$, we have $\dot{\phi} < 0$ for $\phi \in]0, \pi/2[$, and $\dot{\phi} > 0$ for $\phi \in]\pi/2, \pi[$. For $\phi(t) \in [0, \pi/2]$, we have $\lim_{t\to-\infty} \phi(t) = \pi/2$, $\lim_{t\to+\infty} \phi(t) = 0$. For $\phi(t) \in [\pi/2, \pi]$, we have $\lim_{t\to-\infty} \phi(t) = \pi/2$, $\lim_{t\to+\infty} \phi(t) = \pi$.

By the arguments above, for the heteroclinic connection in $\phi(t) \in [0, \pi/2], \forall t \in \mathbf{R}$, (4.86) is equal to

$$\int_{\frac{\pi}{2}}^{0} \frac{-\frac{r^4}{8}\sin(\phi)\sin^2(2\phi)(\beta-\alpha+\delta r^2\cos^2(\phi))(\lambda+3\alpha r^2\sin^2(\phi))}{\frac{r^2}{2}\sin(2\phi)(\beta-\alpha+\delta r^2\cos^2(\phi))J(\phi)}d\phi =$$

$$= \int_{\frac{\pi}{2}}^{0} \frac{-\frac{r^4}{8}\sin(\phi)\sin^2(2\phi)(\beta-\alpha+\delta r^2\cos^2(\phi))(\lambda+3\alpha r^2\sin^2(\phi))\left(1+\tan^2(\frac{\phi}{2})\right)^5\left(1-\tan^2(\frac{\phi}{2})\right)^{\frac{\delta r^2(\beta-\alpha+\delta r^2)}{(\beta-\alpha)(\beta-\alpha+\delta r^2)}}}{\frac{r^2}{2}\sin(2\phi)\left(\beta-\alpha+\delta r^2\cos^2(\phi)\right)\left((\beta-\alpha-\delta r^2)+2(\beta-\alpha-\delta r^2)\tan^2(\frac{\phi}{2})+(\beta-\alpha+\delta r^2)\tan^4(\frac{\phi}{2})\right)^{\frac{5(\alpha-\beta)^2+\delta r^2\left(5(\beta-\alpha)+\delta r^2\right)}{2(\beta-\alpha)(\beta-\alpha+\delta r^2)}}\left(\tan(\frac{\phi}{2})\right)^{\frac{\delta r^2}{\beta-\alpha+\delta r^2}}}d\phi =$$

$$= \int_{\frac{\pi}{2}}^{0} \frac{-\frac{r^2}{4}\sin(\phi)\sin(2\phi)(\lambda+3\alpha r^2\sin^2(\phi))\left(1+\tan^2(\frac{\phi}{2})\right)^5\left(1-\tan^2(\frac{\phi}{2})\right)^{\frac{\delta r^2(\beta-\alpha+\delta r^2)}{(\beta-\alpha)(\beta-\alpha+\delta r^2)}}}{\left((\beta-\alpha-\delta r^2)+2(\beta-\alpha-\delta r^2)\tan^2(\frac{\phi}{2})+(\beta-\alpha+\delta r^2)\tan^4(\frac{\phi}{2})\right)^{\frac{5(\alpha-\beta)^2+\delta r^2\left(5(\beta-\alpha)+\delta r^2\right)}{2(\beta-\alpha)(\beta-\alpha+\delta r^2)}}\left(\tan(\frac{\phi}{2})\right)^{\frac{\delta r^2}{\beta-\alpha+\delta r^2}}}d\phi =$$

$$= \int_{\frac{\pi}{2}}^{0} I(\phi)d\phi$$

We prove that $\int_{\frac{\pi}{2}}^{0} I(\phi)d\phi$ converges by proving that $I(\phi)$ is bounded in $[0, \frac{\pi}{2}]$. For the parameter values we are working with, the factors appearing in the numerator are indeed in the numerator (and the same for the denominator). The numerator in $I(\phi)$ is bounded in $[0, \frac{\pi}{2}]$ and, since $\alpha(\beta - \alpha) + \delta\lambda > 0$,

$$\left((\beta-\alpha-\delta r^2)+2(\beta-\alpha-\delta r^2)\tan^2(\frac{\phi}{2})+(\beta-\alpha+\delta r^2)\tan^4(\frac{\phi}{2})\right)^{\frac{5(\alpha-\beta)^2+\delta r^2\left(5(\beta-\alpha)+\delta r^2\right)}{2(\beta-\alpha)(\beta-\alpha+\delta r^2)}} \neq 0.$$

Thus, it only remains to see that $I(\phi)$ is bounded when $\phi = 0$, that is, when $\left(\tan(\frac{\phi}{2})\right)^{\frac{\delta r^2}{\beta-\alpha+\delta r^2}}$ is zero.

We have that

$$\begin{aligned} &\lim_{\phi\to 0} \frac{\sin(\phi)\sin(2\phi)}{\left(\tan(\frac{\phi}{2})\right)^{\frac{\delta r^2}{\beta-\alpha+\delta r^2}}} = \\ &= \lim_{\phi\to 0} 8\left(\sin(\tfrac{\phi}{2})\right)^{2-\frac{\delta r^2}{\beta-\alpha+\delta r^2}}(2\cos^2(\tfrac{\phi}{2})-1)(\cos(\tfrac{\phi}{2}))^{\frac{\delta r^2}{\beta-\alpha+\delta r^2}+2}, \end{aligned} \tag{4.87}$$

which is zero, since $1 < 2 - \frac{\delta r^2}{\beta-\alpha+\delta r^2} < 2$.

This completes the proof for the heteroclinic connection in $\phi(t) \in [0, \pi/2], \forall t \in \mathbf{R}$. For the heteroclinic connection in $\phi(t) \in [\pi/2, \pi], \forall t \in \mathbf{R}$ the proof is analogous. □

Chapter 5

Dynamics near Shilnikov heteroclinic cycles

In section 3.4 we analysed the structure and symmetry of the Shilnikov heteroclinic network Σ in Field's example. The quotient heteroclinic network Σ/Γ is the union of three heteroclinic cycles, see figures 3.5 and 3.6 in section 3.4. One of the cycles connects two saddle-foci, another the two saddle-foci with a periodic trajectory, and the remaining is a cycle homoclinic to the periodic trajectory.

The aim of this chapter is to study the local dynamics in the neighbourhood of the quotient heteroclinic cycles. We generalize the study to any flow on a three-dimensional manifold having a Shilnikov heteroclinic cycle topologically equivalent to each of the quotient heteroclinic cycles.

In section 5.1 we consider the case of a heteroclinic cycle involving two saddle-foci, and in section 5.2 that of a homoclinic connection to a periodic trajectory. We find conditions for the existence of chaotic dynamics in the neigbourhood of such heteroclinic and homoclinic cycles by finding conditions for horseshoe dynamics.

The heteroclinic cycle involving two saddle-foci and a periodic trajectory leads to considerably bigger technical difficulties, and we will not study it here. Nevertheless, we claim that it is possible to find conditions for horseshoe dynamics in the neighbourhood of such heteroclinic cycle and that techniques as in section 5.1 apply.

The study of the local dynamics in the neighbourhood of homoclinic and heteroclinic cycles containing saddle-foci started with Shilnikov. Shilnikov proved the existence of horseshoe dynamics in the neighbourhood of an orbit homoclinic to a hyperbolic

saddle-focus of a third-order differential equation in Shilnikov [41], and of a fourth--order differential equation in Shilnikov [42]. The local dynamics in the neighbourhood of a heteroclinic cycle containing a saddle-focus in $\mathbf{R}^3$, was first studied by Tresser [44]. The study of these, and other cases of homoclinic and heteroclinic motion, can be found in chapter 3 of [45].

We use standard techniques, we reduce our study to a Poincaré map that describes the underlying flow in a neighbourhood of the cycles. (For an explanation on Poincaré maps, see section 1.5 of Guckenheimer and Holmes [20] and section 1.6 of Wiggins [45].)

In section 5.1, the local dynamics of the flow near the heteroclinic cycle is decomposed into linear dynamics within cylindrical neighbourhoods around the invariant saddles and regular dynamics within tubes around the heteroclinic connections.

In section 5.2, the local flow near the homoclinic cycle is discretized by the derivation of a first return map around the cycle defined on a section transverse to the flow in a point of the periodic trajectory.

We prove that those Poincaré maps are Smale horseshoe maps ([20], section 5.1 and [45], section 2.1). Thus, the local dynamics of the flows in the neighbourhood of the heteroclinic cycles is suspended horseshoe dynamics.

Any Smale horseshoe map Ψ possesses an invariant Cantor set, (Simmons [43], section 11), Λ such that the restriction of Ψ to Λ is homeomorphic to the shift on two symbols ([20], theorem 5.2.7).

This suffices to guarantee that the restriction of Ψ to the invariant Cantor set has a countable set of periodic orbits of arbitrarily long periods, an uncountable set of bounded nonperiodic motions and a dense orbit ([20], theorem 5.1.2), leading to chaotic dynamics.

5.1 Connecting two saddle-foci

5.1.1 Introduction

We consider a generic flow on a three-dimensional manifold satisfying the following hypothesis:

(A) There is a Shilnikov heteroclinic cycle with two equilibria, e_1 and e_2, that are

saddle-foci of type 2, 1 and 1, 2, respectively. There are two invariant curves (see figure 5.1),

$$W^s(e_2) = W^u(e_1), \tag{5.1}$$

and,

$$W^s(e_1) \pitchfork W^u(e_2). \tag{5.2}$$

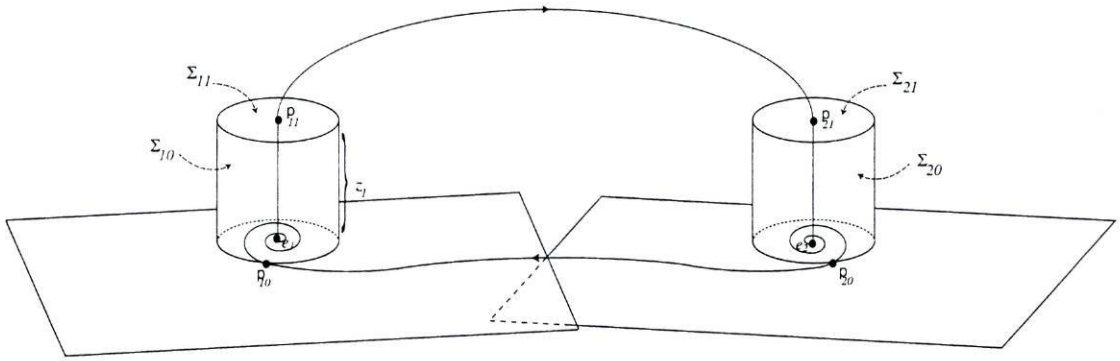

Figure 5.1: Shilnikov heteroclinic cycle in a three-dimensional flow connecting two saddle-foci.

We shall prove that under certain conditions, there is horseshoe dynamics in the neighbourhood of such heteroclinic cycle. The proof is inspired by section 6.5 of [20] and sections 3.2 and 3.3 of [45]. We define a Poincaré map, Ψ, composed of local transition maps defined in cylindrical neighbourhoods of the sadde-foci, given by the linearized flow near those points, and connecting diffeomorphisms between the cylindrical neighbourhood of one saddle and the cylindrical neighbourhood of the other saddle, given by the nonsingular dynamics in a tubular neighbourhood around the heteroclinic connections. Then, we show that the dynamics of the Poincaré map is of horseshoe type.

To prove the existence of Smale horseshoes in the dynamics of the Poincaré map Ψ we shall consider a rectangle, R, iterate it by Ψ and prove the validity of hypotheses $H1$ and $H3$ of theorem 5.2.4 of [20], called here conditions B and C:

(B) We can find two partitions, H and V, of R into strips, such that the strips in H are transverse to the strips in V, and two disjoint strips in H are mapped by Ψ into two disjoint strips in V. When this happens we say that the image of R by the Poincaré map Ψ meets R in a horseshoe-like form. This means that Ψ has the qualitative behavior of a horseshoe map f in which f takes a rectangle

R, stretches it in the vertical direction, compresses it in the horizontal direction, turns it and places it over itself (see section 5.1 of [20] and section 2.1 of [45]).

This geometrical behaviour is the reason for the Poincaré map Ψ on its invariant set to be topologically conjugate to a full shift on two symbols.

(C) We can find two complementary bundles of sectors, S^u and S^s, such that $D\Psi$ maps S^u into S^u while expanding each vector in S^u, and $D\Psi^{-1}$ maps S^s into S^s while expanding each vector in S^s.

This hyperbolicity condition implies the invariant set of the Poincaré map Ψ to be a Cantor set.

By Theorem 5.2.4 in [20], conditions B and C guarantee that the Poincaré map Ψ possesses an invariant Cantor set of points Λ that is hyperbolic and Ψ restricted to Λ is homeomorphic to the shift on two symbols.

For a detailed and more formal explanation see sections 5.1 and 5.2 of [20], or sections2.1 and 2.3 of [45].

In the next sections we define cylindrical neighbourhoods of each of the equilibria e_1 and e_2 in the heteroclinic cycle. Then we define a Poincaré map on the wall of one of those cylindrical neigbourhoods. In Theorem 30 we give sufficient conditions for the existence of rectangles, on the wall of the cylinder, that satisfy condition B and then in Theorem 31 we find conditions under which the rectangles satisfy condition C.

5.1.2 Poincaré map

Let λ_{e_j} and $\alpha_{e_j} \pm i\beta_{e_j}$ be the eigenvalues of e_j, $j = 1, 2$. We assume

(H1) $\lambda_{e_1} > 0$, $\alpha_{e_1} < 0$, $\beta_{e_1} > 0$, $\lambda_{e_2} < 0$ $\alpha_{e_2} > 0$, $\beta_{e_2} > 0$, and $\frac{\alpha_{e_1}\lambda_{e_2}}{\lambda_{e_1}\alpha_{e_2}} < 1$,

and consider a neighbourhood of e_j, N_{e_j}, $j = 1, 2$, where the flow is linearizable.

The stable manifold theorem (see [20], theorem 1.3.2), allows us to introduce local coordinates $(x_{e_1}, y_{e_1}, z_{e_1})$ in N_{e_1} such that the local unstable manifold of e_1, $W^u_{loc}(e_1)$, is contained in the z_{e_1}-axis and the local stable manifold, $W^s_{loc}(e_1)$, is contained in (x_{e_1}, y_{e_1})-plane. Similarly, we introduce local coordinates $(x_{e_2}, y_{e_2}, z_{e_2})$ in N_{e_2} such

that the local stable manifold of e_2, $W^s_{loc}(e_2)$, is contained in the z_{e_2}-axis, and the local unstable manifold, $W^u_{loc}(e_2)$, is contained in (x_{e_2}, y_{e_2})-plane (see figure5.1).

For ease of computations we use polar coordinates (r_{e_j}, θ_{e_j}), $j = 1, 2$, such that

$$\begin{aligned} x_{e_j} &= r_{e_j} \cos(\theta_{e_j}), \\ y_{e_j} &= r_{e_j} \sin(\theta_{e_j}). \end{aligned}$$

In N_{e_j}, $j = 1, 2$ we define the surfaces

$$\begin{aligned} \Sigma_{j0} &= \{(x_{e_j}, y_{e_j}, z_{e_j}) : r_{e_j} = r_0 \text{ and } 0 < z_{e_j} < z_1\}, \\ \Sigma_{j1} &= \{(x_{e_j}, y_{e_j}, z_{e_j}) : r_{e_j} < r_0 \text{ and } 0 < z_{e_j} = z_1\}. \end{aligned}$$

Denote by p_{11} the intersection of $W^u(e_1)$ with Σ_{11}, by p_{21} the intersection of $W^u(e_1)$ with Σ_{21}. Let p_{20} be a point in $W^u(e_2) \cap W^s(e_1) \cap \Sigma_{20}$ and p_{10} the point on the trajectory of p_{20} that intersects Σ_{10}, see figure 5.1. We take p_{j0}, $j = 1, 2$ as the origin of the coordinates (θ_{e_j}, z_{e_j}) in Σ_{j0}.

In what follows we define a Poincaré map Ψ in a rectangular neighbourhood R_{e_1} of p_{10} in Σ_{10}, for points in R_{e_1} whose image by the flow return to R_{e_1}. Then we show the existence of Smale horseshoes in the dynamics of the Poincaré map.

Linearizing the flow in N_{e_j}, $j = 1, 2$ we define two diffeomorphisms

$$\varphi_{e_1} : \Sigma_{10} \to \Sigma_{11} \qquad \text{and} \qquad \varphi_{e_2} : \Sigma_{21} \to \Sigma_{20}.$$

By the Hartman-Grobman theorem, φ_{e_1} and φ_{e_2} are good approximations of the flow near the equilibria.

The trajectory from p_{11} to p_{21} and from p_{20} to p_{10} is nonsingular. Hence we shall define a diffeomorphism from a neighbourhood of p_{11} in Σ_{11} into a neighbourhood of p_{21} in Σ_{21}

$$\phi_{e_1 e_2} : \Sigma_{11} \to \Sigma_{21}$$

and a diffeomorphism from a neighbourhood of p_{20} in Σ_{20} into a neighbourhood of p_{10} in Σ_{10}

$$\phi_{e_2 e_1} : \Sigma_{20} \to \Sigma_{10}.$$

These diffeomorphims are given by applying the flow box theorem around the heteroclinic connections.

The Poincaré map Ψ is defined as the composition of the above diffeomorphisms

$$\Psi = \phi_{e_2e_1} \circ \varphi_{e_2} \circ \phi_{e_1e_2} \circ \varphi_{e_1}.$$

A direct computation yields,

$$\varphi_{e_1}(\theta_{e_1}, z_{e_1}) = \left(r_0 \left(\frac{z_1}{z_{e_1}} \right)^{\frac{\alpha_{e_1}}{\lambda_{e_1}}}, \theta_{e_1} + \frac{\beta_{e_1}}{\lambda_{e_1}} \ln \left(\frac{z_1}{z_{e_1}} \right) \right) = (r_{e_1}, \theta_{e_1}), \tag{5.3}$$

and

$$\varphi_{e_2}(r_{e_2}, \theta_{e_2}) = \left(\frac{\beta_{e_2}}{\alpha_{e_2}} \ln \left(\frac{r_0}{r_{e_2}} \right) + \theta_{e_2}, (\frac{r_0}{r_{e_2}})^{\frac{\lambda_{e_2}}{\alpha_{e_2}}} z_1 \right) = (\theta_{e_2}, z_{e_2}). \tag{5.4}$$

In a flow-box around the one-dimensional connection $W^u(e_1) = W^s(e_2)$ the map $\phi_{e_1e_2} : \Sigma_{11} \to \Sigma_{21}$ can be approximated by a perturbation, with ε, δ small, of the identity map given by the diagonal matrix,

$$\begin{bmatrix} 1+\varepsilon & 0 \\ 0 & 1+\delta \end{bmatrix}.$$

We shall see in the next section that the geometry of the Poincaré map is the same if we take $\phi_{e_1e_2}$ to be the identity, but this perturbation is essential in obtaining hyperbolicity, as we shall see in section 5.1.4. There is no loss of generality in choosing a diagonal perturbation - this may always be obtained by a suitable choice of coordinates and by incorporating any rotation in the map φ_{e_2}.

Since the two-dimensional manifolds $W^u(e_2)$ and $W^s(e_1)$ are transverse, we consider the diffeomorphism $\phi_{e_2e_1}$ as a rotation of angle ρ, and we assume ρ is close to zero. The Poincaré map near p_{e_1} is thus given by

$$\begin{aligned}
\Psi(\theta_{e_1}, z_{e_1}) &= \phi_{e_2e_1} \circ \varphi_{e_2} \circ \phi_{e_1e_2} \circ \varphi_{e_1}(\theta_{e_1}, z_{e_1}) = \\
&= \phi_{e_2e_1} \circ \varphi_{e_2} \left((1+\varepsilon) r_0 \left(\frac{z_1}{z_{e_1}} \right)^{\frac{\alpha_{e_1}}{\lambda_{e_1}}}, (1+\delta) \left(\theta_{e_1} + \ln \left(\frac{z_1}{z_{e_1}} \right)^{\frac{\beta_{e_1}}{\lambda_{e_1}}} \right) \right) \\
&= \varphi_{e_2e_1} \left(\ln \left((1+\varepsilon)^{-\frac{\beta_{e_2}}{\alpha_{e_2}}} \right) + \ln \left(\frac{z_{e_1}}{z_1} \right)^{\frac{\alpha_{e_1}\beta_{e_2} - (1+\delta)\beta_{e_1}\alpha_{e_2}}{\lambda_{e_1}\alpha_{e_2}}} + (1+\delta)\theta_{e_1}, (1+\varepsilon)^{-\frac{\lambda_{e_2}}{\alpha_{e_2}}} \left(\frac{z_{e_1}}{z_1} \right)^{\frac{\alpha_{e_1}\lambda_{e_2}}{\lambda_{e_1}\alpha_{e_2}}} z_1 \right).
\end{aligned}$$

5.1.3 Geometry of the Poincaré map

In this section we show that the Poincaré map Ψ has the geometry of a horseshoe map. This implies that Ψ has an invariant set and that the dynamics of Ψ on the

invariant set is topologically conjugate to the shift on a space of bi-infinite sequences of two symbols.

We consider a rectangular neighbourhood, R_{e_1}, of p_{10} on the surface Σ_{10} of the cylindrical neighbourhood of e_1 and show that it intersects its image by the Poincaré map Ψ in a horseshoe-like way.

In fact, what we actually do is something that is equivalent but easier to compute: we consider the inverse image in Σ_{20} by the rotation $\phi_{e_2e_1}$ of the rectangular neighbourhood R_{e_1} in Σ_{10}. Then we study how the image of R_{e_1} by $\varphi_{e_2} \circ \phi_{e_1e_2} \circ \varphi_{e_1}$ intersects its inverse image by the rotation $\phi_{e_2e_1}$ in Σ_{20} (see figure 5.2).

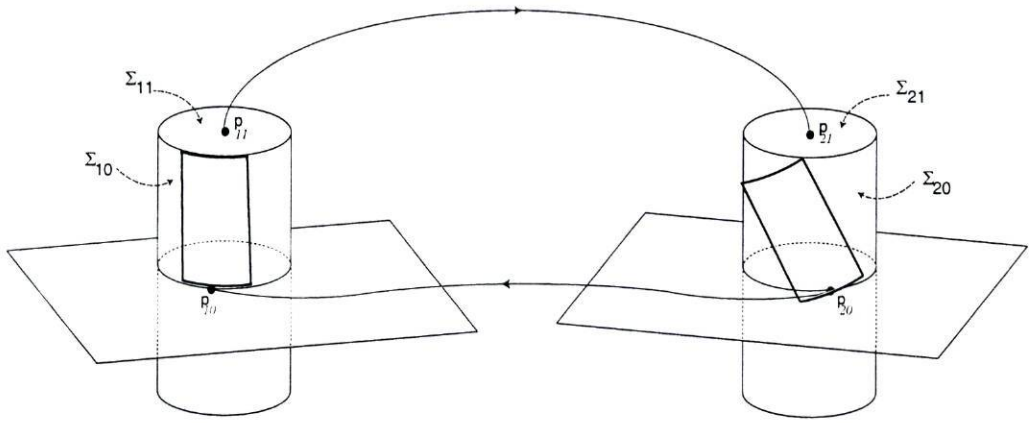

Figure 5.2: Image in Σ_{20} of $\phi^{-1}_{e_2e_1}(R_{e_1})$.

We consider the following rectangular neighbourhood in Σ_{10},

$$R_{e_1} = [-\nu\pi, \nu\pi] \times [0, z_1],$$

with $0 < \nu << 1$ and the covering of R_{e_1} by rectangles

$$R_{e_1k} = [-\nu\pi, \nu\pi] \times \left[z_1 e^{\gamma(k+1)}, z_1 e^{\gamma k}\right],$$

with $\gamma = \frac{5\pi\lambda_{e_1}\alpha_{e_2}}{\alpha_{e_1}\beta_{e_2} - (1+\delta)\beta_{e_1}\alpha_{e_2}}$, $k \in \mathcal{N}_0^+$ and $R_{e_1} = \bigcup_{k=0}^{\infty} R_{e_1k}$. Note that $\gamma < 0$, thus the height of the rectangles $R_{e_1k} \to 0$ as $k \to +\infty$ (see figure 5.3).

The reason for this particular choice of the rectangular partition of R_{e_1} will become clear in the proof of theorem 30.

We want then to study the intersection of $\varphi_{e_2} \circ \phi_{e_1e_2} \circ \varphi_{e_1}(R_{e_1k})$ with $\phi^{-1}_{e_2e_1}(R_{e_1k})$. Note that the image of R_{e_1} by $\phi^{-1}_{e_2e_1}$ is a rectangular neighbourhood of p_{20} in Σ_{20} crossed by $W^u_{loc}(e_2) \cap \Sigma_{20}$ as in see figure 5.2.

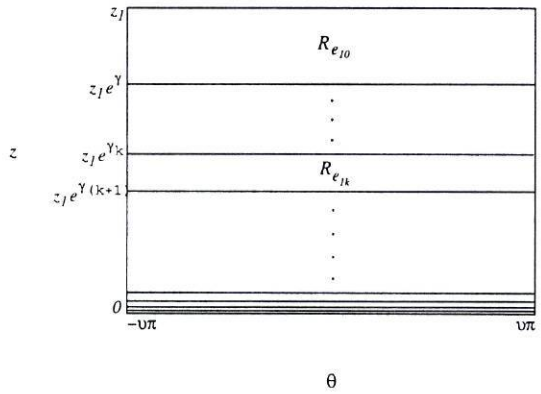

Figure 5.3: Rectangular neighbourhood R_{e_1} and its covering by the rectangles $R_{e_{1k}}$.

We first study the image of R_{e_1} by $\varphi_{e_2} \circ \phi_{e_1 e_2} \circ \varphi_{e_1}$.

Lemma 29 *The rectangular neighbourhood R_{e_1} is mapped by $\varphi_{e_2} \circ \phi_{e_1 e_2} \circ \varphi_{e_1}$ into a strip that winds around Σ_{20} and accumulates in $W^u_{loc}(e_2) \cap \Sigma_{20}$.*

Proof: The image of R_{e_1} by $\varphi_{e_2} \circ \phi_{e_1 e_2} \circ \varphi_{e_1}$ is determined by the image of its boundaries. In fact it is enough to study the image of the boundaries parallel to the z-axis. Let s be one of those boundaries.

Recall that $\frac{\alpha_{e_1}}{\lambda_{e_1}} < 0$ and $\frac{\beta_{e_1}}{\lambda_{e_1}} > 0$ in (5.3).

We have that $\lim_{z_{e_1} \to z_1} \varphi_{e_1}(\theta_{e_1}, z_{e_1}) = (r_0, \theta_{e_1})$. Moreover, $\lim_{z_{e_1} \to 0} \varphi_{e_1}(\theta_{e_1}, z_{e_1}) = (0, +\infty)$.

The image of s by φ_{e_1} is a logarithmic spiral in Σ_{11} that winds around the z_{e_1}-axis, and has p_{11} as an accumulation point, as shown in figure 5.4.

Writing $\phi_{e_1 e_2}(r_{e_1}, \theta_{e_1}) = (r_{e_1} + \varepsilon r_{e_1}, \theta_{e_1} + \delta\theta_{e_1}) = (r, \theta)$, we have $\lim_{r_{e_1} \to 0} r = 0$ and $\lim_{r_{e_1} \to r_0} r = r_0 + \delta r_0$. Moreover, $\lim_{\theta_{e_1} \to 0} \theta = 0$.

The logarithmic spiral in Σ_{11} is perturbed and mapped by $\phi_{e_1 e_2}$ into another spiral in Σ_{21} that winds around the z_{e_1}-axis and has p_{21} as a limit point (a small piece may not be mapped into Σ_{21}).

Recall that $\frac{\beta_{e_2}}{\alpha_{e_2}} > 0$ and $\frac{\lambda_{e_2}}{\alpha_{e_2}} < 0$ in (5.4).

We have that $\lim_{r_{e_2} \to r_0} \varphi_{e_2}(r_{e_2}, \theta_{e_2}) = (\theta_{e_2}, z_1)$. Moreover, $\lim_{r_{e_2} \to 0} \varphi_{e_2}(r_{e_2}, \theta_{e_2}) = (+\infty, 0)$.

The logarithmic spiral in Σ_{21} is transformed by φ_{e_2} into a curve that winds around

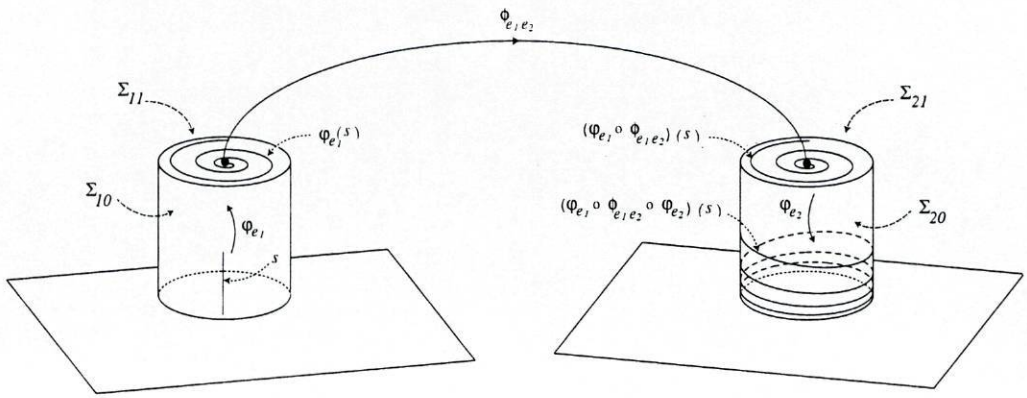

Figure 5.4: Image, in Σ_{20}, by $\varphi_{e_2} \circ \phi_{e_1e_2} \circ \varphi_{e_1}$ of a vertical segment s in Σ_{10}.

Σ_{20} and accumulates on $W^u_{loc}(e_2) \cap \Sigma_{20}$, as in figure 5.4. □

Theorem 30 *Consider the covering of R_{e_1} by the rectangles $R_{e_{1k}}$. Under hypothesis (A) in section 5.1.1 and hypothesis (H1) in section 5.1.2, and for ρ, the angle of the rotation $\phi_{e_2e_1}$, sufficiently close to zero, there are values of k such that the intersection of $\varphi_{e_2} \circ \phi_{e_1e_2} \circ \varphi_{e_1}(R_{e_{1k}})$ with $\phi^{-1}_{e_2e_1}(R_{e_{1k}})$ in Σ_{20} is a topological horseshoe.*

Proof: To compute the image of a rectangle $R_{e_{1k}}$ by $\varphi_{e_2} \circ \phi_{e_1e_2} \circ \varphi_{e_1}$ we compute the image of its boundaries. The boundaries of $R_{e_{1k}}$ are given by

$$U = [-\nu\pi, \nu\pi] \times \left\{z_1 e^{\gamma k}\right\},$$

$$D = [-\nu\pi, \nu\pi] \times \left\{z_1 e^{\gamma(k+1)}\right\},$$

$$L = \{-\nu\pi\} \times \left[z_1 e^{\gamma(k+1)}, z_1 e^{\gamma k}\right],$$

$$R = \{\nu\pi\} \times \left[z_1 e^{\gamma(k+1)}, z_1 e^{\gamma k}\right].$$

Their images in Σ_{20} by $\varphi_{e_2} \circ \phi_{e_1e_2} \circ \varphi_{e_1}$ are given by

$$\varphi_{e_2} \circ \phi_{e_1e_2} \circ \varphi_{e_1}(U) =$$
$$\left[(5k - (1+\delta)\nu)\,\pi + \ln(1+\varepsilon)^{-\frac{\beta_{e_2}}{\alpha_{e_2}}}, (5k + (1+\delta)\nu)\,\pi + \ln(1+\varepsilon)^{-\frac{\beta_{e_2}}{\alpha_{e_2}}}\right] \times \left\{z_1(1+\varepsilon)^{-\frac{\lambda_{e_2}}{\alpha_{e_2}}} e^{\eta k}\right\},$$
$$\varphi_{e_2} \circ \phi_{e_1e_2} \circ \varphi_{e_1}(D) =$$
$$\left[(5(k+1) - (1+\delta)\nu)\,\pi + \ln(1+\varepsilon)^{-\frac{\beta_{e_2}}{\alpha_{e_2}}}, (5(k+1) + (1+\delta)\nu)\,\pi + \ln(1+\varepsilon)^{-\frac{\beta_{e_2}}{\alpha_{e_2}}}\right] \times \left\{z_1(1+\varepsilon)^{-\frac{\lambda_{e_2}}{\alpha_{e_2}}} e^{\eta(k+1)}\right\},$$
$$\varphi_{e_2} \circ \phi_{e_1e_2} \circ \varphi_{e_1}(L) =$$
$$\{((5l - (1+\delta)\nu)\pi + \ln(1+\varepsilon)^{-\frac{\beta_{e_2}}{\alpha_{e_2}}}, (1+\varepsilon)^{-\frac{\lambda_{e_2}}{\alpha_{e_2}}} z_1 e^{\eta l}); k \le l \le k+1\},$$
$$\varphi_{e_2} \circ \phi_{e_1e_2} \circ \varphi_{e_1}(R) =$$
$$\{((5l + (1+\delta)\nu)\pi + \ln(1+\varepsilon)^{-\frac{\beta_{e_2}}{\alpha_{e_2}}}, (1+\varepsilon)^{-\frac{\lambda_{e_2}}{\alpha_{e_2}}} z_1 e^{\eta l}); k \le l \le k+1\},$$

with $\eta = \frac{5\pi\alpha_{e_1}\lambda_{e_2}}{\alpha_{e_1}\beta_{e_2}-(1+\delta)\beta_{e_1}\alpha_{e_2}}$

To simplify computations we consider $\varepsilon = \delta = 0$, i.e., we consider $\phi_{e_1e_2}$ as the identity map. We claim that, for ε and δ not equal zero and small the same kind of conclusions apply. For $\varepsilon = \delta = 0$,

$$\varphi_{e_2} \circ \phi_{e_1e_2} \circ \varphi_{e_1}(\theta_{e_1}, z_{e_1}) = \left(\ln\left(\frac{z_{e_1}}{z_1}\right)^{\frac{\alpha_{e_1}\beta_{e_2}-\beta_{e_1}\alpha_{e_2}}{\lambda_{e_1}\alpha_{e_2}}} + \theta_{e_1}, \left(\frac{z_{e_1}}{z_1}\right)^{\frac{\alpha_{e_1}\lambda_{e_2}}{\lambda_{e_1}\alpha_{e_2}}} z_1 \right) = (\theta_{e_2}, z_{e_2}), \tag{5.5}$$

and the above images simplify to

$$\varphi_{e_2} \circ \phi_{e_1e_2} \circ \varphi_{e_1}(U) = [(5k-\nu)\pi, (5k+\nu)\pi] \times \left\{z_1 e^{\eta k}\right\},$$

$$\varphi_{e_2} \circ \phi_{e_1e_2} \circ \varphi_{e_1}(D) = [(5(k+1)-\nu)\pi, (5(k+1)+\nu)\pi] \times \left\{z_1 e^{\eta(k+1)}\right\},$$

$$\varphi_{e_2} \circ \phi_{e_1e_2} \circ \varphi_{e_1}(L) = \{((5l-\nu)\pi, z_1 e^{\eta l}); k \leq l \leq k+1\},$$

$$\varphi_{e_2} \circ \phi_{e_1e_2} \circ \varphi_{e_1}(R) = \{((5l+\nu)\pi, z_1 e^{\eta l}); k \leq l \leq k+1\},$$

with $\eta = \frac{5\pi\alpha_{e_1}\lambda_{e_2}}{\alpha_{e_1}\beta_{e_2}-\beta_{e_1}\alpha_{e_2}}$

We consider a rectangular neighbourhood of p_{20} in Σ_{20} homeomorphic to R_{e_1} defined by,

$$R_{e_2} = [-\nu\pi, \nu\pi] \times [0, z_1],$$

and a covering of R_{e_2} by rectangles homeomorphic to the covering of R_{e_1}

$$R_{e_{2k}} = [-\nu\pi, \nu\pi] \times \left[z_1 e^{\gamma(k+1)}, z_1 e^{\gamma k}\right],$$

with $k \in \mathcal{N}_0^+$ and $R_{e_2} = \bigcup_{k=0}^{\infty} R_{e_{2k}}$.

We find conditions for $\varphi_{e_2} \circ \phi_{e_1e_2} \circ \varphi_{e_1}(R_{e_{1k}})$ to intersect $R_{e_{2k}}$ in a horseshoe.

In figure 5.5 we represent the kind of intersection of $\varphi_{e_2} \circ \phi_{e_1e_2} \circ \varphi_{e_1}(R_{e_{1k}})$ and $R_{e_{2k}}$ that we want to find in Σ_{20} for a rectangle $R_{e_{1k}}$ in Σ_{10}. The calculations differ if k is even or odd.

We want to find conditions under which $\varphi_{e_2} \circ \phi_{e_1e_2} \circ \varphi_{e_1}(R_{e_{1k}})$ intersects $R_{e_{2k}}$ in two disjoint regions with a horseshoe-like form. We want the rectangle $R_{e_{1k}}$ to be contracted in one direction, expanded in another direction, and wound around Σ_{20}

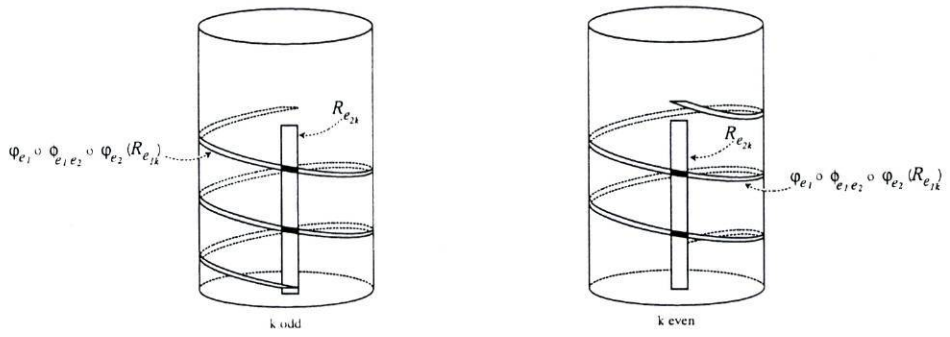

Figure 5.5: Desired intersections of $\varphi_{e_2} \circ \phi_{e_1 e_2} \circ \varphi_{e_1}(R_{e_{1k}})$ with $R_{e_{2k}}$, respectively, when k is odd and even.

in such a way that we can find two disjoint regions of $R_{e_{1k}}$ that are mapped by $\varphi_{e_2} \circ \phi_{e_1 e_2} \circ \varphi_{e_1}$ over their homeomorphic regions in $R_{e_{2k}}$.

Notice that the sign of $\alpha_{e_1}\beta_{e_2} - \beta_{e_1}\alpha_{e_2}$ determines whether θ_{e_2} increases or decreases as $z_{e_1} \to 0$,that is, determines whether the image of $R_{e_{1k}}$ winds to the right or to the left. Since we consider $\beta_{e_i} > 0$, $i = e_1, e_2$, we have that $\alpha_{e_1}\beta_{e_2} - \beta_{e_1}\alpha_{e_2}$ is negative and the strip winds to the right.

As $\frac{\alpha_{e_1}\lambda_{e_2}}{\lambda_{e_1}\alpha_{e_2}} < 1$ we have $z_1 e^{\eta k} > z_1 e^{\gamma k}$.

Notice also that the height of the rectangle $R_{e_{1k}}$ determines the number of times $\varphi_{e_2} \circ \phi_{e_1 e_2} \circ \varphi_{e_1}(R_{e_{1k}})$ winds around Σ_{20}, and this depends on the choice of the scalar on the numerator of the exponent $\gamma = \frac{5\pi\lambda_{e_1}\alpha_{e_2}}{\alpha_{e_1}\beta_{e_2} - (1+\delta)\beta_{e_1}\alpha_{e_2}}$ in the definition of the covering. We have chosen the value 5 for the scalar, since, as can be seen in figure 5.5, this is the smallest value giving the desired intersections.

Let now L and R denote, respectively, the left and right boundaries of $R_{e_{1k}}$. In order to obtain the desired form for the intersection of $\varphi_{e_2} \circ \phi_{e_1 e_2} \circ \varphi_{e_1}(R_{e_{1k}})$ and $R_{e_{2k}}$ it is sufficient to impose that the first time $\varphi_{e_2} \circ \phi_{e_1 e_2} \circ \varphi_{e_1}(R)$ goes through angle $-\nu\pi$ it intersects L, and that the second time $\varphi_{e_2} \circ \phi_{e_1 e_2} \circ \varphi_{e_1}(L)$ goes through angle $\nu\pi$ it intersects R (see figure 5.5).

When k is even this is equivalent, respectively, to

$$z_1 e^{\eta(k+\frac{2}{5}(1-\nu))} < z_1 e^{\gamma k}, \tag{5.6}$$

and

$$z_1 e^{\eta(k+\frac{2}{5}(2+\nu))} > z_1 e^{\gamma(k+1)}. \tag{5.7}$$

Condition (5.6) is equivalent to $k > \frac{\frac{2}{5}(\nu-1)\alpha_{e_1}\lambda_{e_2}}{\alpha_{e_1}\lambda_{e_2} - \lambda_{e_1}\alpha_{e_2}}$, and condition (5.7) is trivially verified for all k, and for ν sufficiently small.

When k is odd it is equivalent, respectively, to

$$z_1 e^{\eta(k+\frac{1}{5}(1-2\nu))} < z_1 e^{\gamma k}, \tag{5.8}$$

and

$$z_1 e^{\eta(k+\frac{3}{5}+\frac{2}{5}\nu)} > z_1 e^{\gamma(k+1)}. \tag{5.9}$$

Condition (5.8) is equivalent to $k > \frac{\frac{1}{5}(2\nu-1)\alpha_{e_1}\lambda_{e_2}}{\alpha_{e_1}\lambda_{e_2}-\lambda_{e_1}\alpha_{e_2}}$, and condition (5.9) is trivially verified for all k, and for ν sufficiently small.

We have shown that under certain conditions there are values of k such that the intersection of $\varphi_{e_2} \circ \phi_{e_1e_2} \circ \varphi_{e_1}(R_{e_{1k}})$ with $R_{e_{2k}}$ in Σ_{20} is a topological horseshoe.

Since we are assuming that the angle ρ of the rotation $\phi_{e_2e_1}$ is small, we can conclude that, under the same conditions, the intersection of $\varphi_{e_2} \circ \phi_{e_1e_2} \circ \varphi_{e_1}(R_{e_{1k}})$ with $\phi^{-1}_{e_2e_1}(R_{e_{1k}})$ is a topological horseshoe. To see this imagine that you rotate sightly the underlying rectangle in the classical horseshoe picture; the intersection points will change but will nevertheless produce a horseshoe-type intersection. □

5.1.4 Hyperbolicity of the Poincaré map

From the results in the last section we can conclude the existence of infinitely many rectangles in R_{e_1}, where Ψ is a topological horseshoe. We now prove the existence for Ψ of sector-bundles in R_{e_1} satisfying condition (C) in section 5.1.1. This and theorem 30 above imply that Ψ possesses an hyperbolic invariant Cantor set Λ in R_{e_1} and that the restriction of Ψ to the Cantor set Λ is homeomorphic to the shift on the space of bi-infinite sequences with elements in an alphabet with two symbols.

Theorem 31 *Assume hypotheses (A) in section 5.1.1 and $(H1)$ in section 5.1.2 hold. Let $z_2 = z_1 \left(\frac{\lambda_{e_1}\alpha_{e_2}}{\alpha_{e_1}\lambda_{e_2}}\right)^{\frac{\lambda_{e_1}\alpha_{e_2}}{\alpha_{e_1}\lambda_{e_2}-\lambda_{e_1}\alpha_{e_2}}}$. If $\delta > 0$, $\varepsilon < 0$ and $z_{e_1} > z_2$, or $\delta < 0$, $\varepsilon > 0$ and $z_{e_1} < z_2$ then the Poincaré map Ψ is hyperbolic.*

Proof: We must prove we can find a sectorial structure satisfying condition (C) in section 5.1.1.

We follow [20], section 6.5: we prove that at each point the derivative $D\Psi$ has one eigenvalue of magnitude less than 1 and the other larger than 1, and that the angle between the eigenvectors is bounded away from zero.

In these circumstances, the sectorial structure is obtained from the bounds of the eigenvectors, by choosing small sectors around the boundary values. Those sectors satisfy condition (C).

The matrix of the derivative of Ψ at a point (θ_{e_1}, z_{e_1}) in R_{e_1} is given by

$$D\Psi\Big|_{(\theta_{e_1},z_{e_1})} = \begin{bmatrix} \cos\rho & -\sin\rho \\ \sin\rho & \cos\rho \end{bmatrix} \begin{bmatrix} a & b \\ 0 & d \end{bmatrix},$$

with

$$\begin{bmatrix} a & b \\ 0 & d \end{bmatrix} = \begin{bmatrix} 1+\delta & \left(\frac{\alpha_{e_1}\beta_{e_2}}{\lambda_{e_1}\alpha_{e_2}} - (1+\delta)\frac{\beta_{e_1}}{\lambda_{e_1}}\right)\frac{1}{z_{e_1}} \\ 0 & \left(\frac{1}{1+\varepsilon}\right)^{\frac{\lambda_{e_2}}{\alpha_{e_2}}} \frac{\alpha_{e_1}\lambda_{e_2}}{\lambda_{e_1}\alpha_{e_2}} \left(\frac{z_1}{z_{e_1}}\right)^{1-\frac{\alpha_{e_1}\lambda_{e_2}}{\lambda_{e_1}\alpha_{e_2}}} \end{bmatrix}.$$

The eigenvalues of $D\Psi\Big|_{(\theta_{e_1},z_{e_1})}$ are,

$$\frac{1}{2}\left((a+d)\cos\rho + b\sin\rho \pm \sqrt{[(a+d)\cos\rho + b\sin\rho]^2 - 4ad}\right),$$

with eigenvectors,

$$\left(1, \frac{\left((d-a)\cos\rho + b\sin\rho \pm \sqrt{[(a+d)\cos\rho + b\sin\rho]^2 - 4ad}\right)}{2(b\cos\rho - d\sin\rho)}\right).$$

We start by analysing the magnitude of the eigenvalues when $\rho = 0$. In this case the eigenvalues are given by a and d. For $\delta > 0$ the absolute value of a is larger than 1, and for $\delta < 0$ it is less than 1.

Let $z_2 = z_1 \left(\frac{\lambda_{e_1}\alpha_{e_2}}{\alpha_{e_1}\lambda_{e_2}}\right)^{\frac{\lambda_{e_1}\alpha_{e_2}}{\alpha_{e_1}\lambda_{e_2} - \lambda_{e_1}\alpha_{e_2}}}$. For $z_{e_1} = z_2$ we have $d = (1+\varepsilon)^{-\frac{\lambda_{e_2}}{\alpha_{e_2}}}$. Thus, when $\varepsilon > 0$ the absolute value of d is larger than 1 at least for $z_{e_1} < z_2$. When $\varepsilon < 0$ the absolute value of d is less than 1 at least for $z_{e_1} > z_2$.

Thus, for $\delta > 0$, $\varepsilon < 0$ and $z_{e_1} > z_2$ we have $|a| > 1$ and $|d| < 1$. For $\delta < 0$, $\varepsilon > 0$ and $z_{e_1} < z_2$ we have $|a| < 1$ and $|d| > 1$.

When $\rho \approx 0$ the eigenvalues are close to a and d. The product of the eigenvalues is $det\,(D\Psi) = ad$. We conclude that, when $\rho \approx 0$, as long as the discriminant $\Delta = [(a+d)\cos\rho + b\sin\rho]^2 - 4ad$ is greater than zero, there are two different eigenvalues, one with absolute value larger than 1 and one with absolute value less than 1.

The angle between the eigenvectors is bounded away from zero as long as Δ is bounded away from zero. Since $\rho \approx 0$ we have $\Delta \approx (a-d)^2$. Thus, it is possible to choose values of δ and ε such that Δ is not close to zero.

We conclude that there are values of δ, ε and z_{e_1} such that the derivative of Ψ has one eigenvalue with absolute value less than 1 and the other with absolute value larger than 1 and the angle between the eigenvectors is bounded away from zero. □

5.1.5 Conclusion

We have proved that, under the conditions of theorem 30 in section 5.1.3 and theorem 31 in the last section, the diffeomorphism Ψ satisfies hypotheses (B) and (C) in section 5.1.1. Thus, by Theorem 5.2.4 in [20], we can conclude that, under those conditions, the diffeomorphism Ψ has a hyperbolic invariant Cantor set Λ, such that, Ψ restricted to Λ is topologically conjugate to a shift σ on the set X of bi-infinite sequences of two symbols. That is, there is a homeomorphism $h : X \to \Lambda$, such that $\Psi\Big|_{\Lambda} = h \circ \sigma \circ h^{-1}$.

The invariant Cantor set Λ is structurally stable since small C^1 perturbations of Ψ still satisfy hypotheses (B) and (C).

An analogous treatment shows the existence in R_{e_2} of a Cantor set invariant by that Poincaré map and with the same properties of Λ.

The case of the unperturbed example we constructed in section 4.1.1, where, in the restriction to the invariant three-sphere, the two-dimensional manifolds of the two saddles in the heteroclinic cycle coincide, is non-generic since $\rho = 0$.

If we simplify the problem and consider the still more degenerate situation where $\phi_{e_1e_2}$ and $\phi_{e_2e_1}$ are the identity map, then

$$D\Psi = \begin{bmatrix} 1 & (\frac{\alpha_{e_1}\beta_{e_2}}{\lambda_{e_1}\alpha_{e_2}} - \frac{\beta_{e_1}}{\lambda_{e_1}})\frac{1}{z_{e_1}} \\ 0 & \frac{\alpha_{e_1}\lambda_{e_2}}{\lambda_{e_1}\alpha_{e_2}}(\frac{z_{e_1}}{z_1})^{\frac{\alpha_{e_1}\lambda_{e_2}}{\lambda_{e_1}\alpha_{e_2}}-1} \end{bmatrix}.$$

In this case we can still prove the existence of a topological horseshoe, but it is nonhyperbolic since one of the eigenvalues equals 1.

Moreover, if the eigenvalues of the equilibria e_1 and e_2 verify the relations,

$$\frac{\alpha_{e_1}}{\beta_{e_1}} = \frac{\alpha_{e_2}}{\beta_{e_2}} \qquad \text{and} \qquad \frac{\alpha_{e_1}}{\lambda_{e_1}} = \frac{\alpha_{e_2}}{\lambda_{e_2}}, \tag{5.10}$$

then Ψ is the identity.

5.1.6 Resonance in Field's example

The resonance (5.10) appears in Field's example (described in section 3.1).

Restricted to the invariant sphere, the equilibria in $[a]$ have eigenvalues λ_a, $\alpha_a \pm i\beta_a$ with

$$\lambda_a = \tfrac{4\lambda\gamma}{\beta+\gamma-2}, \quad \alpha_a = \tfrac{\lambda(\gamma+3\beta)}{\beta+\gamma-2} \qquad \text{and} \qquad \beta_a = \tfrac{\lambda(3\gamma-\beta)}{\beta+\gamma-2},$$

and the equilibria in $[b]$ have eigenvalues λ_b, $\alpha_b + i\beta_b$ with

$$\lambda_b = \tfrac{4\lambda\gamma}{\beta+\gamma+2}, \quad \alpha_b = \tfrac{\lambda(\gamma+3\beta)}{\beta+\gamma+2} \qquad \text{and} \qquad \beta_b = \tfrac{\lambda(3\gamma-\beta)}{\beta+\gamma+2}.$$

For the parameter values we are considering,

$$\lambda > 0, \quad \gamma < 0, \quad \beta > 0, \quad \gamma + 3\beta > 0 \quad \text{and} \quad |\beta + \gamma| < 2, \tag{5.11}$$

we have,

$$\lambda_a > 0, \ \alpha_a < 0, \quad \beta_a > 0, \quad \lambda_b < 0, \quad \alpha_b > 0 \text{ and } \beta_b < 0.$$

We identify the equilibria in $[a]$ and in $[b]$, respectively, with equilibria e_1 and e_2 of the generic situation we have studied in the last sections.

The eigenvalues of the equilibria in $[a]$ and $[b]$ are resonant since they verify the equalities in (5.10). Since we do not know the transition maps $\phi_{e_1e_2}$ and $\phi_{e_2e_1}$, one way around this problem is to perturb Field's example. We use as perturbation an equivariant polynomial of degree 5. Note that this is the next lowest degree for polynomials to be equivariant by the symmetry group Γ since it contains $-I_V$. Note also that we can conclude that the family of vector fields in Field's example is not 3-determined.

Lemma 32 *A basis for the space of Γ-equivariant homogeneous polynomial maps from $\mathbf{R}^4$ to $\mathbf{R}^4$ of degree 5 is given by*

$$\begin{aligned}
p_1(z_1,z_2) &= (|z_1|^2+|z_2|^2)^2(z_1,z_2),\\
p_2(z_1,z_2) &= (|z_1|^2+|z_2|^2)(\overline{z}_1^2\overline{z}_2, z_1\overline{z}_2^2),\\
p_3(z_1,z_2) &= (|z_1|^2+|z_2|^2)(z_2^3,\overline{z}_1^3),\\
p_4(z_1,z_2) &= (z_1^4z_2,\overline{z}_1z_2^4),\\
p_5(z_1,z_2) &= (\overline{z}_1^3z_2^2,\overline{z}_1^2\overline{z}_2^3),\\
p_6(z_1,z_2) &= (z_1^2\overline{z}_2^3, z_1^3z_2^2),\\
p_7(z_1,z_2) &= (\overline{z}_1\overline{z}_2^4, z_1^4\overline{z}_2).
\end{aligned}$$

Proof: The proof is a straighforward computation. □

Notice that the family of perturbed vector fields will no longer be of the form

$$x' = \lambda x + Q(x),$$

with $Q(x)$ a homogeneous polynomial map with odd degree, so we can no longer apply the Invariant Sphere Theorem as it is stated in [14], [15].

However, in the case of normal hyperbolicity of the invariant sphere (see Hirsch, Pugh and Shub [26]), for small enough perturbations there still exists a globally attracting invariant sphere close to that of the unperturbed system. When X is a flow invariant normally hyperbolic manifold, theorem 4.1 in [26] guarantees that under perturbation there is a unique flow invariant manifold X_ε near X, and X_ε is diffeomorphic to X. See also the equivariant version of this theorem in [36], proposition 1.1.

Let V be a finite dimensional real vector space with inner product $(.,.)$ and unit sphere $S(V)$.

Let $P^d(V,V)$ be the space of homogeneous polynomial maps from V to V of degree $d \geq 1$.

Let $Q \in P^d(V,V)$. We define $\rho_Q : S(V) \longrightarrow \mathbf{R}$ by

$$\rho_Q(u) = (Q(u),u).$$

For $Q \in P^{2p+1}(V,V)$, we say that Q is *contracting* if

$$\rho_Q(u) < 0, \qquad \text{for all } u \in S(V).$$

We have the following:

Conjecture 33 *Let V be an n-dimensional vector space and $Q_{2p+1} : V \to V$ a homogeneous polynomial of degre $2p+1$, $p \geq 1$. Consider the vector field*

$$x' = \lambda x + Q_{2p+1}(x) + \Sigma_L Q_L(x), \tag{5.12}$$

with Q_L homogeneous polynomials in V of degree $L \geq 2p+2$. Let Q_{2p+1} be contracting and $M \in \mathbf{R}^-$ be the upper bound of $\rho_{Q_{2p+1}}$ in $S(V)$. If

$$\Sigma_L c^L (\frac{1}{-M})^{\frac{L}{2p}} \rho_{Q_L} < 0, \tag{5.13}$$

for all $c > 1$, then for values of $\lambda > 0$ near 0 there is a unique invariant sphere, $S(\lambda) \subset V \backslash \{0\}$, that is globally attracting in $V \backslash \{0\}$.

Note that (5.13) is naturally satisfied when the homogeneous polynomials Q_L are contracting.

Although we were not able to prove the above conjecture extending the Invariant Sphere theorem, we confirmed numerically, for some parameter values, that the conjecture is valid.

In the next lemma we state conditions for fifth degree Γ-equivariant polynomials, with Γ defined in section 3.1, to be contracting.

Lemma 34 *Let $z = (z_1, z_2)$ and*

$$Q(z) = \Sigma_{i=1}^{7} \alpha_i p_i(z),$$

where $\alpha_i \in I\!R$ and the p_i are as in lemma 32. Then Q is contracting if

$$\alpha_1 < 0, \text{ and } |\alpha_1| > |\alpha_2 + \alpha_3| + \frac{|\alpha_4|}{2} + \frac{|\alpha_5| + |\alpha_6| + |\alpha_7|}{4}.$$

Proof: We follow the proof of lemma A.10 in [15].

We have

$$\begin{aligned}(Q(z), z) \;=\; & \alpha_1 ||z||^6 + (\alpha_2 + \alpha_3)(\overline{z}_1^3 \overline{z}_2 + z_1^3 z_2 + \overline{z}_1 z_2^3 + z_1 \overline{z}_2^3) + \\ & + (\frac{\alpha_4}{2}|z_1|^2 + \frac{\alpha_5}{2}|z_2|^2)(z_1^3 z_2 + \overline{z}_1^3 \overline{z}_2) + (\frac{\alpha_4}{2}|z_2|^2 + \frac{\alpha_5}{2}|z_1|^2)(\overline{z}_1 z_2^3 + z_1 \overline{z}_2^3) + \\ & + \frac{\alpha_6 + \alpha_7}{2}(\overline{z}_1^4 z_2^2 + z_1^4 \overline{z}_2^2 + \overline{z}_1^2 \overline{z}_2^4 + z_1^2 z_2^4).\end{aligned}$$

Changing to polar coordinates, $z_1 = r_1 e^{i\theta_1}$ and $z_2 = r_2 e^{i\theta_2}$, after some simplifications we obtain,

$$\begin{aligned}(Q(z), z) &= \alpha_1(r_1^2 + r_2^2)^3 + \\ &+2(\alpha_2 + \alpha_3)r_1 r_2(r_1^2\cos(3\theta_1 + \theta_2) + r_2^2\cos(\theta_1 - 3\theta_2)) + \\ &+(\alpha_4 r_1^2 + \alpha_5 r_2^2)r_1^3 r_2\cos(3\theta_1 + \theta_2) + (\alpha_4 r_2^2 + \alpha_5 r_1^2)r_1 r_2^3\cos(\theta_1 - 3\theta_2) + \\ &+(\alpha_6 + \alpha_7)r_1^2 r_2^2(r_1^2\cos(4\theta_1 - 2\theta_2) + r_2^2\cos(2\theta_1 + 4\theta_2)).\end{aligned}$$

So,

$$(Q(z), z) \leq (\alpha_1 + |\alpha_2 + \alpha_3| + \frac{|\alpha_4|}{2} + \frac{|\alpha_5| + |\alpha_6| + |\alpha_7|}{4})(r_1^2 + r_2^2)^3.$$

□

We consider a small perturbation of the family of vector fields in Field's example in the conditions of the above conjecture of extension of the Invariant Sphere Theorem. We must consider $\alpha_1 < 0$ to verify the conditions in lemma 34 and at least one $\alpha_i \neq 0$ for $i = 2, ..., 7$ to break the resonance relation between the eigenvalues of the equilibria. For ease of computations we choose $\alpha_2 \neq 0$ with $|\alpha_1| > |\alpha_2|$. As in [15], there is no loss of generality in assuming that $\alpha_1 = -1$. We also assume $\alpha_2 > 0$ and thus we must have $\alpha_2 < 1$.

Writing the equivariant perturbed system in real coordinates and renaming α_2 as α, we have

$$\left\{\begin{array}{rcl}\dot{x}_1 &=& \lambda x_1 - ||x||^2 x_1 + \beta(x_1^2 x_2 - y_1^2 x_2 - 2x_1 y_1 y_2) + \gamma(x_2^3 - 3x_2 y_2^2) - ||x||^4 x_1 + \\ & & +\alpha||x||^2(x_1^2 x_2 - y_1^2 x_2 - 2x_1 y_1 y_2) \\ \dot{y}_1 &=& \lambda y_1 - ||x||^2 y_1 + \beta(-x_1^2 y_2 + y_1^2 y_2 - 2x_1 y_1 x_2) + \gamma(-y_2^3 + 3x_2^2 y_2) - ||x||^4 y_1 + \\ & & +\alpha||x||^2(-x_1^2 y_2 + y_1^2 y_2 - 2x_1 x_2 y_1) \\ \dot{x}_2 &=& \lambda x_2 - ||x||^2 x_2 + \beta(x_1 x_2^2 - x_1 y_2^2 + 2y_1 x_2 y_2) + \gamma(x_1^3 - 3x_1 y_1^2) - ||x||^4 x_2 + \\ & & +\alpha||x||^2(x_1 x_2^2 - x_1 y_2^2 + 2y_1 x_2 y_2) \\ \dot{y}_2 &=& \lambda y_2 - ||x||^2 y_2 + \beta(y_1 x_2^2 - y_1 y_2^2 - 2x_1 x_2 y_2) + \gamma(y_1^3 - 3x_1^2 y_1) - ||x||^4 y_2 + \\ & & +\alpha||x||^2(y_1 x_2^2 - y_1 y_2^2 - 2x_1 x_2 y_2)\end{array}\right. \tag{5.14}$$

Lemma 35 *For the parameter values in (5.11) and $\beta + \gamma \geq 0$ the dynamics of the perturbed system (5.14) in the restriction to the planes of symmetry is topologically equivalent to the nonperturbed dynamics, but without the resonance relation between*

the eigenvalues, that is, we have

$$\frac{\alpha_a\beta_b}{\beta_a\alpha_b} \neq 1 \qquad \textit{and} \qquad \frac{\alpha_a\lambda_b}{\lambda_a\alpha_b} \neq 1.$$

Proof: In the restriction to the invariant plane **S**, equations (5.14) restrict to,

$$\begin{cases} \dot{x}_1 &= \lambda x_1 - (x_1^2+x_2^2)x_1 + \beta x_1^2 x_2 + \gamma x_2^3 - (x_1^2+x_2^2)^2 x_1 + \alpha(x_1^2+x_2^2)x_1^2 x_2 \\ \dot{x}_2 &= \lambda x_2 - (x_1^2+x_2^2)x_2 + \beta x_1 x_2^2 + \gamma x_1^3 - (x_1^2+x_2^2)^2 x_2 + \alpha(x_1^2+x_2^2)x_1 x_2^2 \end{cases} \tag{5.15}$$

On the axis **A**, we have the pair of equilibria $\pm a(\lambda) = \pm(x_a, 0, x_a, 0)$, with

$$x_a^2 = \frac{-(\beta+\gamma-2) - \sqrt{(\beta+\gamma-2)^2 - 8\lambda(\alpha-2)}}{4(\alpha-2)}.$$

The eigenvalues of the linearization of (5.14) at $\pm a(\lambda)$ are given by

$$r_a = -2\lambda + 4(\alpha-2)x_a^4,$$

$$\lambda_a = -4\gamma x_a^2,$$

and

$$\alpha_a \pm i\beta_a = \left(-x_a^2\left[6\alpha x_a^2 + (\gamma+3\beta)\right]\right) \pm i\left(-x_a^2\left[(3\gamma-\beta) - 2\alpha x_a^2\right]\right).$$

On the axis **B**, we have the pair of equilibria $\pm b(\lambda) = \pm(x_b, 0, -x_b, 0)$, with

$$x_b^2 = \frac{-(\beta+\gamma+2) + \sqrt{(\beta+\gamma+2)^2 + 8\lambda(\alpha+2)}}{4(\alpha+2)}.$$

The eigenvalues of the linearization of (5.14) at $\pm b(\lambda)$ are given by

$$r_b = -2\lambda - 4(\alpha+2)x_b^4,$$

$$\lambda_b = 4\gamma x_b^2,$$

and,

$$\alpha_b \pm i\beta_b = \left(-x_b^2\left[-6\alpha x_b^2 - (\gamma+3\beta)\right]\right) \pm i\left(-x_b^2\left[(3\gamma-\beta) - 2\alpha x_b^2\right]\right).$$

It is easy to verify that the eigenvalues of the perturbed equilibria maintain the same sign and are nonresonant.

Following the proof of lemma A.11 in [15], we conclude that, for the parameter values we are working with, there are no other nonzero equilibria in the restriction to **S**.

In the restriction to the invariant plane $\mathbf{P}$, equations (5.14) restrict to,

$$\begin{cases} \dot{y}_1 &= \lambda y_1 - (y_1^2+y_2^2)y_1 + \beta y_1^2 y_2 - \gamma y_2^3 - (y_1^2+y_2^2)^2 y_1 + \alpha(y_1^2+y_2^2)y_1^2 y_2 \\ \dot{y}_2 &= \lambda y_2 - (y_1^2+y_2^2)y_2 - \beta y_1 y_2^2 + \gamma y_1^3 - (y_1^2+y_2^2)^2 y_2 - \alpha(y_1^2+y_2^2)y_1 y_2^2 \end{cases} \tag{5.16}$$

We have that a nontrivial equilibrium of (5.16) satisfies

$$2\beta y_1^2 y_2^2 - \gamma(y_1^4+y_2^4) + 2\alpha(y_1^2+y_2^2)y_1^2 y_2^2 = 0. \tag{5.17}$$

Setting $X = 2y_1^2 y_2^2 \geq 0$ and $Y = y_1^2 + y_2^2 \geq 0$, equation (5.17) transforms to

$$\beta X - \gamma Y^2 + \gamma X + \alpha XY = 0,$$

that is,

$$X = \frac{\gamma Y^2}{\beta + \gamma + \alpha Y}. \tag{5.18}$$

Since $\gamma < 0$, $\alpha > 0$ and $\beta + \gamma \geq 0$, equation (5.18) has no solutions. □

In the dynamics of system (5.14) we still observe numerical evidence of the existence of a Shilnikov heteroclinic network topologically equivalent to that of the unperturbed system.

This is what was expected since, as it is conjectured, the invariant manifolds with dimension ≥ 2 of the invariant saddles in the Shilnikov heteroclinic network intersect transversely, and thus the network is structurally stable.

5.2 Homoclinic connection to a periodic trajectory

In this section we consider a generic flow on a three-dimensional manifold satisfying the following hypothesis:

(A) There is a transverse homoclinic orbit to a hyperbolic periodic trajectory c. The term transverse meaning that the homoclinic orbit is given by

$$W^s(c) \pitchfork W^u(c). \tag{5.19}$$

We justify very shortly the existence of horseshoe dynamics in the neighbourhood of such homoclinic cycle. For a more detailed and technical explanation see [45], section 3.4.

We consider a section S transverse to the vector field in a point p of the periodic trajectory c. Consider $V \subset S$ a small neighbourhood of p where the vector field is linearizable and consider the associated Poincaré map Ψ in V.

We reduce the study of the local dynamics of the flow in the neighbourhood of the periodic trajectory c to the study of the local dynamics of the corresponding Poincaré map Ψ in V near the fixed point p.

Given the hypothesis of transverse intersection of the invariant manifolds of the periodic trajectory c, we have that the stable and unstable manifolds of the hyperbolic fixed point p of the Poincaré map Ψ intersect transversely at a given point q in V. The point q is called a *transverse homoclinic point.* Due to the invariance of the stable and unstable manifolds of p by Ψ, the points in the Ψ-trajectory of q are also transverse homoclinic points. By the λ-lemma ([38], §7), the stable and unstable manifolds of p accumulate on themselves.

These are the fundamental aspects in the proof of the Smale-Birkhoff Homoclinic Theorem which guarantees the existence of a hyperbolic Cantor set invariant by the Poincaré map Ψ and topologically conjugate to a subshift of finite type.

Theorem 36 (The Smale-Birkhoff Homoclinic Theorem) *([20], theorem 5.3.5) Let $f : \mathbf{R}^n \to \mathbf{R}^n$ be a diffeomorphism such that p is a hyperbolic fixed point and there exists a point $q \neq p$ of transverse intersection between $W^s(p)$ and $W^u(p)$. Then f has a hyperbolic invariant set Λ on which f is topologically conjugate to a subshift of finite type.*

Chapter 6

Symbolic dynamics in Field's example

Our numerical study (section 3.2) of Field's example sustains Field's conjecture on the existence of a Shilnikov heteroclinic network involving the equilibria in $[a] \cup [b]$ and periodic trajectories in $[c]$. It allowed us to find evidence of the existence of heteroclinic connections from the equilibria in $[b]$ to equilibria in $[a]$ and to the periodic trajectories in $[c]$, and from the periodic trajectories in $[c]$ to the equilibria in $[a]$ and to periodic trajectories in $[c]$. The invariant saddles in $[a] \cup [b] \cup [c]$, the heteroclinic connections found analitically by Field [15] and the heteroclinic connections found numerically by us form a Shilnikov heteroclinic network Σ.

In section 3.3 we studied the structuring properties of the network Σ. Those properties motivated our approach to the study of the local dynamics in the neighbourhood of Σ. In that section we defined the quotient heteroclinic network Σ/Γ and noted that it is the union of three quotient heteroclinic cycles, one connecting the two equivalence classes of equilibria, another connecting the equivalence classes of equilibria and the equivalence class of the periodic trajectories and one homoclinic to the equivalence class of the periodic trajectories.

In chapter 4 we constructed two simple examples, each having a heteroclinic cycle topologically equivalent to a quotient heteroclinic cycle in Σ/Γ.

In chapter 5 we studied the local dynamics in the neighbourhood of generic heteroclinic cycles involving two saddle-foci with their two-dimensional invariant manifolds intersecting transversely, and the local dynamics in the neighbourhood of a generic homoclinic cycle to a periodic trajectory. We concluded that, under certain conditions,

there is horseshoe dynamics in the neighbourhood of those cycles and it can be modelled by the dynamics of a subshift in the space of sequences with elements in an alphabet with two symbols. We claim existence of horseshoe dynamics in the neighbourhood of generic heteroclinic cycles involving two saddle-foci and a periodic trajectory such that their two-dimensional invariant manifolds intersect transversely.

This way, we can conclude that, under certain conditions, in the neighbourhood of the quotient heteroclinic cycles there is horseshoe dynamics and thus it can be modelled by the dynamics of a two-subshift.

In the next section we characterize what we call the dynamics along the heteroclinic network. To simplify matters we see a trajectory close to the heteroclinic network qualitatively as a path along the network (section 3.3). A path along the network is characterized by the trail of the nodes in the network where it passes. The dynamics along the network is given by a characterization of the set of possible trails. We do this by defining a subshift dynamics on the space of sequences with elements in an alphabet with 25 symbols, where 25 is the number of invariant saddles in the network Σ.

Finally, in section 6.2, we define symbolic dynamics that represents the chaotic dynamics in the neighbourhood of Σ. We characterize it by using the description of the dynamics in the neighbourhood of the quotient heteroclinic cycles and the codification of the dynamics along the heteroclinic network Σ. The final conclusion is that in the neighbourhood of the network Σ we have horseshoe of horseshoe dynamics.

6.1 Symbolic dynamics along the heteroclinic network

In this section we define symbolic dynamics given by a subshift of finite type that codifies the dynamics along the heteroclinic network. Using this codification we conclude that the dynamics along the heteroclinic network is of horseshoe type. We introduce the concepts on subshifts of finite type as we need them; for a more detailed explanation on the subject see Kitchens [31], Wiggins ([45], section 2.2). Notice that we use a different notation for the spaces of two-sided sequences.

We number the equilibria in $[a] \cup [b]$ and the periodic trajectories in $[c]$ in the following

way:

$a \to 1$	$-a \to 6$	$b \to 11$	$-b \to 16$	$c \to 21$
$sa \to 2$	$-sa \to 7$	$sb \to 12$	$-sb \to 17$	$sc \to 22$
$s^2a \to 3$	$-s^2a \to 8$	$s^2b \to 13$	$-s^2b \to 18$	$s^2c \to 23$
$s^3a \to 4$	$-s^3a \to 9$	$s^3b \to 14$	$-s^3b \to 19$	$s^3c \to 24$
$s^4a \to 5$	$-s^4a \to 10$	$s^4b \to 15$	$-s^4b \to 20$	$s^4c \to 25$

and define the alphabet $L_M = \{a, sa, s^2a, ..., s^4c\}$.

With this alphabet we build the space of two-sided sequences $X_{25} = L_M^{\mathbf{Z}}$, that contains points of the form, $x = (...x_{-n}...x_{-2}x_{-1}.x_0x_1x_2...x_n...)$, where each $x_i \in L_M, i \in \mathbf{Z}$.

We define a metric on X_{25} by

$$\begin{cases} d(x,y) = 0 & \text{if} \quad x = y, \\ d(x,y) = 1/2^N & \text{with} \quad N \text{ such that } x_i = y_i \text{ for } |i| < N \text{ and } x_N \neq y_N \text{ or } x_{-N} \neq y_{-N}. \end{cases} \tag{6.1}$$

The space X_{25} with the topology given by this metric is compact, totally disconnected, perfect and homeomorphic to the usual middle thirds Cantor set ([31]).

The shift transformation $\sigma : X_{25} \to X_{25}$ is defined by $[\sigma(x)]_i \equiv x_{i+1}$, that is, if $x = (...x_{-n}...x_{-2}x_{-1}.x_0x_1x_2...x_n...)$, then $\sigma(x) = (...x_{-n}...x_{-2}x_{-1}x_0.x_1x_2...x_n...)$.

The space X_{25} together with the map σ is a dynamical system and is called the *full shift on 25 symbols* or the *full 25-shift.*

The term "full" indicates that X_{25} contains all the sequences defined by the alphabet L_M. We want to consider only those sequences where there exists a connection between two consecutive invariant saddles.

To indicate the admissible sequences we define a 25×25 transition matrix, M, with rows and colums indexed by the elements of the alphabet. The entry in row i, column j is 1 if and only if there is a connection from invariant saddle i to invariant saddle j, otherwise it is zero.

The matrix M has a block structure, and is defined as follows

$$M = \begin{bmatrix} 0 & A_1 & 0 \\ A_2 & 0 & A_3 \\ A_4 & 0 & A_5 \end{bmatrix},$$

where

$$A_1 = \begin{bmatrix} I_{5\times5} & I_{5\times5} \\ I_{5\times5} & I_{5\times5} \end{bmatrix}, A_2 = \begin{bmatrix} A_5 & A_5 \\ A_5 & A_5 \end{bmatrix}, A_3 = \begin{bmatrix} \mathbf{1}_{5\times5} \\ \mathbf{1}_{5\times5} \end{bmatrix}, A_4 = \begin{bmatrix} \mathbf{1}_{5\times5} & \mathbf{1}_{5\times5} \end{bmatrix}, A_5 = \mathbf{1}_{5\times5} - I_{5\times5},$$

where $I_{5\times5}$ denotes the identity matrix of order 5, and $\mathbf{1}_{5\times5}$ denotes the square matrix of order 5 with all entries equal to 1. This matrix M defines the subset $X_M \subset X_{25}$ of the allowed sequences,

$$X_M = \left\{x \ : \ M_{x_i x_{i+1}} = 1 \text{ for all } i \in \mathbf{Z}\right\},$$

which is closed and invariant by the shift.

The restriction of the shift transformation to X_M defines a dynamical system called the *two-sided shift of finite type defined by* M. The symbolic dynamics of the shift transformation on the subset X_M reproduces the dynamics along the heteroclinic network. The following theorem shows that, as X_{25}, X_M is homeomorphic to the usual middle thirds Cantor set. It guarantees the existence of dense periodic trajectories in the dynamics of the subshift defined by the matrix M and the existence of a point whose trajectory by the subshift is dense ([31]).

Theorem 37 *The space of the sequences defined by M is homeomorphic to the usual middle thirds Cantor set.*

Proof: The matrix M is irreducible since for $l \geq 5$, we have for all pair of indices i and j that $(M^l)_{ij} > 0$. It is known that the space of sequences defined by an irreducible transition matrix is either a periodic trajectory or is homeomorphic to the usual middle thirds Cantor set [31].

In the case of the space sequences defined by M it is obvious that it is not a periodic trajectory since we can easily point out two different allowed sequences: $(absasb)$ and $(a - bs^2as^2b)$, where (w) denotes the sequence $(...wwwwww...)$. We conclude that the space of the sequences defined by M is homeomorphic to the usual middle thirds Cantor set. □

We can measure the randomness of the dynamics of a subshift by computing its topological entropy. The topological entropy measures the rate of exponential growth of the number of allowed words,

$$h(X) = lim_{l\to\infty}\frac{1}{l}\log|\mathcal{W}(X,l)|,$$

where $\mathcal{W}(X,l) = \{[x_0,...,x_{l-1}]\,|x \in X\}$ denotes the words in X of lenght l and $|\cdot|$ denotes the cardinality of the set.

By observation 1.4.2 of [31], we have that $h(X_M, \sigma) = \log \lambda$, where λ is the spectral radius of M. That is,

$$\lambda = max \{ \|\mu\| : \mu \text{ is an eigenvalue for } M \} .$$

For the matrix M, Maple provides the value $\lambda \simeq 7.013293248$, and we conclude that the subshift defined by M has topological entropy $h(X_M, \sigma) \simeq \log(7.013293248)$.

Identifying the dynamics along the heteroclinic network Σ with the subshift defined by M the following corollary holds:

Corollary 38 *The dynamics along the heteroclinic network* Σ

(1) has dense periodic points,

(2) has at least one point with dense trajectory,

(3) is of horseshoe type.

Proof: The dynamics along the heteroclinic network is described by the subshift of finite type defined by matrix M. Since the matrix M is irreducible we have proved in theorem 37 that the space of the sequences defined by M is topologically conjugate to the usual middle thirds Cantor set. Thus, the statements (1) and (2) are an immediate consequence of this conjugacy, since the dynamics on the Cantor set has dense periodic points and at least one point with dense trajectory.

Statement (3) follows from the fact that the dynamics of the shift transformation is topologically conjugate to the dynamics of the Smale horseshoe; see [20], section 5.1 and [45], section 2.1. □

If we consider the alphabet $L_Q = \{[a], [b], [c]\}$, numbering its elements by the given order, the transition matrix that translates the dynamics along the quotient heteroclinic network is given by

$$Q = \begin{bmatrix} 0 & 1 & 0 \\ 1 & 0 & 1 \\ 1 & 0 & 1 \end{bmatrix} .$$

Note that matrices M and Q have the same structure. The topological entropy of the subshift defined by Q is $\log(\frac{1+\sqrt{5}}{2}) \simeq \log(1.618033989)$.

6.2 Symbolic dynamics in the neighbourhood of the network

In this section we put together the information on the dynamics obtained in the previous section with the symbolic dynamics in chapter 5 to obtain the local dynamics in the neighbourhood of the heteroclinic network Σ. That is, we put together information contained in sequences such as $(... - sb.absa...)$, describing the dynamics along the heteroclinic network, with that contained in sequences of the type $(...221.1221...)$, describing the dynamics on a Cantor set.

Consider the invariant saddles $[a]$, $[b]$ and $[c]$ in the quotient heteroclinic network Σ/Γ. Define neighbourhoods of these invariant saddles and Poincaré maps as in chapter 5. This is enough, by the study and claim in chapter 5, to assert the existence, under certain conditions, of horseshoe dynamics in the neigbourhood of each of the quotient heteroclinic cycles in the network Σ/Γ.

Further, the symmetry allows us to use those neighbourhoods to define neighbourhoods of the invariant saddles in the heteroclinic network Σ. A neighbourhood of the whole heteroclinic network Σ can be obtained from the latter using the flow. Each closed path along a heteroclinic cycle in the network Σ, determines a Poincaré map with properties analogous to the Poincaré maps defined in chapter 5.

Recall that each invariant saddle is part of more than one heteroclinic connection. There are several heteroclinic trajectories entering and leaving the neighbourhood of each invariant saddle, producing several Cantor sets in each neighbourhood. All Cantor sets in a given neighbourhood can be identified since they are topologically equivalent. They can be distinguished via the trails of the closed paths.

Let e be an invariant saddle in $[a]\cup[b]\cup[c]$. Let X_e be the space of bi-infinite sequences of elements in the alphabet $L_e = \{1_e, 2_e\}$. The dynamics of the shift map in X_e is topologically equivalent to the dynamics on the Cantor set in the neighbourhood of the invariant saddle e. We define the symbolic dynamics in the neighbourhood of the network Σ using the shift dynamics (X_M, σ) and (X_e, σ), for each e in L_M.

Let x be a sequence in X_M that defines the trail of a trajectory along the network Σ, and y^e a sequence in X_e, for each $e \in L_M$. For example, $x = (...s^3bc.sa - sb - s^2as^2b...)$ and $y^a = (...1_a.1_a1_a1_a...)$, ..., $y^{s^4c} = (...2_{s^4c}.1_{s^4c}1_{s^4c}2_{s^4c}...)$.

Each closed trajectory in a sequence x, let us say $(...x_i...x_i...)$, corresponds to a closed path along the network that starts and ends at the same node x_i. The closed path

determines one iteration of the Poincaré map defined in the neighbourhood of x_i, and this corresponds to a shift operation on a sequence $y^{x_i} \in X_{x_i}$.

In fact, each shift operation in x, with $[\sigma(x)]_{i-1} = x_i$, determines a shift operation in $y^{x_i} \in X_{x_i}$. This is because every time a trajectory passes a node more than once, it determines another closed path starting and ending at that node.

Let $L_R = \cup_{e \in L_M} L_e$ and X_R be the space of the sequences with elements in the alphabet L_R. Let $X_N \subset X_R$ be the subset of the sequences in X_R describing the dynamics in the neighbourhood of the heteroclinic network Σ.

We define a multi-tape Turing machine that constructs the sequences in X_N. Each sequence in X_N is constructed using a sequence in X_M and a sequence in X_e, for each $e \in L_M$. A sequence in X_N looks like $(...2_{s^3b}2_c.1_{sa}2_{-sb}1_{-s^2a}1_{s^2b}...)$.

We could have defined the subshift (X_N, σ) codifying the dynamics in the neighbourhood of the heteroclinic network Σ without defining a Turing machine. The Turing machine is just a tool that helps to explain how the symbolic dynamics in the neighbourhood of the network Σ is defined using the symbolic dynamics along the network Σ and the symbolic dynamics that codifies the dynamics in the neighbourhood of the heteroclinic cycles in the network. The use of the Turing machine can be useful in connecting our study to Complexity theory.

A *Turing machine* is a simple mathematical model of a computer (that is as powerful as any other computer - Church's thesis). We give here a very brief description of a multi--tape Turing machine, for a more detailed explanation see (Hopcroft and Ullman [28], chapter 7) and (Homer and Selman [27], chapter 2). As the name indicates, a multi--tape Turing machine has more than one tape. A multi-tape Turing machine consists of a finite state control connected to the output and input tapes and a read-write head for each of them, see figure 6.1. The finite control consists of a set of states, a transition function δ and the tape heads. Each tape is divided into cells and the tape heads scan one cell of the tape at a time. The tapes are infinite in both directions and we refer to the two directions on the tapes as left and right. The tape heads can be moved one cell to the left or to the right or can remain in the same position. Before the Turing machine starts computing, an input string is placed on each input tape, one symbol in each cell, and the ouput tape is blank. The tape head of each tape is positioned on a distinguished cell on the tape called the start cell, and the finite control is in a distinguished state, i, called the initial state. The Turing machine computes via the transition function δ. On a single move, depending on the state of the finite control and the symbol scanned by each of the tape heads, the machine can do the following

operations: change state; print a new symbol on the cell scanned by the output tape head; and move each of its tape heads, independently, one cell to the left or right, or keep it stationary.

Formally, we denote a multi-tape Turing machine, with k tapes, as

$$\mathcal{T} = (Q, A_1, ..., A_k, M_1, ..., M_k, \Delta, \delta, i, F),$$

where

Q	is the finite set of *states*,
A_j	is the set of *input symbols* in tape j, $j \in \{1, ..., k\}$ and is a subset of M_j not including Δ,
M_j	is the finite set of allowable tape *symbols* in tape j, $j \in \{1, ..., k\}$
Δ	is the *blank*, and is a symbol of M_j, $j \in \{1, ..., k\}$
δ	is the *next move function*, a map from $Q \times M_1 \times ... \times M_k$ to $Q \times M_1 \times ... \times M_k \times \{L, R, S\}^k$,
$i \in Q$	is the *initial state*,
$F \subseteq Q$	is the set of *final states*.

(6.2)

Let X_2 be the space of bi-infinite sequences of elements in the alphabet $L_2 = \{1, 2\}$.

We could define a multi-tape Turing machine $\mathcal{T}$ constructing X_N by considering 27 tapes. The first one would initially be blank and during the computation would be replaced by the output sequence, the second would contain a sequence $x \in X_M$ and the others contain a sequence $y^e \in X_2$, one for each invariant saddle $s \in L_M$. The Turing machine $\mathcal{T}$ would read an element $x_i = e$, $s \in L_M$, in the second tape, read an element $y^e_j = d$, $d \in L_2$, in the tape containing the sequence y^e corresponding to e and would write d_e in the output tape (first tape).

Consider a full shift (X, σ) on n-symbols and consider k sequences $x^1, ..., x^k$ in X. Define a new sequence x satisfying $x_i \in \{x^1_i, ..., x^k_i\}$. Since (X, σ) is a full shift, it is immediate that $x \in X$.

Considering the above observation, instead of defining a Turing machine with 27 tapes we define it with only 3 tapes. The first tape is initially blank and will contain the output sequence, the second tape contains a sequence $x \in X_M$, and the third tape contains a sequence $y \in X_2$. Assume, for example, $x = (...sa\ s^3b\ c\ \ sa\ .\ -\ sb\ -\ s^2a\ s^2b\ a\ b...)$ and $y = (...1112.12122...)$.

Since the sequences are bi-infinite, the Turing machine that we define inspects alternately one cell at the right and one cell at the left of the tapes.

Each state contains information regarding the number of the next cell of the tapes to be inspected and the number of cells the tape heads must move to the left or to the right until they reach that cell.

If the tape heads are not positioned at the cell to be inspected, they move to the left or to the right accordingly to the information in the state. When the tape heads are positioned at the cell to be inspected, the Turing machine $\mathcal{T}$ reads the element $x_i = e$, $e \in L_M$ in the second tape and the element $y_i = d$, $d \in L_2$ in the third tape, writes d_e in the output tape, advances the tapes one element to the left or to the right, adjusts the state information, and continues with the same procedure. For the example sequences given, the output sequence in the first tape is $(...1_{sa}1_{s^3b}1_c2_{sa}.1_{-sb}2_{-s^2a}1_{s^2b}2_a2_b...)$. See figure 6.1.

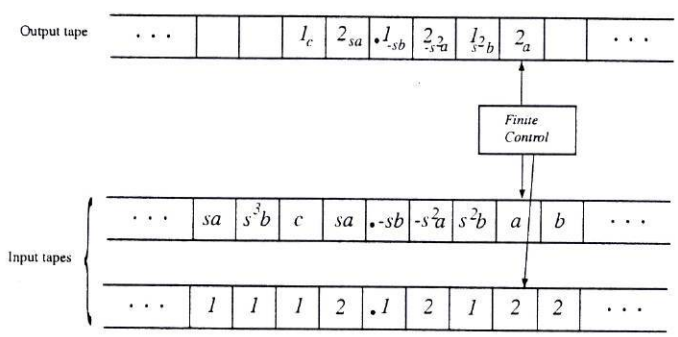

Figure 6.1: The Turing machine $\mathcal{T}$ that takes a sequence in X_M, a sequence in X_2 and outputs a sequence in X_N.

The set of possible output sequences is the set of bi-infinite sequences with elements in L_R, such that, d_e and l_k are two consecutive elements in a sequence if and only if there is a connection in the heteroclinic network Σ from saddle e to saddle k.

The Turing machine $\mathcal{T}$ that constructs the sequences in X_N is formally defined as

$$\mathcal{T} = (Q, A_1, A_2, A_3, M_1, M_2, M_3, \Delta, \delta, i, F),$$

where

$$\begin{array}{lllllllll} Q & = & \{(p,l,r)\}, p \in \mathbf{Z},\ l,r \in \mathcal{N}_0, & i & = & (0,0,0) \in Q, & F & = & \{\}, \\ A_1 & = & \{\}, & A_2 & = & L_M, & A_3 & = & L_2, \\ M_1 & = & L_R \cup \{\Delta\}, & M_2 & = & L_M \cup \{\Delta\}, & M_3 & = & L_2 \cup \{\Delta\}. \end{array} \tag{6.3}$$

For each state $(p, l, r) \in Q$, the variable p contains the number of the next cell to be inspected and the variables l and r give the number of cells the tape heads should move, respectively, to the left or to the right to reach the cell p. The transition function is defined as

$$\delta \; : \; Q \times M_1 \times M_2 \times M_3 \to Q \times M_1 \times M_2 \times M_3 \times \{L, R, S\}^3, \tag{6.4}$$

with

$$\begin{aligned}
\delta((0,0,0),[\;,e,d]) &= ((1,0,0),[d_e,e,d],[R,R,R]),\\
\delta((n,0,k),[w,e,d]) &= ((n,0,k-1),[w,e,d],[R,R,R]),\\
\delta((n,0,0),[\;,e,d]) &= ((-n,2n-1,0),[d_e,e,d],[L,L,L]),\\
\delta((-n,k,0),[w,e,d]) &= ((-n,k-1,0),[w,e,d],[L,L,L]),\\
\delta((-n,0,0),[\;,e,d]) &= ((n+1,0,2n),[d_e,e,d],[R,R,R]),
\end{aligned} \tag{6.5}$$

$n \in \mathcal{N}$, $e \in L_M$, $d \in L_2$, and $d_e \in L_R$.

Notice that the set of final states is empty since the sequences are infinite. However, at any time we can stop the computation of the Turing machine and inspect the contents of the output tape.

We construct the space X_N of the sequences that define the symbolic dynamics that characterizes the local dynamics in the neighbourhood of the heteroclinic network Σ using the map

$$\begin{array}{ccc} X_M \times X_2 & \longrightarrow & X_N \\ (x,y) & \mapsto & z = \mathcal{T}(x,y) \end{array} \tag{6.6}$$

which given two sequences in X_M and X_2 produces a sequence in X_N that is the output sequence of the defined Turing machine $\mathcal{T}$.

We order the elements in the alphabet L_R as follows,

$1_a \to 1$	$1_{-a} \to 11$	$1_b \to 21$	$1_{-b} \to 31$	$1_c \to 41$
$2_a \to 2$	$2_{-a} \to 12$	$2_b \to 22$	$2_{-b} \to 32$	$2_c \to 42$
$1_{sa} \to 3$	$1_{-sa} \to 13$	$1_{sb} \to 23$	$1_{-sb} \to 33$	$1_{sc} \to 43$
$2_{sa} \to 4$	$2_{-sa} \to 14$	$2_{sb} \to 24$	$2_{-sb} \to 34$	$2_{sc} \to 44$
$1_{s^2a} \to 5$	$1_{-s^2a} \to 15$	$1_{s^2b} \to 25$	$1_{-s^2b} \to 35$	$1_{s^2c} \to 45$
$2_{s^2a} \to 6$	$2_{-s^2a} \to 16$	$2_{s^2b} \to 26$	$2_{-s^2b} \to 36$	$2_{s^2c} \to 46$
$1_{s^3a} \to 7$	$1_{-s^3a} \to 17$	$1_{s^3b} \to 27$	$1_{-s^3b} \to 37$	$1_{s^3c} \to 47$
$2_{s^3a} \to 8$	$2_{-s^3a} \to 18$	$2_{s^3b} \to 28$	$2_{-s^3b} \to 38$	$2_{s^3c} \to 48$
$1_{s^4a} \to 9$	$1_{-s^4a} \to 19$	$1_{s^4b} \to 29$	$1_{-s^4b} \to 39$	$1_{s^4c} \to 49$
$2_{s^4a} \to 10$	$2_{-s^4a} \to 20$	$2_{s^4b} \to 30$	$2_{-s^4b} \to 40$	$2_{s^4c} \to 50$

The transition matrix N that defines the subshift of finite type codifying the dynamics in the neighbourhood of the heteroclinic network has the same block structure as the

matrix M that defines the subshift of finite type that codifies the dynamics along the heteroclinic network.

We have,

$$N = \begin{bmatrix} 0 & A_1 & 0 \\ A_2 & 0 & A_3 \\ A_4 & 0 & A_5 \end{bmatrix},$$

where

$$A_1 = \begin{bmatrix} P & P \\ P & P \end{bmatrix}, P = \begin{bmatrix} \mathbf{1}_{2\times 2} & 0 & 0 & 0 & 0 \\ 0 & \mathbf{1}_{2\times 2} & 0 & 0 & 0 \\ 0 & 0 & \mathbf{1}_{2\times 2} & 0 & 0 \\ 0 & 0 & 0 & \mathbf{1}_{2\times 2} & 0 \\ 0 & 0 & 0 & 0 & \mathbf{1}_{2\times 2} \end{bmatrix},$$

$$A_2 = \begin{bmatrix} A_5 & A_5 \\ A_5 & A_5 \end{bmatrix}, A_3 = \begin{bmatrix} \mathbf{1}_{10\times 10} \\ \mathbf{1}_{10\times 10} \end{bmatrix}, A_4 = \begin{bmatrix} \mathbf{1}_{10\times 10} & \mathbf{1}_{10\times 10} \end{bmatrix}, A_5 = \mathbf{1}_{10\times 10} - P.$$

The space of sequences defined by matrix N is homeomorphic to the usual middle thirds Cantor set, similarly to what happens with the subshift defined by the matrix M.

The topological entropy of the subshift defined by $h(X_N, \sigma) \simeq \log(14.02658650)$ (determined numerically with Maple).

Identifying the local dynamics in the neighbourhood of the heteroclinic network Σ with the shift dynamics defined by matrix N we conclude that, it

- has dense periodic trajectories,
- has at least one point with dense trajectory,
- has topological entropy $\simeq \log(14.02658650)$, and
- is of horseshoe type.

As expected, the topological entropy of the dynamics in the neighbourhood of the heteroclinic network is greater than the topological entropy of the dynamics along the heteroclinic network.

Assembling the information obtained, we have that, under certain conditions,

Proposition 39 *(1) There are dense periodic trajectories in the neighbourhood of the network Σ and dense periodic trajectories in the neigbourhood of the heteroclinic cycles in Σ.*

(2) There is at least one point with dense trajectory in the neighbourhood of the network Σ and at least one point with dense trajectory in the neighbourhood of each heteroclinic cycle in Σ.

(3) the dynamics in the neighbourhood of each heteroclinic cycle in Σ is horseshoe dynamics, and the dynamics in the neighbourhood of the network Σ is a horseshoe of horseshoe dynamics.

Chapter 7

Future work

Finally, we point out some aspects related to the work in this thesis that we find interesting for future research.

We would like to study the local behaviour in the neighbourhood of a generic heteroclinic cycle topologically equivalent to that of the example that we construct in section 4.2 involving two saddle-foci and a periodic trajectory.

As we have mentioned, it seems that we can find conditions for horseshoe dynamics in the neighbourhood of such heteroclinic cycle using similar techniques and computations as in section 5.1 with some added difficulties.

Moreover, it would be interesting to inspect, for the examples we constructed, if there is other kind of complicated behaviour, such as mixing properties. Consider, for example, the system constructed in section 4.1, where in the unperturbed system we have a two--dimensional heteroclinic connection that is a two-sphere on the invariant three-sphere, and then we perturb the rotational symmetry to get the transverse intersection of the two-dimensional invariant manifolds.

As conjectured by M. Field [17], there can be the creation of shaped regions where orbits can escape from the 'inside' of the two-sphere. This is what we observe in the time series 4.8 in section 4.1.3.1. What are the asymptotics of these regions? To what extent can they create mixing between the 'inside' and the 'outside' of the original two-sphere?

M. Field's guess is that the regions become streched out and spiral around the one--dimensional unperturbed connection (that would allow for reentry). What is the asymptotic probability of a point in one of these regions to reenter the 'inside' of the

two-sphere the next time round? After n-times? Does the series sum to a number strictly less than one?

We think that the symmetry breaking perturbations of the unperturbed examples in sections 4.1.1.2 and 4.2.1.2 deserve further study.

We have proved that, under certain conditions, the dynamics in the neighbourhood of the Shilnikov heteroclinic network Σ of Field's example is a horseshoe of horseshoe dynamics. This implies chaotic dynamics, but does not imply the existence of a chaotic attractor. Nevertheless, numerical integration with Dstool appears to yield trajectories asymptotic to chaotic motion, as in figure 3.3. The question remains: is the Field's example a chaotic attractor?

Another interesting question is whether the chaotic behaviour in Field's example persists for small symmetry breaking perturbations, and how it bifurcates. Numerical computations with Dstool revealed the persistence of the chaotic behaviour for small linear perturbations. Increasing the value of the perturbation factor we observed the flow jumping alternately between two regions and staying in each region for a while. Further increasing the perturbing value the two regions seem to bifurcate to four attracting periodic trajectories. A detailed investigation is worth while.

It is interesting to notice that the topological entropy of the symbolic dynamics in the neighbourhood of the heteroclinic network Σ equals the sum of the topological entropy of the symbolic dynamics along the network and of the topological entropy of the symbolic dynamics in the neighbourhood of the heteroclinic cycles in Σ. This is valid for heteroclinic networks where the symbolic dynamics that codifies the dynamics in the neighbourhood of the heteroclinic cycles are topologically conjugate.

This raises an interesting question: In general, given a heteroclinic network with some structure, is it possible to establish a relation between the entropy in the neighbourhood of the heteroclinic network with the entropy along the heteroclinic network and the entropy in the neighbourhood of parts of the network?

The use of symbolic dynamics and of a Turing machine that generates the space of allowed sequences connects to the part of complexity theory supported by concepts from probability and information theory. We would like to explore this connection (see Badii and Politi [5]).

We would like to prove the conjecture 33 in section 5.1.6 of the extension of the Invariant sphere theorem [15].

Appendix A

Dstool programming and results

A.1 Dstool program

The basic Dstool specification of a dynamical system (vector field or mapping) comprizes essentially the definition of the set of governing equations for the dynamical system and the definition of the initial settings of the variables and parameters. Additionally, procedures can be written to define derivatives or auxiliary scalar-valued functions.

We give a brief explanation of how the Dstool program that we defined to study Field's example works. At the end of the section we present a complete printing of the Dstool program.

The routine `field()` is called in each iteration; it reads the current state variables in array `x` and the current parameters in array `p`, and places the new state in the array `f`. The routine `field()` calls the routine `field_aux()`.

The routine `field_aux()` is the routine that we define to control whether a trajectory is near an equilibrium or periodic trajectory. The array `equilibrio` contains the coordinates of the equilibria, and the array `nomes` contains the identification of those equilibria.

For each coordinate of the actual position in phase space, the routine `field_aux()` first computes its distance to the coordinates of an equilibrium. Then it compares each of those values with the pre-defined distance in variable `dist`. This is repeated for each point in the array of equilibria.

The pre-defined distance is considered as a parameter and so its value can be changed during the Dstool execution.

If the distance computed in each coordinate is less than the fixed distance, this means that the trajectory passes near the equilibrium that is being analised. In this case it prints the identification of the equilibrium and the distance in each coordinate.

This same procedure is then executed for each of the points in the array `ciclo` that correspond to points of the periodic trajectories. We study the proximity of a trajectory to a periodic trajectory by its proximity to some points of the periodic trajectory. The values `c11,...,c82` defined in the begining of the routine were numerically computed using Dstool and represent coordinates in the (y_1, y_2)-plane of 8 points that belong to the periodic trajectory c. The points of the remaining periodic trajectories are computed using the group action.

The definition is completed with the information in routine `field_init()` about the structure of the phase space, the names of the variables, initial values and the maximum and minimum values. This routine also provides information on parameters, auxiliary functions and numerical algorithms.

In what concerns interpretation of data in the sequences, we emphasize two facts.

One is that the network in the Field's example is not asymptotically stable, so there are some parts of the sequences that we have ignored because we think that the trajectory did not come sufficiently close to the equilibrium or periodic trajectory so as to draw any conclusion. The other important aspect is the value that we consider to be the radius of the neighbourhoods.

```
/*  ------------------------------------------------------------------

This program is the property of:

                          Cornell University
                    Center for Applied Mathematics
                          Ithaca, NY 14853

and may be used, modified and distributed freely, subject to the
following restrictions:

       Any product which incorporates source code from the dstool
       program or utilities, in whole or in part, is distributed
       with a copy of that source code, including this notice. You
       must give the recipients all the rights that you have with
       respect to the use of this software. Modifications of the
       software must carry prominent notices stating who changed
       the files and the date of any change.
```

```
DsTool is distributed in the hope that it will be useful, but
WITHOUT ANY WARRANTY; without even the implied warranty of FITNESS
FOR A PARTICULAR PURPOSE.  The software is provided as is without
any obligation on the part of Cornell faculty, staff or students to
assist in its use, correction, modification or enhancement.

  ------------------------------------------------------------  */
#include <model_headers.h>

/* ---------------------------------------------------------------------
   Required function used to define the vector field or map.
   The values of the vector field mapping at point x with parameter
   values p are returned in the pre-allocated array f. For vector fields,
   the last components of both f and x are time components. All arrays are
   indexed starting from 0.
   --------------------------------------------------------------------- */
int field(f,x,p)
double *f,*x,*p;
{
  double l=p[0], b=p[1], g=p[2];

  field_aux(f,x,p);

  f[0]=l*x[0]-(x[0]*x[0]+x[1]*x[1]+x[2]*x[2]+x[3]*x[3])*x[0]+
             +b*(x[0]*x[0]*x[2]-x[1]*x[1]*x[2]-2*x[0]*x[1]*x[3])+
             +g*(x[2]*x[2]*x[2]-3*x[2]*x[3]*x[3]);

  f[1]=l*x[1]-(x[0]*x[0]+x[1]*x[1]+x[2]*x[2]+x[3]*x[3])*x[1]+
             +b*(-x[0]*x[0]*x[3]+x[1]*x[1]*x[3]-2*x[0]*x[1]*x[2])+
             +g*(-x[3]*x[3]*x[3]+3*x[2]*x[2]*x[3]);

  f[2]=l*x[2]-(x[0]*x[0]+x[1]*x[1]+x[2]*x[2]+x[3]*x[3])*x[2]+
             +b*(x[0]*x[2]*x[2]-x[0]*x[3]*x[3]+2*x[1]*x[2]*x[3])+
             +g*(x[0]*x[0]*x[0]-3*x[0]*x[1]*x[1]);

  f[3]=l*x[3]-(x[0]*x[0]+x[1]*x[1]+x[2]*x[2]+x[3]*x[3])*x[3]+
             +b*(x[1]*x[2]*x[2]-x[1]*x[3]*x[3]-2*x[0]*x[2]*x[3])+
             +g*(x[1]*x[1]*x[1]-3*x[0]*x[0]*x[1]);
}

/* ---------------------------------------------------------------------
   Optional function used to define the Jacobian m at point x with
   parameters p. The matrix m is pre-allocated (by the routine dmatrix);
   At exit, m[i][j] is to be the partial derivative of the i'th component
   of f with respect to the j'th component of x.
   --------------------------------------------------------------------- */
/*

int user_jac(m,x,p)
double  **m, *x, *p;
{
}
*/

/* ---------------------------------------------------------------------
   Optional function used to define the inverse or approximate inverse y at
```

```
   the point x with parameter values p. The array y is pre-allocated.
   ------------------------------------------------------------------------ */
/*
int user_inv(y,x,p)
double    *y,*x,*p;
{
}
*/

/* ------------------------------------------------------------------------
   Optional function used to define aux functions f of the varbiables x
   and parameters p. The array f is pre-allocated. Time is available as the
   last component of x.
   ------------------------------------------------------------------------ */
/*
   ----------------------------
   ROUTINE field_aux STARTS HERE
   ----------------------------
                                */
int field_aux(f,x,p)
double *f,*x,*p;
{
   int flag=0;
   int viz=0;
   int i=0;
   double dist=p[3];
   double  d[4]= {0,0,0,0};
   double         sin(),cos();

   double         roota=sqrt((-p[0])/(p[1]+p[2]-2));
   double         rootb=sqrt((p[0])/(p[1]+p[2]+2));

   double         c11=1.0228068;
   double         c12=-0.0067817186;

   double         c21=-1.0123465;
   double         c22=0.083224282;

   double         c31=0.021242525;
   double         c32=1.0214375;

   double         c41=-0.097350043;
   double         c42=-1.0095621;

   double         c51=0.35436298;
   double         c52=-0.94794071;

   double         c61=-0.08908218;
   double         c62=0.96830921;

   double         c71=0.3958211;
   double         c72=0.89402183;

   double         c81=-0.90502673;
   double         c82=-0.49743481;

   char*   nomes[21]={"zero",
```

```
                    "a","sa","s2a","s3a","s4a","-a","-sa","-s2a","-s3a","-s4a",
                    "b","sb","s2b","s3b","s4b","-b","-sb","-s2b","-s3b","-s4b",
                    };
  char*   nomeciclos[41]={"zero","c","sc","s2c","s3c","s4c","c","sc","s2c","s3c","s4c",
                                "c","sc","s2c","s3c","s4c","c","sc","s2c","s3c","s4c",
                                "c","sc","s2c","s3c","s4c","c","sc","s2c","s3c","s4c",
                                "c","sc","s2c","s3c","s4c","c","sc","s2c","s3c","s4c"};

  double  equilibrio[21][4]= {
           {0,0,0,0},
           {roota,0,roota,0}
           {roota*cos(2*PI/5),roota*sin(2*PI/5),roota*cos(4*PI/5),roota*sin(4*PI/5)},
           {roota*cos(4*PI/5),roota*sin(4*PI/5),roota*cos(-2*PI/5),roota*sin(-2*PI/5)},
           {roota*cos(-4*PI/5),roota*sin(-4*PI/5),roota*cos(2*PI/5),roota*sin(2*PI/5)},
           {roota*cos(-2*PI/5),roota*sin(-2*PI/5),roota*cos(-4*PI/5),roota*sin(-4*PI/5)},
           {-roota,0,-roota,0},
           {-roota*cos(2*PI/5),-roota*sin(2*PI/5),-roota*cos(4*PI/5),-roota*sin(4*PI/5)},
           {-roota*cos(4*PI/5),-roota*sin(4*PI/5),-roota*cos(-2*PI/5),-roota*sin(-2*PI/5)},
           {-roota*cos(-4*PI/5),-roota*sin(-4*PI/5),-roota*cos(2*PI/5),-roota*sin(2*PI/5)},
           {-roota*cos(-2*PI/5),-roota*sin(-2*PI/5),-roota*cos(-4*PI/5),-roota*sin(-4*PI/5)},
           {rootb,0,-rootb,0},
           {rootb*cos(2*PI/5),rootb*sin(2*PI/5),rootb*cos(9*PI/5),rootb*sin(9*PI/5)},
           {rootb*cos(4*PI/5),rootb*sin(4*PI/5),rootb*cos(3*PI/5),rootb*sin(3*PI/5)},
           {rootb*cos(-4*PI/5),rootb*sin(-4*PI/5),rootb*cos(7*PI/5),rootb*sin(7*PI/5)},
           {rootb*cos(-2*PI/5),rootb*sin(-2*PI/5),rootb*cos(PI/5),rootb*sin(PI/5)},
           {-rootb,0,rootb,0},
           {-rootb*cos(2*PI/5),-rootb*sin(2*PI/5),-rootb*cos(9*PI/5),-rootb*sin(9*PI/5)},
           {-rootb*cos(4*PI/5),-rootb*sin(4*PI/5),-rootb*cos(3*PI/5),-rootb*sin(3*PI/5)},
           {-rootb*cos(-4*PI/5),-rootb*sin(-4*PI/5),-rootb*cos(7*PI/5),-rootb*sin(7*PI/5)},
           {-rootb*cos(-2*PI/5),-rootb*sin(-2*PI/5),-rootb*cos(PI/5),-rootb*sin(PI/5)},
                        };

double  ciclo[41][4]= {
          {0,0,0,0},
          {0,c11,0,c12},
          {c11*cos(2*PI/5+PI/2),c11*sin(2*PI/5+PI/2),c12*cos(4*PI/5-PI/2),c12*sin(4*PI/5-PI/2)},
          {c11*cos(4*PI/5+PI/2),c11*sin(4*PI/5+PI/2),c12*cos(-2*PI/5-PI/2),c12*sin(-2*PI/5-PI/2)},
          {c11*cos(-4*PI/5+PI/2),c11*sin(-4*PI/5+PI/2),c12*cos(2*PI/5-PI/2),c12*sin(2*PI/5-PI/2)},
          {c11*cos(-2*PI/5+PI/2),c11*sin(-2*PI/5+PI/2),c12*cos(-4*PI/5-PI/2),c12*sin(-4*PI/5-PI/2)},
          {0,c21,0,c22},
          {c21*cos(2*PI/5-PI/2),c21*sin(2*PI/5-PI/2),c22*cos(4*PI/5+PI/2),c22*sin(4*PI/5+PI/2)},
          {c21*cos(4*PI/5-PI/2),c21*sin(4*PI/5-PI/2),c22*cos(-2*PI/5+PI/2),c22*sin(-2*PI/5+PI/2)},
          {c21*cos(-4*PI/5-PI/2),c21*sin(-4*PI/5-PI/2),c22*cos(2*PI/5+PI/2),c22*sin(2*PI/5+PI/2)},
          {c21*cos(-2*PI/5-PI/2),c21*sin(-2*PI/5-PI/2),c22*cos(-4*PI/5+PI/2),c22*sin(-4*PI/5+PI/2)},
          {0,c31,0,c32},
          {c31*cos(2*PI/5+PI/2),c31*sin(2*PI/5+PI/2),c32*cos(4*PI/5+PI/2),c32*sin(4*PI/5+PI/2)},
          {c31*cos(4*PI/5+PI/2),c31*sin(4*PI/5+PI/2),c32*cos(-2*PI/5+PI/2),c32*sin(-2*PI/5+PI/2)},
          {c31*cos(-4*PI/5+PI/2),c31*sin(-4*PI/5+PI/2),c32*cos(2*PI/5+PI/2),c32*sin(2*PI/5+PI/2)},
          {c31*cos(-2*PI/5+PI/2),c31*sin(-2*PI/5+PI/2),c32*cos(-4*PI/5+PI/2),c32*sin(-4*PI/5+PI/2)},
          {0,c41,0,c42},
          {c41*cos(2*PI/5-PI/2),c41*sin(2*PI/5-PI/2),c42*cos(4*PI/5-PI/2),c42*sin(4*PI/5-PI/2)},
          {c41*cos(4*PI/5-PI/2),c41*sin(4*PI/5-PI/2),c42*cos(-2*PI/5-PI/2),c42*sin(-2*PI/5-PI/2)},
          {c41*cos(-4*PI/5-PI/2),c41*sin(-4*PI/5-PI/2),c42*cos(2*PI/5-PI/2),c42*sin(2*PI/5-PI/2)},
          {c41*cos(-2*PI/5-PI/2),c41*sin(-2*PI/5-PI/2),c42*cos(-4*PI/5-PI/2),c42*sin(-4*PI/5-PI/2)},
          {0,c51,0,c52},
          {c51*cos(2*PI/5+PI/2),c51*sin(2*PI/5+PI/2),c52*cos(4*PI/5-PI/2),c52*sin(4*PI/5-PI/2)},
          {c51*cos(4*PI/5+PI/2),c51*sin(4*PI/5+PI/2),c52*cos(-2*PI/5-PI/2),c52*sin(-2*PI/5-PI/2)},
```

```
            {c51*cos(-4*PI/5+PI/2),c51*sin(-4*PI/5+PI/2),c52*cos(2*PI/5-PI/2),c52*sin(2*PI/5-PI/2)},
            {c51*cos(-2*PI/5+PI/2),c51*sin(-2*PI/5+PI/2),c52*cos(-4*PI/5-PI/2),c52*sin(-4*PI/5-PI/2)},
            {0,c61,0,c62},
            {c61*cos(2*PI/5-PI/2),c61*sin(2*PI/5-PI/2),c62*cos(4*PI/5+PI/2),c62*sin(4*PI/5+PI/2)},
            {c61*cos(4*PI/5-PI/2),c61*sin(4*PI/5-PI/2),c62*cos(-2*PI/5+PI/2),c62*sin(-2*PI/5+PI/2)},
            {c61*cos(-4*PI/5-PI/2),c61*sin(-4*PI/5-PI/2),c62*cos(2*PI/5+PI/2),c62*sin(2*PI/5+PI/2)},
            {c61*cos(-2*PI/5-PI/2),c61*sin(-2*PI/5-PI/2),c62*cos(-4*PI/5+PI/2),c62*sin(-4*PI/5+PI/2)},
            {0,c71,0,c72},
            {c71*cos(2*PI/5+PI/2),c71*sin(2*PI/5+PI/2),c72*cos(4*PI/5+PI/2),c72*sin(4*PI/5+PI/2)},
            {c71*cos(4*PI/5+PI/2),c71*sin(4*PI/5+PI/2),c72*cos(-2*PI/5+PI/2),c72*sin(-2*PI/5+PI/2)},
            {c71*cos(-4*PI/5+PI/2),c71*sin(-4*PI/5+PI/2),c72*cos(2*PI/5+PI/2),c72*sin(2*PI/5+PI/2)},
            {c71*cos(-2*PI/5+PI/2),c71*sin(-2*PI/5+PI/2),c72*cos(-4*PI/5+PI/2),c72*sin(-4*PI/5+PI/2)},
            {0,c81,0,c82},
            {c81*cos(2*PI/5-PI/2),c81*sin(2*PI/5-PI/2),c82*cos(4*PI/5-PI/2),c82*sin(4*PI/5-PI/2)},
            {c81*cos(4*PI/5-PI/2),c81*sin(4*PI/5-PI/2),c82*cos(-2*PI/5-PI/2),c82*sin(-2*PI/5-PI/2)},
            {c81*cos(-4*PI/5-PI/2),c81*sin(-4*PI/5-PI/2),c82*cos(2*PI/5-PI/2),c82*sin(2*PI/5-PI/2)},
            {c81*cos(-2*PI/5-PI/2),c81*sin(-2*PI/5-PI/2),c82*cos(-4*PI/5-PI/2),c82*sin(-4*PI/5-PI/2)},
                        };

/* while  ( viz < 21 && flag == 0) */
  while  ( viz < 21)
   {
    for(i=0;i<4;i++)
     {
       d[i]=x[i]-equilibrio[viz][i];
       if (d[i] < 0) d[i]=-d[i];
      }
    if (d[0] < dist && d[1] < dist && d[2] < dist && d[3] < dist)
     {
       flag=1;
       printf("equilibrium %s distance (%f,%f,%f,%f) \n",nomes[viz],d[0],d[1],d[2],d[3]);
      }
    viz=viz+1;
   }
   viz=0;

/* while  ( viz < 41 && flag == 0) */
  while  ( viz < 41)
   {
    for(i=0;i<4;i++)
     {
       d[i]=x[i]-ciclo[viz][i];
       if (d[i] < 0) d[i]=-d[i];
      }

    if (d[0] < dist && d[1] < dist && d[2] < dist && d[3] < dist)
     {
       flag=1;
       printf("periodic trajectory %s distance (%f,%f,%f,%f)  point %i \n",
                                    nomeciclos[viz],d[0],d[1],d[2],d[3],viz);
      }
    viz=viz+1;
   }
}

/*
   ---------------------------
```

```
   ROUTINE field_aux ENDS HERE
   ---------------------------
                              */
/* ------------------------------------------------------------------------
   Required procedure to define default data for the dynamical system. NOTE: You
   may change the entries for each variable but PLEASE DO NOT change the list of
   items.  If a variable is unused, NULL or zero the entry, as appropriate.
   ------------------------------------------------------------------------ */
int field_init()
{
/* ------------ define the dynamical system in this segment --------------- */

int            n_varb=4;                        /* dim of phase space */
static char    *variable_names[]={"x1","y1","x2","y2"};    /* list of phase varb names */
static double  variables[]={0.790,0.000001,0.790,-0.00001}; /* default varb initial values */
static double  variable_min[]={-3.,-3.,-3.,-3.};        /* default varb min for display */
static double  variable_max[]={3.,3.,3.,3.};         /* default varb max for display */

static char    *indep_varb_name="time";         /* name of indep variable  */
double         indep_varb_min=0.;               /* default indep varb min for display */
double         indep_varb_max=10000.;           /* default indep varb max for display */

int            n_param=4;                       /* dim of parameter space */
static char    *parameter_names[]={"lambda","beta","gamma",''distancia''}; /* list of param names */
static double  parameters[]={1.,1,-0.6,0.15};           /* initial parameter values */
static double  parameter_min[]={1.,-1.,-1.,-1.};        /* default param min for display */
static double  parameter_max[]={1.,1.,1.,1.};        /* default param max for display */

int            n_funct=1;                       /* number of user-defined functions */
static char    *funct_names[]={"sequence"};     /* list of funct names; {""} if none */
static double  funct_min[]={0.};              /* default funct min for display */
static double  funct_max[]={1000};              /* default funct max for display */

int            manifold_type=EUCLIDEAN;         /* PERIODIC (a periodic varb) or EUCLIDEAN */
static int     periodic_varb[]={FALSE, FALSE,FALSE,FALSE}; /* if PERIODIC, which varbs are periodic? */
static double  period_start[]={0.,0.};          /* if PERIODIC, begin fundamental domain */
static double  period_end[]={1., 1.};           /* if PERIODIC, end of fundamental domain */

int            mapping_toggle=FALSE;             /* this is a map? TRUE or FALSE */
int            inverse_toggle=FALSE;            /* if so, is inverse FALSE, APPROX_INV, */
                                                /* or EXPLICIT_INV? FALSE for vec field */

/*  In this section, input NULL or the name of the function which contains... */
int            (*def_name)()=field;              /* the eqns of motion */
int            (*jac_name)()=NULL;              /* the jacobian (deriv w.r.t. space) */
int            (*aux_func_name)()=NULL;         /* the auxiliary functions */
int            (*inv_name)()=NULL;              /* the inverse or approx inverse */
int            (*dfdt_name)()=NULL;             /* the deriv w.r.t time */
int            (*dfdparam_name)()=NULL;         /* the derivs w.r.t. parameters */

/* ------------------ end of dynamical system definition ----------------- */
#include <ds_define.c>
}
```

References

[1] V.I. Arnold, 1973 *Ordinary Differential Equations*, The MIT Press

[2] P. Ashwin, 1997, Cycles homoclinic to chaotic sets; robustness and resonance, *Chaos*, Vol. **7**, pages207–220

[3] P. Ashwin and P. Chossat, 1998, Attractors for Robust Heteroclinic Cycles with Continua of Connections, *J. Nonlinear Sci.*, Vol. **8**, pages103–129

[4] P. Ashwin and M. Field, 1999 Heteroclinic Networks in Coupled Cell Systems *Arch. Rational Mech. Anal.*, **148**, pages 107–143

[5] R. Badii and A. Politi, 1997, *Complexity. Hierarchical Structures and Scaling in Physics*, Cambridge Nonlinear Science Series, Vol. **6**,Cambridge University Press

[6] A.L. Bertozzi, 1988, Heteroclinic orbits and chaotic dynamics in planar fluid flows, *SIAM J. Math. Anal.*, Vol. **19**, No. **6**, pages1271–1294

[7] G. E. Bredon, 1972 *Introduction to Compact transformation Groups*, Pure and Applied Mathematics, **46**,Academic Press, New York, London

[8] P. Chossat and M. Field, 1995, Geometric analysis of the effect of symmetry breaking perturbations on an $O(2)$ invariant homoclinic cycle, *Fields Institute Communications*, **4**, pages 21–42

[9] P. Chossat, F. Guyard and R. Lauterbach, 1999, Generalized Heteroclinic Cycles in Spherically Invariant Systems and their Perturbations, *J. Nonlin. Science*, Vol. **9**, Nr. **5**, pages479–524

[10] M. Dellnitz, M. Field, M. Golubitsky, A. Hohmann and J. Ma, 1995, Cycling Chaos, *IEEE Transactions on Circuits and Systems-I: Fundamental Theory and Applications*, **42(10)**, pages 821–823

[11] M. Dellnitz, G. Froyland and O. Junge *The Algorithms Behind GAIO - Set Oriented Numerical Methods for Dynamical Systems* Department of Mathematics and Computer Science University of Paderborn

[12] A.P.S. Dias, B. Dionne and I. Stewart, 2000 Heteroclinic Cycles and Wreath Product Symmetries *Dynamics and Stability of systems*, vol **15**, No **4**, pages 353–385

[13] M.J. Field, 1980 Equivariant Dynamical Systems *Transactions of the Amer. Math. Soc.*, Vol.**259**, No.**1**, pages 185–205

[14] M.J. Field, 1989, Equivariant bifurcation theory and symmetry breaking, *J. Dynamics and Diff. Equations*, **1**, pages 369–421

[15] M.J. Field, 1996, *Lectures on Bifurcations, Dynamics and Symmetry*, Pitman Research Notes in Mathematics Series 356, Longman

[16] M. Field, 2000 *Complex Dynamics in Symmetric Systems*, Summer School on Bifurcations, Symmetry, and Patterns, 5-14 July, 2000, Centro de Matemática Aplicada da Universidade do Porto,Notes CMA/1/00

[17] M. Field, Private communication.

[18] M.J. Field, R.W. Richardson, 1992, Symmetry-Breaking and Branching Patterns in Equivariant Bifurcation Theory, II, *Arch. Rational Mech. Anal.*, number 120, pages 147-190

[19] M. Golubitsky and D. G. Schaeffer, 1988, *Singularities and Groups in Bifurcation Theory*, Vol. **II**, Springer-Verlag

[20] J. Guckenheimer and P. Holmes,1983, *Nonlinear Oscillations, Dynamical Systems, and Bifurcations of Vector Fields*, Applied Mathematical Sciences, number 42, Springer-Verlag

[21] J. Guckenheimer and P. Holmes, 1988, Structurally stable heteroclinic cycles, *Math. Proc. Camb. Phil. Soc.*, **103**, pages 189–192

[22] J. Guckenheimer , M.R. Myers, F.J. Wicklin, P.A. Worfolk, 1995, *Dstool: A Dynamical System Toolkit with an Interactive Graphical Interface - Reference Manual*, Center For Applied Mathematics, Cornell University

[23] J. Guckenheimer, 1995, *DsTool: A Dynamical System Toolkit with an Interactive Graphical Interface - Tutorial*, Center for Applied Mathematics, Cornell University

[24] J. Guckenheimer, M.R. Myers, F.J. Wicklin, P.A. Worfolk, 1995, *DsTool: A Dynamical System Toolkit with an Interactive Graphical Interface - User's Manual*, Center for Applied Mathematics, Cornell University

[25] J. Guckenheimer, B.A. Meloon, M.R. Myers, F.J. Wicklin, P.A. Worfolk, 1997, *DsTool: A Dynamical System Toolkit with an Interactive Graphical Interface - User's Manual*,Version Tk Draft, Center for Applied Mathematics, Cornell University

[26] M.W.Hirsch, C.C.Pugh, M.Shub, 1977 *Invariant Manifolds* Lecture Notes in Mathematics, **583**, Springer-Verlag

[27] S.Homer and A.L. Selman *Computability and Complexity Theory*, Texts in Computer Science,Springer

[28] J.E. Hopcroft and J.D. Ullman, 1979 *Introduction to Automata theory, Languages, and Computation*, Addison-Wesley

[29] O. Junge, 2000 *GAIO - Reference Manual Version 1.2* Department of Mathematics and Computer Science University of Paderborn

[30] V. Kirk and M. Silber, 1994, A competition between heteroclinic cycles, *Nonlinearity*, **7** pages 1605–1621

[31] B.P. Kitchens, 1998, *Symbolic Dynamics One-Sided, Two-Sided and Countable State Markov Shifts*, Springer

[32] M. Krupa, 1990 Bifurcations of relative equilibria, *SIAM J. Math. Anal.*, Vol.**21**, No.**6**, pages 1453–1486

[33] M. Krupa, 1997, *Robust Heteroclinic Cycles*, J. Nonlinear Sci., , pages 129–176

[34] M. Krupa and I. Melbourne, 1995, Asymptotic stability of heteroclinic cycles in systems with symmetry, *Ergod. Th. & Dynam. Sys.*, **15**, pages 121–147

[35] R. Lauterbach, S. Maier-Paape and E. Reissner, 1996 A systematic study of heteroclinic cycles in dynamical systems with broken symmetries, *Proc. of the Royal Soc. of Edinburgh*, **126A** pages885–909,

[36] R. Lauterbach and M. Roberts, 1992, Heteroclinic Cycles in Dynamical Systems with Broken Spherical Symmetry, *Journal of Differential Equations*, **100**, pages 22–48

[37] I. Melbourne, P. Chossat and M. Golubitsky, 1989 Heteroclinic cycles involving periodic solutions in mode interactions with $O(2)$ symmetry *Proc. of the Royal Soc. of Edinburgh*, **113A**, pages 315–345

[38] J. Palis Jr. and W. de Melo, 1982 *Geometric Theory of Dynamical Systems. An Introduction.*, Springer-Verlag

[39] E. Reissner, 1999, *On flows with Spatio-Temporal Symmetries near Heteroclinic Networks*, Shaker Verlag, Augsburg University Dissertation

[40] G. Schwarz, 1980, Lifting smooth homotopies of orbit spaces, *Inst. Hautes Études Sci. Publ. Math.*, **51**, pages37–135,

[41] L.P. Shilnikov, 1965, A case of the existence of a denumerable set of periodic motions, *Sov. Math. Dokl.*, **6**, pages163–166,

[42] L.P. Shilnikov, 1967, The Existence of a Denumerable Set of Periodic Motions in Four-Dimensional Space in an Extended Neighborhood of a Saddle-Focus, *Sov. Math. Dokl.*, **8**, pages54–58,

[43] G.F. Simmons, 1963 Introduction to Topology and Modern Analysis, *International Student Edition*,Mc Graw-Hill

[44] C. Tresser, 1984, About some theorems by L. P. Sil'nikov, *Ann. Inst. Henri Poincaré*, **40(4)**, pages 441–461

[45] S. Wiggins, 1988, *Global Bifurcations and Chaos - Analytical Methods*, Springer-Verlag